



Muthalagu, Nathiya (2015) *Understanding the mechanism of MYC induced vulnerabilities*. PhD thesis.

<https://theses.gla.ac.uk/7464/>

Copyright and moral rights for this work are retained by the author

A copy can be downloaded for personal non-commercial research or study, without prior permission or charge

This work cannot be reproduced or quoted extensively from without first obtaining permission in writing from the author

The content must not be changed in any way or sold commercially in any format or medium without the formal permission of the author

When referring to this work, full bibliographic details including the author, title, awarding institution and date of the thesis must be given

Enlighten: Theses

<https://theses.gla.ac.uk/>
research-enlighten@glasgow.ac.uk

Understanding the mechanism of MYC induced vulnerabilities

Nathiya Muthalagu, MSc.,

This thesis is submitted to the University of Glasgow in accordance with the requirement for the Degree of Doctor of Philosophy in the Institute of Cancer Sciences, College of Medical, Veterinary, and Life Sciences

The Beatson Institute for Cancer Research
Garscube Estate
Switchback Road
Bearsden
Glasgow

Institute of Cancer Sciences
College of Medical, Veterinary and Life Sciences
University of Glasgow

March 2015



CANCER
RESEARCH
UK

BEATSON
INSTITUTE



University
of Glasgow

Abstract

On average, 50% of all human cancers have high MYC expression and a variety of human cancer cells have been found to be dependent on MYC for survival. An effective MYC centric therapy could therefore have a great impact on cancer survival rates. Several efforts are currently being made to target MYC both directly and indirectly and one of these strategies is to exploit MYC-induced vulnerabilities such as apoptosis and synthetic lethality.

MYC can drive apoptosis and can also sensitize cells to other pro-apoptotic stimuli. MYC-induced apoptosis presents a formidable restraint to tumourigenesis *in vivo*. However, the mechanism(s) through which MYC induces apoptosis remains controversial, with some studies implicating p19Arf-mediated stabilization of p53, while others argue for direct regulation of BH3 only proteins, especially Bim. In order to directly compare the relative contributions of p19Arf and Bim to MYC-induced apoptosis, I have made use of the Rosa26-MycER mouse model, wherein the tamoxifen dependent MycER fusion protein is expressed in all tissues. *In vivo*, activation of MYC drives apoptosis only in those tissues where MycER expression is highest (i.e. small intestine and colon). Nevertheless, MycER activation sensitizes several other tissues to synthetic killing by Doxorubicin. To investigate the role of p19Arf and Bim, I have bred the Rosa26-MycER line onto p19Arf and Bim nullizygous mouse lines and measured MYC induced killing under a variety of settings. The results presented in this thesis indicate that MYC-induced apoptosis is dependent upon Bim expression, and proceeds independently of p19Arf. Moreover, I have also shown that Bim is a direct transcriptional target of MYC.

MYC is overexpressed in different human cancer types including pancreatic cancer. Recent studies using mouse models for pancreatic cancer revealed that endogenous Myc expression is required for the initiation and maintenance of pancreatic ductal adenocarcinoma. In this study, using GEMMs I have shown that MYC can drive pancreatic cancer and also cooperates with oncogenic Kras to accelerate pancreatic ductal adenocarcinoma. I have used MYC/Kras pancreatic cancer model to test the MYC induced dependency on AMPK related kinase Ark5 (Nuak1). Synthetic lethal screening strategies have recently revealed a number of kinases such as Nuak1, upon which cells that overexpress MYC selectively depend for their survival. To investigate the requirement of Nuak1 for MYC driven pancreatic tumourigenesis, I have used the previously described, *Nuak1^{FL/FL}* mouse. Deletion of *Nuak1* specifically in the pancreas did not significantly

impact survival or tumour burden of the mice. However, my data suggest that tumours arise by failing to knockout Nuak1 completely, suggesting that MYC overexpressing cells may impose a selective pressure to retain the Nuak1 allele, whereas normal pancreatic cells can tolerate the deletion of Nuak1.

In vitro, primary murine pancreatic cancer cells derived from MYC/Kras^{G12D} tumours are sensitive to BH3-mimetic ABT-737 and Nuak1 inhibitor HTH-01-015. Taken together, my data suggest that augmenting MYC induced apoptosis by using ABT-737 and exploiting MYC induced dependence upon Nuak1 may be a successful therapeutic strategy for MYC dependent cancers.

Table of contents

Abstract.....	2
Acknowledgements.....	12
List of Publications.....	14
Author's Declaration	15
Abbreviations.....	16
1 Introduction.....	21
1.1 Cancer.....	21
1.2 MYC and Cancer.....	21
1.2.1 Mechanism of MYC deregulation.....	21
1.3 MYC: structure and function.....	23
1.3.1 MYC-structure.....	23
1.3.1.1 Function of Myc boxes.....	24
1.3.2 Transcriptional function of MYC.....	25
1.3.3 Target genes and functions.....	25
1.3.3.1 Cell cycle and Cell growth.....	26
1.3.3.2 Stemness.....	26
1.3.3.3 Cell adhesion and cytoskeleton.....	27
1.3.3.4 Metabolism.....	28
1.4 Targeting MYC.....	28
1.4.1 Apoptosis.....	30
1.4.1.1 The two major pathways of apoptosis.....	30
1.4.2 MYC induced apoptosis.....	33
1.4.2.1 Role of p19Arf-p53 pathway in MYC-induced apoptosis.....	33
1.4.2.2 Role of Bcl2 family proteins in MYC-induced apoptosis.....	34
1.4.3 Synthetic lethality.....	35
1.5 ARK5/NUAK 1.....	36
1.5.1 Nuak1 functions.....	37
1.5.1.1 Role of Nuak1 in mitochondrial respiration.....	38
1.5.2 Reactive oxygen species.....	39
1.6 Pancreatic cancer.....	40
1.6.1 Basic function of the pancreas.....	40
1.6.2 Pancreatic cancer: Statistics, causes and types.....	40
1.6.2.1 Pancreatic ductal adenocarcinoma.....	41
1.6.2.2 Current treatment of pancreatic cancer.....	42

1.7	Conditional transgenic techniques	43
1.7.1	Site specific DNA recombination	43
1.7.2	Modelling pancreatic cancer	45
1.7.2.1	Conditional Kras mouse models	46
1.7.2.2	Other mouse models for pancreatic cancer	46
1.8	Aim and Objectives	47
2	Materials and Methods	49
2.1	Animal work	49
2.1.1	Colony Maintenance	49
2.1.2	Genotyping	50
2.1.3	Experimental cohorts	50
2.1.3.1	Spontaneous genetically-engineered mouse models (GEMM) of pancreatic tumourigenesis	50
2.1.3.2	End points	50
2.1.3.3	Acute MYC activation model	51
2.1.4	Administration of Tamoxifen	51
2.1.5	Administration of Doxorubicin	51
2.1.6	Tissue sample preparation	51
2.1.6.1	Processing the tissues	52
2.1.6.2	Sectioning of fixed tissues	52
2.2	Cell specific staining	52
2.2.1	Preparation of sections for IHC or cell specific staining	52
2.2.2	Hematoxylin & Eosin staining	53
2.2.3	Alcian blue/PAS staining	53
2.2.4	Picro-sirius red staining	53
2.3	Immunohistochemistry	54
2.3.1	Preparation of sections for IHC	54
2.3.2	Antigen retrieval	54
2.3.3	Blocking endogenous peroxidase	54
2.3.4	Blocking of non-specific antibody binding	54
2.3.5	Primary antibody incubation	55
2.3.6	Secondary antibody incubation	55
2.3.7	Signal amplification	55
2.3.8	Visualizing the signal	55
2.3.9	Counterstaining and slide mounting	56
2.3.10	TUNEL staining	57
2.3.11	Epithelial cell extraction from the small intestine	57
2.4	PCR-Genotyping	58
2.4.1.1	Genomic DNA isolation	58

2.4.1.2	PCR genotyping.....	58
2.4.1.3	Agarose gel electrophoresis.....	59
2.5	Cell Culture techniques.....	61
2.5.1	Fibroblast cell culture.....	61
2.5.2	Generation of primary pancreatic cells.....	61
2.5.3	Passaging cells in culture.....	62
2.5.4	Freezing down cell lines.....	62
2.5.5	Thawing cells in culture.....	62
2.5.6	siRNA transfection.....	62
2.6	Analysis of cell death.....	63
2.6.1	Annexin V/PI staining.....	63
2.6.2	SYTOX green cell death assay.....	63
2.6.3	Crystal violet staining.....	63
2.7	ROS detection.....	64
2.8	RNA isolation and quantitative real-time PCR.....	64
2.8.1	RNA isolation by Trizol method.....	64
2.8.2	cDNA synthesis.....	65
2.8.3	Primer Design.....	65
2.8.4	qRT-PCR.....	66
2.9	Protein Extraction and Western Blot Analysis.....	66
2.9.1	Protein Extraction.....	66
2.9.2	Protein quantification.....	67
2.9.3	Preparation of protein samples.....	68
2.9.4	SDS-PAGE.....	68
2.9.5	Western blot.....	68
2.10	Chromatin immunoprecipitation.....	70
2.11	Data Analysis.....	71
2.11.1	Graphical representation of the data.....	71
2.11.2	Comparision of Means.....	71
2.11.3	Survival analysis.....	71
3	Evaluating the relative contribution of p19Arf and BIM in MYC-induced apoptosis.....	72
3.1	Introduction.....	72
3.1.1	Mouse models used to address the aims.....	73
3.2	Results.....	74
3.2.1	Bim is required for MYC-induced apoptosis.....	74
3.2.2	Bim mediates the pro-apoptotic signalling by MYC.....	77
3.2.3	Bim is a specific BH3-only protein required for MYC-induced apoptosis.....	81
3.2.4	Bim is required specifically downstream of MYC.....	84

3.2.5	Bim is directly regulated by MYC	85
3.2.6	A threshold level of BIM is required for MYC induced- apoptosis	87
3.3	Discussion.....	88
3.4	Future work.....	90
4	Investigating the synergy between MYC and Kras^{G12D} in pancreatic tumourigenesis	92
4.1	Introduction.....	92
4.1.1	Mouse models used to address these aims.....	93
4.2	Results.....	94
4.2.1	Pancreas specific expression of mutant Kras and MYC.....	94
4.2.2	MYC accelerates Kras ^{G12D} induced pancreatic tumourigenesis	95
4.2.3	mTOR and Raf/MEK/Erk pathways are active in MYC and Kras ^{G12D} induced tumours	98
4.2.4	KMC tumours resemble human pancreatic cancer in terms of mucin expression and collagen deposition	100
4.2.5	Dose dependent effect of MYC on pancreatic tumourigenesis	101
4.2.6	mTOR but not Raf/MEK/Erk pathway is active in R26 ^{LSL-MYC} tumours	104
4.2.7	Primary pancreatic tumour cells are sensitive to BH3-mimetic, ABT-737... ..	104
4.3	Discussion.....	106
4.4	Future work.....	108
5	Evaluating the role of Nuak1 in MYC driven pancreatic tumourigenesis	109
5.1	Introduction.....	109
5.2	Mouse models used to address the aim.....	110
5.3	Results.....	111
5.3.1	Pancreas specific Knockout of Ark5/Nuak 1.....	111
5.3.2	MYC and mutant Kras impose selective pressure to retain Nuak1	112
5.3.3	Primary pancreatic tumour cells are sensitive to Nuak1 inhibitor.....	114
5.3.4	Discussion.....	115
5.4	Future work.....	117
6	Conclusion, discussion and future directions	118
6.1	Tumours are addicted to MYC	118
6.2	Targeting MYC.....	118
6.2.1	MYC-induced apoptosis	120
6.2.1.1	Role of Bim in MYC-induced apoptosis	121
6.2.1.2	Role of p19Arf in MYC-induced apoptosis.....	124
6.2.1.3	Exploiting MYC-induced apoptosis as a therapeutic strategy.....	126
6.3	MYC in pancreatic tumourigenesis	126
6.4	‘Synthetic lethality’- an approach to target MYC selectively	127
6.5	Future directions	128
6.5.1	Establishing tamoxifen inducible MYC/Kras ^{G12D} pancreatic model	128

6.5.2	Exploiting MYC-induced vulnerabilities	128
6.5.3	Characterizing the functions of Nuak1 in vitro	129
6.6	Therapeutic implications	129
References	131

List of Figures

Figure 1-1- Domains of MYC and its binding partners.....	23
Figure 1-2- The mitochondrial regulation of caspase dependent cell death.....	32
Figure 1-3 Activation of the AMPK-related kinases by LKB1.....	36
Figure 1-4 Decreased expression of ETC components upon NUAK1 depletion.....	39
Figure 1-5- The progression model for PDAC.....	42
Figure 1-6- Outline of Cre-LoxP system for generating a gene knockout.....	44
Figure 1-7- Outline of Cre-LoxP system for generating overexpression or Knockin strains.	45
Figure 3-1- Mouse models used to study MYC-induced apoptosis.....	74
Figure 3-2- Bim is required for MYC-induced apoptosis in the intestine.....	75
Figure 3-3- Bim is required for MYC-induced apoptosis in MEFs.....	76
Figure 3-4- <i>Bim</i> null cells are resistant to MYC-induced apoptosis after 72hrs of MYC activation.....	77
Figure 3-5- Bim is required for MYC-induced sensitization to Doxorubicin.....	78
Figure 3-6- Bim is not induced by Doxorubicin.....	79
Figure 3-7- Bim is required for MYC-induced sensitization to irradiation and ABT-737..	80
Figure 3-8- Puma is not required for MYC-induced apoptosis in the intestine.....	81
Figure 3-9- Puma is required for MYC induced sensitization to Doxorubicin.....	82
Figure 3-10- Puma is required for Doxorubicin induced apoptosis in the small intestine ..	83
Figure 3-11- Bad is not required for MYC-induced apoptosis <i>In vitro</i>	83
Figure 3-12- Bim is not required for Doxorubicin induced apoptosis in the small intestine	84
Figure 3-13- Bim is not required for Doxorubicin induced apoptosis in MEFs.....	85
Figure 3-14- MYC activation results in increase in Bim expression in the small intestine	85
Figure 3-15- MYC activation induces Bim expression <i>in vitro</i>	86
Figure 3-16- MYC binds to the Bim promoter region.....	87
Figure 3-17- A threshold level of Bim is required for MYC induced apoptosis.....	88
Figure 4-1- Schematic representation of Conditional <i>LSL-Kras</i> ^{G12D/+} and <i>R26</i> ^{LSL-MYC/+} mouse model.....	94
Figure 4-2- Pancreas specific expression of <i>MYC</i> and mutant <i>Kras</i>	95
Figure 4-3- MYC cooperates with mutant <i>Kras</i> in driving pancreatic ductal adenocarcinoma.....	96
Figure 4-4- KMC mice exhibit tumours with mixed pathology.....	98
Figure 4-5- IHC for Ki67 revealed that KMC tumours are actively proliferating.....	98
Figure 4-6- IHC for pS6 (ser240/244) confirmed activation of mTOR pathway in <i>R26</i> ^{LSL- MYC/+} ; <i>LSL-Kras</i> ^{G12D} driven pancreatic tumours.....	99
Figure 4-7- IHC for p-ERK revealed active Raf/MEK/Erk pathway in PanINs and PDAC	100
Figure 4-8- KMC tumours display high mucin expression and collagen deposition.....	101
Figure 4-9- Dose dependent effect of MYC on pancreatic tumourigenesis.....	102
Figure 4-10- MYC induced tumours are primarily neuro-endocrine tumours.....	103
Figure 4-11- IHC for Ki67 on MYC only pancreatic tumours.....	103
Figure 4-12- MYC only tumours have active mTOR pathway but not Raf/MEK/ERk pathway.....	104
Figure 4-13- Primary pancreatic tumour cells derived from KMC tumours are sensitive to BH3-mimetic, ABT-737.....	105
Figure 5-1- NUAK1 depletion kills MYC overexpressing cells.....	110
Figure 5-2- Schematic representation of <i>Nuak1</i> floxed allele.....	111
Figure 5-3- Pancreas specific deletion of <i>Nuak1</i>	111
Figure 5-4- <i>Nuak1</i> deleted mice display pancreas with normal histological feature.....	112
Figure 5-5- <i>Nuak1</i> deletion had no significant effect on survival of the KMC mice.....	113

Figure 5-6- KMC <i>Nuak1^{FL/FL}</i> tumours show partial deletion of the allele	114
Figure 5-7- Primary murine pancreatic tumour cells are sensitive to Nuak1 inhibitor HTH-01-015	115
Figure 5-8- Nuak1 inhibition is not toxic to primary mouse embryonic fibroblasts	115
Figure 6-1- Schematic representation of ways of targeting MYC	119
Figure 6-2- Model for the regulation of Bcl2 proteins by MYC	123
Figure 6-3- Proposed model for role of p19Arf and Bim in MYC-driven processes	125

List of Tables

Table 2-1- Outline of genetic models used in this study	49
Table 2-2- IHC conditions	56
Table 2-3- Primers used for genotyping PCR.....	58
Table 2-4- Outline of PCR reactions, cycling conditions and product sizes	60
Table 2-5- Genomic DNA elimination components.....	65
Table 2-6- Reverse-transcription reaction components	65
Table 2-7- Primers used for Q-RT PCR	65
Table 2-8- Q-RT PCR reaction components	66
Table 2-9- Q-RT PCR cycling condition.....	66
Table 2-10- SDS-PAGE gel composition.....	68
Table 2-11- Buffers used during Protein analysis	69
Table 2-12- Antibody conditions for western blot analysis.....	69
Table 2-13- Buffers used for Chromatin immunoprecipitation.....	70
Table 4-1 Table summarising the histological features of pancreatic tumours in KMC and MC mice	97
Table 4-2- Table summarising the histological features of tumours from R26 ^{LSL-MYC} homozygous and heterozygous cohorts	102

Acknowledgements

Initially I would like to thank Graduate school of life sciences (GSLs) and Cancer Research UK (CRUK), for funding my PhD at University of Wurzburg and Beatson institute for cancer research, respectively.

To my supervisor Daniel Murphy, who has helped to nurture my research interest and allowed me to develop the skills required for further academic career. My special thanks to Daniel for giving me this exciting project and for all the motivation and encouragements he has given throughout my research period and most of all I will always be grateful for the faith he has shown in me. My sincere thanks to Martin Eilers and all his lab members, for all the stimulating lab meetings and journal clubs.

My sincere thanks to all our collaborators, Gerard Evan, Stephen Tait, Martin Eilers and their lab members, without whom this work would not have been possible. I take this opportunity to thank Alasdair Fraser from Gerry Graham's group, for his immense help in doing B cell FACS analysis.

My special thanks to my dear friend Sarah Neidler, who was always there to listen and share good and bad experiences and without her, our move from Germany to Glasgow would have been difficult. Special mention to Barbara and Jannes from Germany for all their help and support. From the M10 lab, my special thanks to Meera Raja, for her immense help in correcting my thesis. Thanks to Tiziana and Jennifer for all those laughs and refreshing coffee breaks. Thanks to Jacqueline for all the scientific inputs and helping me in designing certain experiments. Special thanks to Allan Mcvie, for all the technical help and taking care of my lab duties during my absence.

There are good few 'Beatsonites' who deserve a mention here. Evangelos, for all those enthusiastic scientific discussions and mind-blowing ideas he shared with me. Gabriel, for all the help in microscopy and image analysis. Mohindar, Karthik, Jacob, Vinay, and Linda my fellow Indians, who have made my life away from home little bit easier.

Without the excellent biological and histological services at the Beatson institute this work would not have been possible. My special thanks to Colin and his team for doing all my urgent histology requests at short notice. Katherine from Germany and Tom Gilbey from Beatson Advanced imaging resource (BAIR), without their hours of training, I could never

have achieved as much I have at the FACS. I take this opportunity to thank Dimitris Athineos for hours of training he provided on pancreatic cancer mouse model.

Finally to my family; My mum, dad and my sisters who have supported me through all the years of education and also encouraged me to travel several thousands of miles to do my PhD. I am always grateful to my grandfather Mr.Thiruvupillai and my uncle Mr.Thennavan, who have helped me financially throughout my school and college education, without their support I would not have come this far. Also, I am blessed to have my husband Prabhu, who put his career second to mine and came all the way from India to the UK, just to see me happy.

List of Publications

Ichim, G., Lopez, J., Ahmed, S. U., **Muthalagu, N.**, Giampazolias, E., Delgado, M. E., Haller, M., Riley, J. S., Mason, S. M., Athineos, D., *et al.* (2015). Limited mitochondrial permeabilization causes DNA damage and genomic instability in the absence of cell death. **Molecular cell** 57, 860-872.

Murphy, D. J., and **Muthalagu, N.** (2015). Bim's up first. **Molecular & cellular oncology** 2, 2.

Muthalagu, N., Junttila, M. R., Wiese, K. E., Wolf, E., Morton, J., Bauer, B., Evan, G. I., Eilers, M., and Murphy, D. J. (2014). BIM is the primary mediator of MYC-induced apoptosis in multiple solid tissues. **Cell reports** 8, 1347-1353.

Liu, L., Ulbrich, J., Muller, J., Wustefeld, T., Aeberhard, L., Kress, T. R., **Muthalagu, N.**, Rycak, L., Rudalska, R., Moll, R., *et al.* (2012). Deregulated MYC expression induces dependence upon AMPK-related kinase 5. **Nature** 483, 608-612.

Author's Declaration

I hereby declare that the work presented in this thesis is the result of my own independent investigation unless otherwise stated.

This work has not been accepted for any other degree, nor it is being currently submitted for any other degree.

Nathiya Muthalagu

Abbreviations

Mouse models

$R26^{MER/MER}$ = MycER^{T2} expressed under the control of Rosa26 locus

KMC = $Pdx1-Cre; R26^{LSL-MYC/+}; LSL-Kras^{G12D}$

KC = $Pdx1-Cre; LSL-Kras^{G12D}$

MC = $Pdx1-Cre; R26^{LSL-MYC/+}$

KMCⁱ = $Pdx1-CreER; R26^{LSL-MYC/+}; LSL-Kras^{G12D}$

Symbols

°C = Degrees Celsius

µg = Micrograms

µl = Microlitres

µm = Micrometre

µM = Micromolar

nm = nanometre

mg = milligrams

Kg = Kilograms

ml = millilitres

A

ABC = Avidin Biotin Complex

ADM = Acinar-to-Ductal Metaplasia

ADP = Adenosine Diphosphate

AMP = Adenosine Monophosphate

APC = Adenomatous Polyposis Coli

ARF = Alternative reading frame

ATP = Adenosine Triphosphate

B

Bad = Bcl2-associated death promoter

BCA = Bicinchoninic Acid

Bcl2 = B-cell lymphoma 2

BET = Bromodomain and Extraterminal domain family

bHLHZ = Basic helix loop helix leucine zipper motif

BH3 = Bcl2-homology domain 3

Bim = Bcl2-interacting mediator of cell death

BL = Burkitt lymphoma

Bmi1 = polycomb ring finger oncogene

Bp = base pair

BSA = Bovine serum albumin

C

CAMKK = calcium/calmodulin- dependent kinase kinase

CDK = Cyclin-dependent kinase

cDNA = complementary DNA

Chk1 = Checkpoint kinase 1

CHIP = Chromatin immunoprecipitation

CIP2A = Cancerous inhibitor of protein phosphatase 2A

Cre = recombinant enzyme derived from P1 bacteriophage

CTD = Carboxy terminal domain

D

DAB = 3,3'-Diaminobenzidine

DEDs = Death interacting domains

dH₂O = distilled water

DMSO = Dimethyl sulfoxide

dMyc = Drosophila Myc

DNA = Deoxyribonucleic acid

dNTP = Deoxynucleotide triphosphate

DTT = Dithiothreitol

DUBs = Deubiquitinating enzyme

E

ECM = Extra cellular matrix

EDTA = Ethylenediaminetetraacetic acid

EGFR = Epidermal growth factor receptor

EMT = Epithelial to Mesenchymal Transition

E_μ-Myc = Enhancer of immunoglobulin heavy chain μ linked to Myc transgene

ER = Estrogen receptor

ES cells = Embryonic Stem cells

ETC = Electron transport chain

F

FADD = Fas-associated protein with death domain

FBS = Fetal bovine serum

FLP = Flippase

G

GADD45 = Growth arrest and DNA damage inducible protein

GAPs = GTPase activating proteins

gDNA = Genomic DNA

GDP = Guanosine diphosphate

GEMMs = Genetically engineered mouse models

GLS = Glutamine synthetase

GLUT1 = Glucose transporter 1

GTP = Guanosine-5'-triphosphate

H

HAT = histone acetyl transferase

HECTH9 = HECT domain-containing ubiquitin E3 ligase

HEPES = 4-(2-hydroxyethyl)-1-piperazineethanesulfonic acid

HK2 = Hexokinase 2

HRP = Horse radish peroxidase

HSC = Hematopoietic stem cells

H&E = Hematoxylin and Eosin staining

I

IHC = Immuno histochemistry

Ig = Immunoglobulin

IP injection = Intraperitoneal injection

IPMNs = Intraductal Papillary Mucinous Neoplasms

IVCs = Individually ventilated cages

γ -IR = Gamma-Irradiation

L

LDHA = Lactate dehydrogenase A

M

MB I-IV = Myc boxes

MCNs = Mucinous cystic neoplasms

MEFs = Mouse embryonic fibroblasts

MLC2 = Myosin light chain 2

MMP = Matrix metalloproteinase

MOMP = Mitochondrial outer membrane permeabilization

mTOR = Mammalian target of rapamycin

MYPT1 = Myosin phosphatase target subunit 1

Myc-ER = Myc-oestrogen receptor fusion transgene

P

PAS = Periodic acid-Schiff stain

PBS = Phosphate buffered saline

PCR = Polymerase chain reaction

PDAC = Pancreatic ductal adenocarcinoma

PDGF = Platelet derived growth factor

PanIN = Pancreatic intraepithelial neoplasia

Pdx1 = Pancreatic and duodenal homeobox1

PFK = phosphofructo kinase

PIN1 = Peptidylprolyl Cis/Trans isomerase, NIMA-interacting 1

PI = Propidium iodide

PLL slides = Poly-L-Lysine coated slides

POZ domain = Pox virus and Zing finger domain

p-TEFb = Positive transcription elongation factor

Puma = p53 upregulated modulator of apoptosis

Q

Q-RT PCR = Quantitative- Real Time PCR

R

RIPA = Radioimmunoprecipitation assay buffer

ROS = Reactive oxygen species

RNA = Ribonucleic acid

rRNA = Ribosomal RNA

S

SAE = Sumo activating enzyme

SDS = Sodium Dodecyl sulphate

Ser = serine

siRNA = Small interfering RNA

shRNA = Short hairpin RNA

Skp2 = S-phase kinase-associated protein

SOD = Superoxide dismutase

T

TAD = Transactivation domain

TAE = Tris-acetate-EDTA buffer

T-ALL = T-cell acute lymphoblastic leukemia

Tam = Tamoxifen

TAK1 = Transforming growth factor beta- activated kinase 1

TBS = Tris-Buffered saline

TBS-T = Tris-Buffered saline and Tween20

TCA = Tricarboxylic acid cycle

TdT = Terminal nucleotidyl transferase enzyme

TGF = Transforming growth factor

TNF = Tumour necrosis factor

Thr = Threonine

TUNEL = Terminal nucleotidyl transferase dUTP nick end labelling

Tyr = Tyrosine

U

USP37/38 = Ubiquitin specific peptidases (DUBs)

V

VEGF = Vascular endothelial growth factor

Volts = Voltage

123

4E-BP1 = Eukaryotic translation initiation factor 4E-binding protein1

4-OHT = 4-Hydroxy tamoxifen

1 - Introduction

1.1 Cancer

Cancer is one of the leading causes of death worldwide, with approximately 14 million new cases and 8.2 million cancer related deaths in 2012 (www.who.int/mediacentre/factsheets/fs297/en/). There are more than 200 different types of cancer with different risk factors and causes. The fundamental cause of cancer is genetic alterations in two different categories of genes called tumour suppressors and oncogenes. These alterations are usually somatic events, although germ-line mutations can predispose to familial cancer. The function of tumour suppressor genes is to inhibit cell proliferation, act as “brakes” for the cell cycle, or to act as guardians of genome integrity. The genetic mutations that inactivate tumour suppressors liberate the cell from growth constraints, leading to uncontrolled growth of cancer cells. On the other hand, proto-oncogenes encode proteins that stimulate cellular proliferation, block apoptosis, or both. The products of proto-oncogenes can be broadly classified into six groups: transcription factors, chromatin remodelers, growth factors, growth factor receptors, signal transducers, and apoptosis regulators. The proto-oncogene can become an oncogene, after genetic mutations, leading to increased expression or increased activity, thus conferring a growth advantage to the cancer cells (Croce, 2008; Weinberg, 1991).

1.2 MYC and Cancer

MYC is one of the most frequently deregulated oncogenes in human cancer. *MYC* overexpression correlates with poor clinical outcome, aggressiveness of disease and relapse (Wolfer et al., 2010; Zhou et al., 2014). *MYC* was discovered as a cellular homolog of viral oncogene v-myc (myelocytomatosis virus) (Sheiness and Bishop, 1979). The oncogene *MYC* is a transcription factor, regulating a variety of cellular functions (see section 1.3.3). *MYC* is deregulated in a variety of cancers by different mechanisms such as chromosomal translocation, amplification, somatic mutation or is overexpressed because of deregulated upstream pathways.

1.2.1 Mechanism of *MYC* deregulation

One of the first studied mechanisms of *MYC* deregulation involves translocation of the *MYC* gene to an immunoglobulin locus. For example, in Burkitt Lymphoma (BL) *MYC* translocation involves the juxtaposition of *MYC*, located in chromosome 8, with

immunoglobulin heavy chain (μ) or light chain (λ and κ) located on chromosomes 14, 22, or 2, respectively, leading to an increase in MYC protein expression (Nesbit et al., 1999). The experiments performed by Adams, et al., (Adams et al., 1985) demonstrating the development of pre-B cell and B cell lymphomas in E μ -Myc mice suggest that MYC deregulation is essential for BL development. E μ -Myc is a spontaneous model of lymphomagenesis, where *Myc* is linked to Ig heavy chain enhancer, thus expressed exclusively in B-lymphoid cells. In addition, MYC translocation is also found in some cases of acute T cell lymphoblastic leukemia (T-ALL), diffused large cell B-cell lymphoma and multiple myeloma (Boxer and Dang, 2001).

MYC gene amplification is found in many human cancers and is often associated with aggressive nature of the disease. For example, Escot, et al., (Escot et al., 1986) reported variable level of *MYC* gene amplification in 38% of the primary breast cancer cases analysed and this initial discovery has been confirmed by numerous subsequent studies (Harada et al., 1994; Rodriguez-Pinilla et al., 2007). *MYC* amplification is also reported in human lung cancer (Baykara et al., 2015) and in high grade prostatic intraepithelial neoplasia (Jenkins et al., 1997).

In addition to the *MYC* gene translocation, somatic mutations have been found in a number of tumour samples and cell lines of Burkitt Lymphoma. Interestingly, these mutations were clustered in the Exon 2 region between codons 57 and 63 (Bhatia et al., 1993). These sites were later found to be important in determining MYC protein stability (see section 1.3.1.1).

It has become increasingly clear that MYC deregulation is not just restricted to gross genetic changes at the *MYC* locus. MYC can be deregulated via disruption of upstream pathways that otherwise keep MYC levels in check. At the level of transcription, MYC is downstream of many pathways that are overexpressed in multiple cancer settings. For example, tumour suppressor Adenomatous polyposis coli (APC), a commonly mutated gene in colorectal cancers, leads to accumulation of β -catenin, which binds to the TCF activator and drives constitutive expression of MYC (He et al., 1998). Similarly, MYC is an important target of Notch signalling, which is mutated in T-ALL (Weng et al., 2006). At the level of protein, MYC can be stabilized by loss of critical regulators of protein stability such as F-box family of proteins, which are mutated in approximately 6% of human cancers (Akhoondi et al., 2007) and therefore present at high level in human cancers.

1.3 MYC: structure and function

The proto-oncogene MYC (c-Myc) belongs to the family of Myc genes that include L-Myc and N-Myc (Brodeur et al., 1984; Nau et al., 1985). Although the Myc family members share high sequence similarity and remarkable conservation in structure and functions, they have stage and tissue specific patterns of expression during development (Zimmerman et al., 1986).

1.3.1 MYC-structure

MYC is a basic helix-loop-helix/leucine zipper (bHLHZ) transcription factor. It consists of N-terminal trans activation domain (TAD), which comprises two highly conserved regions called Myc homology box I and II; a middle segment containing another two conserved Myc boxes (MBIII and MBIV) and a nuclear localization signal; and a carboxy terminal bHLHZ domain, which is required for DNA binding and dimerization with its partner proteins (Fig.1-1) (Conacci-Sorrell et al., 2014; Kato et al., 1990).

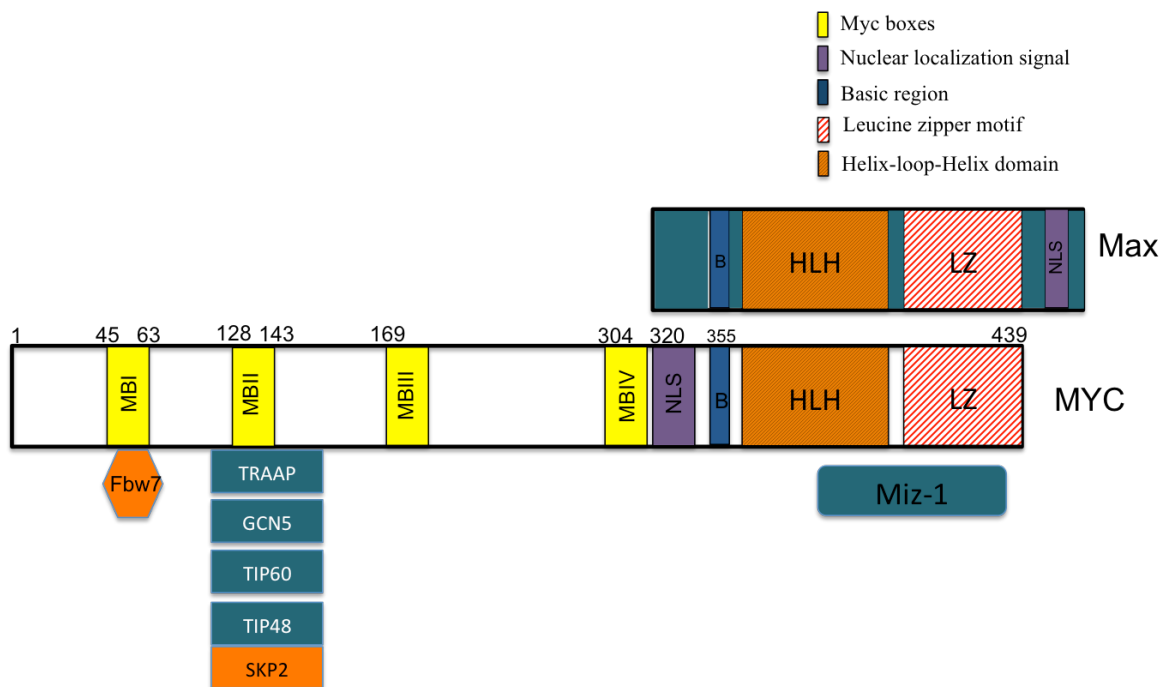


Figure 1-1- Domains of MYC and its binding partners.

The N terminus of MYC has three conserved elements known as Myc boxes I-III. The C terminus contains the basic helix-loop-helix/leucine zipper (bHLH/LZ) motif. In blue are the major functionally characterized transcriptional binding partners and in orange are major E3 ligases involved in MYC turnover.

The search to identify MYC binding partners resulted in the discovery of the protein Max by Blackwood and Eisenmann (Blackwood and Eisenman, 1991). Max is a ubiquitous, basic helix-loop-helix/leucine zipper protein, which does not have a transactivation domain, but heterodimerizes with MYC through its leucine zipper motif in order to bind and activate target genes. Myc/Max heterodimers binds to a specific DNA sequence “CAC(A/G)TG” called E-boxes (Blackwell et al., 1990; Kato et al., 1992). However, Max can also interact with other bHLHZ proteins such as Mad family proteins. Mad family proteins act as transcriptional antagonists for MYC. Mad proteins compete with MYC for interaction with Max and repress transcription by binding to the same E-box sequence as the Myc/Max complex (Ayer et al., 1993). Interestingly, MYC can also repress transcription when it binds to transcription factor Miz-1. Miz-1, a Pox virus and Zinc finger (POZ) domain protein was identified in a yeast two-hybrid screen as a new interacting partner responsible for MYC repression (Peukert et al., 1997; Staller et al., 2001). However, recently it has been demonstrated that Miz-1 is required for repression of a large but not entire fraction of MYC target genes (Walz et al., 2014).

1.3.1.1 Function of Myc boxes

Myc box I (MBI) is involved in the ubiquitylation and proteosomal degradation of MYC. MYC is a tightly regulated protein with short half-life of 20-30 mins. MAP kinase signalling is responsible for Ser-62 phosphorylation of MBI, which increases protein stability, whereas Gsk3 β mediated Thr-58 phosphorylation destabilizes MYC. The phosphorylated form of MYC is then recognized by prolyl isomerase PIN1, which promotes access of protein phosphatase 2A to dephosphorylate Ser-62. The Thr-58 only phosphorylated form of MYC is then recognized by the F-box protein FBW7, which leads to ubiquitination and degradation (Sears, 2004; Yada et al., 2004). Additional E3-ligases such as Skp2, HectH9, and β -TrCP are also implicated in MYC protein regulation. The two phosphorylation sites of Myc Box I, Thr-58 and Ser-62 are of great importance as they fall within a mutational hotspot found in human cancer.

Myc box II acts as a hub for many interacting proteins including, histone acetyl transferase (HAT) complexes such as TRAPP-GCN5, Tip60 and Tip48 (Frank et al., 2003; McMahon et al., 1998), which promote histone acetylation and gene activation (Fig. 1-1).

1.3.2 Transcriptional function of MYC

MYC and other family members were initially proposed to bind specific DNA sequences (E-boxes) and regulate a specific set of target genes (“gene-specific” model). Expression analysis conducted to identify MYC target genes by different research groups resulted in an endless list of putative target genes with little overlap. This questions the “gene-specific” model of regulation. Furthermore, canonical E-boxes are found in the whole genome at a frequency of once per 4 kb on average and not all MYC binding is E-box dependent (Eilers and Eisenman, 2008).

Some studies suggest that MYC, in contrast to other conventional transcription factors, plays an important role in transcriptional elongation and promoter pause release. MYC recruits positive elongation factor p-TEFb (consisting of cdk9 and cyclin T proteins) to phosphorylate RNA pol II carboxy terminal domain (CTD) and stimulate elongation at specific genes (Eberhardy and Farnham, 2001; Eberhardy and Farnham, 2002; Kanazawa et al., 2003). Promoter-proximal pausing of RNA Polymerase II is one of the post initiation regulatory events. MYC, again through recruitment of p-TEFb contributes to promoter proximal pause release in most actively transcribed genes in embryonic stem cells (Rahl et al., 2010). All these observations led to the proposal of a new model called “amplifier model” where MYC is proposed to have a more global effect. Two reports argue that MYC binds and amplifies genes, which are already in an “on” state (Lin et al., 2012; Nie et al., 2012). Thus, it works more as a global factor, enhancing what cells are already doing.

However, two recent reports refute the general amplifier model. Both the reports suggest that MYC regulates differential expression of a distinct set of target genes and different levels of MYC regulates functionally different classes of target genes (Sabo et al., 2014; Walz et al., 2014). Importantly, the “amplifier model” fails to accommodate MYC mediated gene repression. Hence, it is more plausible that MYC regulates the expression of a distinct set of target genes and thereby changes the state of the cell while at the same time functions as an amplifier in a certain cellular context.

1.3.3 Target genes and functions

A large scale screen for MYC binding sites revealed that MYC could regulate almost 15% of the gene in the genome, (Fernandez et al., 2003; Orian et al., 2003) thereby controlling an array of functions, such as proliferation, apoptosis, cell cycle regulation, protein synthesis, cell adhesion and cytoskeleton, and metabolism.

1.3.3.1 Cell cycle and Cell growth

One of the earliest observations about MYC function was its ability to promote proliferation and block differentiation. Since then, many studies have found cell cycle regulators such as Cyclin D1, Cyclin D2, Cyclin B1, and Cdk4 as MYC target genes (Bouchard et al., 2001; Hanson et al., 1994; Hermeking et al., 2000; Menssen and Hermeking, 2002). Also, MYC has been shown to repress CDK inhibitors p21 and p15Ink4a (Staller et al., 2001; Wu et al., 2003) and growth arrest genes such as Gadd45 (Marhin et al., 1997). The experimental evidence showing delayed S-phase entry in MYC null cells and entry of quiescent cells into S-phase by ectopic expression of MYC further strengthened its role in cell cycle and cell growth (Eilers et al., 1989; Kaczmarek et al., 1985; Mateyak et al., 1997). In drosophila, overexpression of dMyc results in an increase in cell size, while loss of function mutant Myc results in flies with reduced body size and smaller cells (Johnston et al., 1999).

Given its role in cell growth, cells over-expressing MYC would demand a higher rate of macromolecular synthesis. As such, the rates of RNA and protein synthesis were higher in MYC proficient cells compared to MYC deficient counterparts (Mateyak et al., 1997). The expression analysis conducted to identify MYC target genes repeatedly identified genes that encode ribosomal RNAs and ribosome biogenesis proteins. MYC regulates multiple stages of ribosome biogenesis from rRNA processing to export of ribosomal subunits from the nucleus to the cytoplasm (Grandori et al., 2005; van Riggelen et al., 2010). In addition, MYC enhances the translational capacity of the cell by increasing RNA Pol I dependent increase in ribosomal RNA synthesis (Arabi et al., 2005; Grandori et al., 2005) and Pol III dependent tRNA synthesis (Gomez-Roman et al., 2003). MYC also regulates translation initiation and elongation factors (Schuhmacher et al., 2001). In essence, MYC regulates proteins involved in cell cycle regulation and regulates protein synthesis at multiple levels to meet the demand of cell growth.

1.3.3.2 Stemness

Myc, along with classical stem cell factors Oct4, Sox2 and Nanog are important for induction and maintenance of induced pluripotent stem cells derived from mouse embryonic fibroblasts (MEFs). In this scenario, expression of stem cell factors (minus c-Myc) in MEFs resulted in a flat, non-ES –cell like morphology, whereas co-expression of Myc restored ES cell morphology and growth properties (Takahashi and Yamanaka, 2006). It has also been reported that Myc expression is necessary for hematopoietic stem cell

(HSC) survival and proliferation (Laurenti et al., 2008). Myc controls the balance between HSC self renewal and differentiation by regulating HSC interaction with its niche (Murphy et al., 2005; Wilson et al., 2004). Moreover, the Myc transcriptional network forms a distinct module termed the Myc module, which together with core (targets of core pluripotency factors) and polycomb (targets of polycomb proteins) modules makes up the embryonic stem cell expression pattern. The Myc module is also active in a variety of cancers, suggesting that MYC partly accounts for shared similarities between ES cells and cancer cells (Kim et al., 2010).

1.3.3.3 Cell adhesion and cytoskeleton

Down regulation of genes involved in adhesion and cytoskeleton by Myc family members might contribute to its ability to transform primary cells and to promote anchorage independent growth (Small et al., 1987). In a human small cell lung cancer cell line, MYC enhances anchorage independent growth by suppressing expression of $\alpha_3\beta_1$ integrins (Barr et al., 1998). Activation of MYC-ER in mouse keratinocytes led to the identification of 81 genes that were consistently down regulated. Thirty percent of those were genes involved in cellular adhesion, cell-cell adhesion and components of the extra cellular matrix (Frye et al., 2003).

A growing body of evidence suggests that MYC has a vital role in cancer cell metastasis, invasion and seeding (Wolfer and Ramaswamy, 2011). Depletion of endogenous MYC in human breast cancer cell line MDA-MB-231 inhibited the ability of these cells to form lung metastasis in an orthotopic mammary tumour model. Conversely, transplantation experiments revealed that overexpression of v-myc is sufficient to give metastatic potential to non-metastatic human lung tumour line A-549 (Rapp et al., 2009; Wolfer et al., 2010). MYC regulates epithelial-to-mesenchymal transition (EMT), an important process in invasion and motility of cancer cells, by promoting TGF β mediated activation of the transcription factor SNAIL (Cho et al., 2010; Smith et al., 2009). MYC, also promotes metastasis indirectly by promoting vasculogenesis and angiogenesis in a VEGF dependent manner (Baudino et al., 2002; Knies-Bamforth et al., 2004). Myc has also been shown to inhibit thrombospondin-1, an angiogenesis inhibitor (Tikhonenko et al., 1996). However, paradoxically MYC also inhibits migration and metastasis depending on context and cell type. Activation of Myc in mouse skin causes a delay in wound healing due to impaired keratinocytes motility and spreading (Frye et al., 2003). A recent report shows that MYC

suppresses metastasis by inhibiting $\alpha_v\beta_3$ integrin expression and thereby reducing its interaction with extra cellular matrix (ECM) components (Liu et al., 2012a).

1.3.3.4 Metabolism

MYC is critical in reprogramming of metabolic pathways, which act to support the growth of cancer cells and to meet energy demands (Dang, 2013). It is now widely accepted that cancer cell preferentially uses aerobic glycolysis to generate ATP even in the presence of oxygen, a phenomenon termed “The Warburg effect”. Aerobic glycolysis is an inefficient way to generate ATP, however the advantage it confers to cancer cells is unclear (Vander Heiden et al., 2009). MYC contributes to the “Warburg effect” by regulating different glycolytic enzymes. MYC up-regulates LDH-A (lactate dehydrogenase A), which converts pyruvate to lactate as part of the glycolytic pathway (Lewis et al., 1997; Shim et al., 1997). MYC also stimulates glycolysis by regulating other glycolytic regulators including, glucose transporter GLUT1, hexokinase2 (HK2), phosphofructokinase (PFK) and enolase 1(ENO1) (Miller et al., 2012). In addition to glucose, glutamine is another energy source that cells rely on. Glutamine is a major source of nitrogen for biosynthesis and also a carbon source for anabolic processes. Glutamine can enter the TCA cycle by a series of reactions called glutaminolysis. MYC enhances glutamine metabolism by enhancing the expression of glutamine transporters and key enzymes such as glutaminase (GLS) (Gao et al., 2009; Wise et al., 2008). Thus, MYC overexpression pushes the cells to a state where they are addicted to either glucose or glutamine depending on the metabolic programme switched on. In addition, MYC also regulates mitochondrial biogenesis at least in part by regulating transcriptional co-activator PGC-1 β (Dang, 2013). Further more, TFAM, a nuclear encoded transcription factor, which plays an important role in mitochondrial transcription and mitochondrial DNA replication, is a direct MYC target (Li et al., 2005). MYC induced mitochondrial biogenesis is important because mitochondria are not only the source of cellular ATP, but also an important source of several intermediates necessary for biosynthesis pathways. For example, acetyl-coA derived from citrate (generated in mitochondria) is essential for fatty acid biogenesis and many TCA cycle intermediates are important for de novo nucleotide biosynthesis (Wallace, 2012).

1.4 Targeting MYC

Targeting MYC is an attractive strategy, given the pivotal role it plays in tumour development and maintenance. One of the challenges in targeting MYC is its widespread

expression in all proliferating cells and inhibiting such a central protein might affect tissue homeostasis. However, Soucek and colleagues (2008) showed that the proliferation defects in the skin, intestinal crypts, and testis upon systemic MYC inhibition using a dominant negative mutant of Myc (“Omomyc”) are well tolerated and completely reversible (Soucek et al., 2004).

One of the different ways to target MYC is to inhibit Myc/Max interaction, thereby inhibiting its transcriptional function. In an attempt to disturb Myc/Max interaction Yin et al., (2003) identified small molecule inhibitors using a yeast two-hybrid screen (Yin et al., 2003). One compound, 10058-F4 was further studied and found successful in *in vitro* analysis (Huang et al., 2006), however it was unstable and rapidly degraded *in vivo* (Guo et al., 2009). Alternatively, MYC can be blocked by conditional expression of dominant negative mutant of Myc (“Omomyc”), which has the ability to bind and sequester all forms of Myc and deny access to Max, thereby blocking transcriptional function of Myc. Such an approach was reported to be effective against multiple tumour types (Annibali et al., 2014; Soucek et al., 2004; Soucek et al., 2008). There are numerous efforts currently being made to develop this as a therapeutic agent.

MYC is a tightly regulated protein with a short half-life. Increasing evidence suggests that MYC is stabilized in human malignancies. A point mutation leading to more stable protein is often found in human tumours (Bhatia et al., 1993). Hence, one strategy is to hamper protein stability or increase degradation by the ubiquitin proteasome system. Deubiquitinating enzymes (DUBs) USP37 and USP28, and CIP2A (cancerous inhibitor of protein phosphatase 2A) are all reported to positively regulate MYC protein stability (Khanna et al., 2009; Pan et al., 2014; Popov et al., 2007). These enzymes are often overexpressed in different types of cancer and their expression has been shown to be required for the proliferation of cancer cells. Thus, designing small molecule inhibitors that specifically target these proteins could provide a possible therapeutic avenue.

There are also efforts being made to target MYC expression itself. Bromodomain and extraterminal (BET) subfamily of human bromodomain proteins are associated with acetylated chromatin and facilitate transcriptional activation. Surprisingly, MYC was found as a transcriptional target for BET BRD4 proteins. A novel BRD4 inhibitor JQ1 repressed both MYC expression and its transcriptional program. Importantly, treatment with JQ1 inhibits growth of tumour cells both *in vitro* and in xenograft models (Delmore et al., 2011; Sahai et al., 2014; Shao et al., 2014).

Although the above mentioned strategies are attractive, safety and specificity are a concern. A novel approach to circumvent this is the synthetic lethal strategy. “Two genes are said to be ‘synthetic lethal’ if mutation of either gene alone is compatible with viability but simultaneous mutation of both genes causes death” (Kaelin, 2005). In other words, exploiting oncogene-mediated addiction could be a more tumour-specific way of targeting cancer cells (further discussed in section 1.4.3). Alternatively, one might exploit the intrinsic tumour suppressive function of oncogene MYC, which drives apoptosis. MYC can both drive and sensitize cells for apoptosis. In lymphomas driven by Myc, anti-apoptotic proteins such as Bcl2 block Myc induced apoptosis and blocking the anti-apoptotic Bcl2 pathway using a small molecule inhibitor ABT-737 has proven to be successful in this model (Mason et al., 2008).

1.4.1 Apoptosis

Evading apoptosis is one of the “hallmarks” of cancer (Hanahan and Weinberg, 2000) and its deregulation can lead to cancer (Cory and Adams, 2002). Uncontrolled growth of cancer cells is usually the net result of an increase in the rate of proliferation and reduced apoptosis. The link between impaired apoptosis and tumourigenesis came into the limelight when the Bcl2 (B cell lymphoma 2) gene that is translocated to an immunoglobulin locus was found to inhibit cell death rather than promoting proliferation (Vaux et al., 1988). Also, impaired apoptotic machinery is a barrier for effective chemotherapy. In particular, modulation of components of cell death pathways is a major factor in conferring drug resistance (Minn et al., 1995; Schmitt et al., 2000; Strasser et al., 1991).

1.4.1.1 The two major pathways of apoptosis

Apoptosis, which is a programmed form of cell death, can be executed by two different pathways: the mitochondrial (intrinsic) pathway; or the death receptor (extrinsic) pathway.

The important components of the mitochondrial pathway are Bcl2 family proteins. They act as a “life/death switch” integrating various intracellular and extracellular stress signals to determine whether the apoptotic pathway is activated or not. The proteins involved in the mitochondrial pathway of apoptosis can be categorized into three groups: anti-apoptotic or survival Bcl2 members; pro-apoptotic effector proteins; and pro-apoptotic BH3-only proteins. The anti and pro-apoptotic protein shares similar globular structure with four Bcl2 homology regions (BH1, BH2, BH3 and BH4). On the other hand, BH3

only proteins, only share a small BH3 domain (9-16 amino acid) with other family members.

The anti-apoptotic proteins include Bcl2 and its close relatives Bcl-x_L, Bcl-w, Mcl1 and A1. The carboxy terminal hydrophobic region targets these proteins to the cytoplasmic region of the outer mitochondrial membrane (Janiak et al., 1994). The function of these proteins is to maintain the integrity of the mitochondrial outer membrane. On the other hand, pro-apoptotic executioner proteins such as Bax and Bak are crucial for inducing mitochondrial outer membrane permeabilization (MOMP). In healthy cells, Bax is largely cytosolic, whereas Bak is an integral outer mitochondrial membrane protein and both are held inactive by anti-apoptotic Bcl2 proteins. In response to pro-apoptotic stimuli, Bax and Bak undergo structural changes; Bax is targeted to outer mitochondrial membrane, where both Bax and Bak forms homo oligomers and leading to MOMP (Fig. 1-2). This triggers the release of inter membrane space proteins cytochrome C, SMAC/DIABLO and Omi, which in turn leads to a sequence of events that activates cysteine proteases called Caspases, resulting in cell death (Fig. 1-2) (Czabotar et al., 2014; Tait and Green, 2013).

The BH3 only proteins include at least eight members including, Bim, Bad, Puma, and Noxa (Doerflinger et al., 2015). These proteins act as damage sensors and natural antagonists for survival proteins. BH3-only proteins bind and neutralize survival proteins, however they differ in their specificity for survival proteins. For example, Bim can bind to all the survival proteins, whereas Bad can bind only to Bcl2, Bcl-x_L and Bcl-w. Some BH3 only proteins (Bim, puma and tBid) have the ability to bind and activate Bax and Bak directly (Llambi et al., 2011).

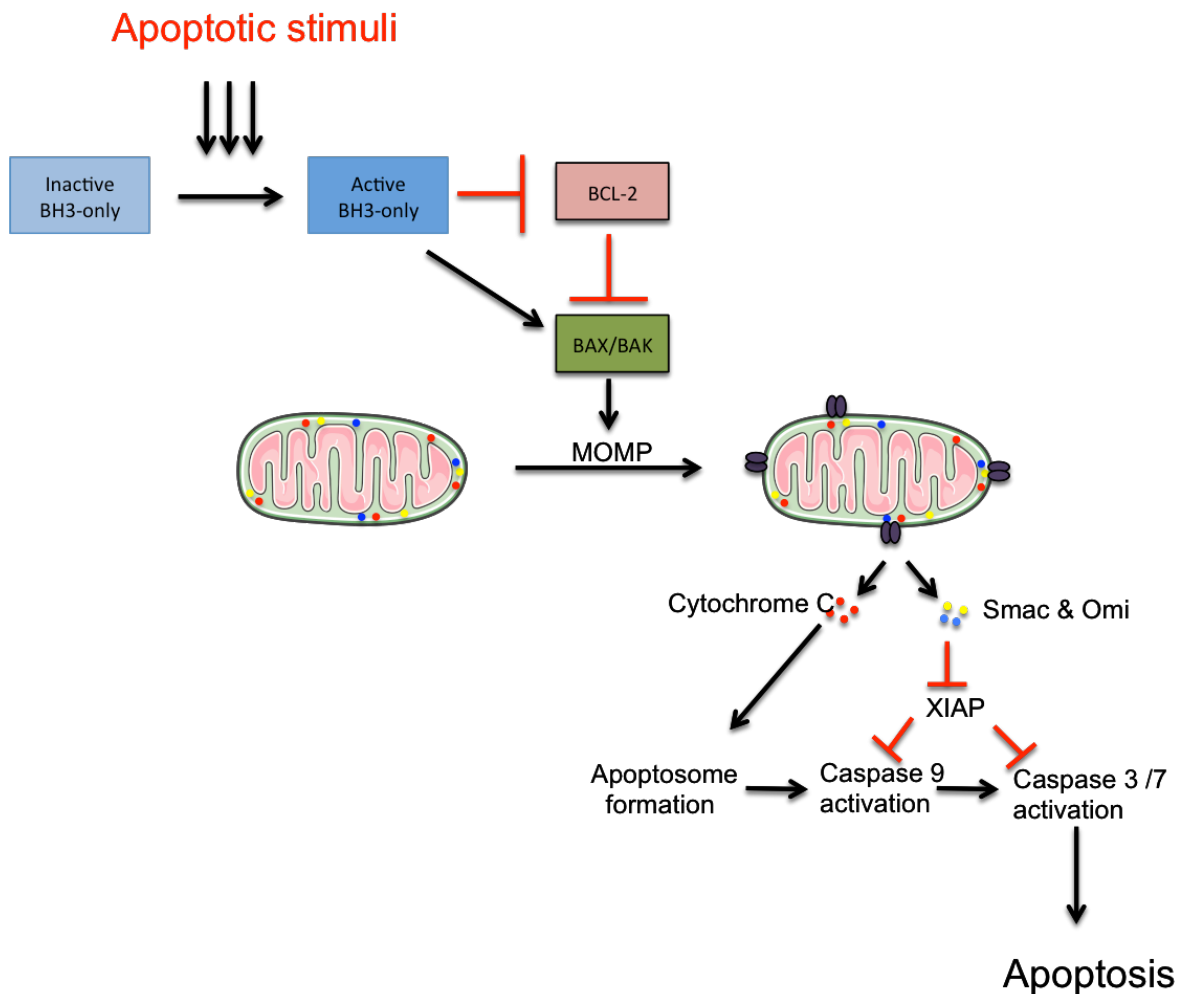


Figure 1-2- The mitochondrial regulation of caspase dependent cell death.

Activation of BH3 only proteins leads to Bax/Bak-mediated mitochondrial membrane permeabilization (MOMP). Following MOMP, soluble proteins are released from the mitochondrial intermembrane space into the cytoplasm. Cytochrome C binding results in an apoptosome formation by Apaf-1. Procaspase-9 is recruited to heptameric Apaf-1 complexes and this leads to its activation. Executioner caspases-3 and -7 are activated through caspase-9 mediated cleavage leading to cell death. Smac and Omi facilitates caspase activation by neutralizing the caspase inhibitor XIAP.

The extrinsic pathway is triggered when “death receptors” are ligated by their cognate ligands of the tumour necrosis factor (TNF) family. Binding of ligand results in receptor aggregation and recruitment of adaptor proteins (e.g. FADD). The receptor and adaptor proteins interact through its respective death domains. The adaptor proteins also contain additional protein-protein interaction modules, such as death interacting domains (DEDs). DEDs mediate the recruitment of initiator caspases (8/10) and cFLIP_L and the resulting complex is termed as death-inducing signalling complex (DISC). The processing of caspase 8/10 at the DISC leads to its activation, which further leads to activation of ‘effector caspases’ such as caspase 3/6/7 and finally cell death (Guicciardi and Gores, 2009).

The two pathways are largely independent. However, the extrinsic pathway can intersect the intrinsic pathway by cleavage dependent activation of BH3 only protein Bid by Caspase 8.

1.4.2 MYC induced apoptosis

Oncogenes that deregulate the cell cycle can often induce apoptosis or sensitize the cells to pro-apoptotic stimuli and MYC serves as a paradigm for this phenomenon (Harrington et al., 1994b). MYC-induced apoptosis was first reported in myeloid cells, and later in fibroblasts, upon growth factor deprivation (Askew et al., 1991; Evan et al., 1992). MYC expression can drive both proliferation and apoptosis at the same time and it is the level of MYC, which determines the output. As such the threshold of MYC required to induce apoptosis is set higher than the level required for ectopic proliferation (Murphy et al., 2008). Although it has been almost two decades since MYC-induced apoptosis was first reported, the mechanism for this process is controversial.

1.4.2.1 Role of p19Arf-p53 pathway in MYC-induced apoptosis

p19Arf (p14ARF in human) is a tumour suppressor protein encoded by alternative splicing of the Ink4a-Arf locus (Sherr, 1998). It interacts with and inhibits Mdm2, a negative regulator of p53, thereby stabilizing p53 protein (Kamijo et al., 1998). Overexpression of MYC induces accumulation of p19Arf and consequent stabilization of p53. Mouse embryonic fibroblasts (MEFs) that lack p19Arf were reported to be resistant to apoptosis induced by ectopic overexpression of MYC in low serum conditions (Zindy et al., 1998). However, it is to be noted that, in this particular study p19Arf null MEFs did undergo apoptosis initially and a resistant population emerged over time. Also, because the level of MYC protein expression declined over the course of these experiments, it is likely that a level of MYC that no longer breached the apoptosis threshold was inadvertently selected for.

The Arf-Mdm2- p53 pathway is frequently inactivated in Myc-induced lymphoma and several lines of evidence suggest that this particular pathway might constrain MYC induced lymphoma. For example, *Myc* expression under the control of immunoglobulin heavy chain enhancer (E μ) develop B cell lymphoma with a mean survival of approximately 6 months and *p19Arf* loss in these mice accelerated lymphomagenesis (Eischen et al., 1999; Schmitt et al., 1999). Heterozygous loss of Bmi-1, a polycomb transcriptional repressor, reduces lymphomagenesis in E μ -Myc mice by enhancing Myc-

induced apoptosis in B-cells. This was attributed to the ability of Bmi-1 to repress expression of p19Arf (Jacobs et al., 1999). In a similar study, Foxo4 transcription factor was shown to suppress Myc-induced lymphoma by directly activating p19Arf expression and thereby promoting apoptosis (Bouchard et al., 2007). Although, the above mentioned studies suggest that Arf-p53 pathway-mediated apoptosis is a barrier for Myc induced B cell lymphoma, it is to be noted that apoptosis is not the only outcome of tumour suppressor p53. To support this, an elegant study utilising acetylation defective mutant of p53 (K117R), which compromises the ability of p53 to induce Puma and Noxa and thereby apoptosis, shows that apoptotic activity is not absolutely required for p53 mediated tumour suppression (Li et al., 2012). Additionally, several independent groups have reported MYC-induced apoptosis in the absence of either p19Arf or p53, suggesting the existence of alternative pathways for MYC-induced death (Blyth et al., 2000; Eischen et al., 2001; Finch et al., 2006).

1.4.2.2 Role of Bcl2 family proteins in MYC-induced apoptosis

A growing body of evidence supports a central role for Bcl2 family proteins in mediating MYC-induced apoptosis. MYC-induced apoptosis involves the release of cytochrome C, a typical event in the mitochondrial apoptotic pathway (Juin et al., 1999). Two independent studies using different model systems suggest that MYC-induced apoptosis requires pro-apoptotic effector protein Bax (Dansen et al., 2006; Juin et al., 2002). Furthermore, overexpression of anti-apoptotic Bcl2 family proteins Bcl-2 and Bcl-x_L can block MYC-induced apoptosis (Bissonnette et al., 1992; Fanidi et al., 1992; Pelengaris et al., 2002). Conversely, suppression of some anti-apoptotic family proteins (e.g. Bcl2, Bcl-x_L) by MYC can sensitize cells to γ -irradiation-induced apoptosis and this regulation is bypassed during lymphomagenesis (Eischen et al., 2001; Maclean et al., 2003). There is also evidence that overexpression of survival proteins dramatically accelerates lymphoma development in E μ -Myc mice (Strasser et al., 1990; Swanson et al., 2004) whereas, pro-apoptotic proteins such as Bim and Puma inhibit Myc induced lymphomagenesis (Egle et al., 2004; Michalak et al., 2009).

Although there are many possible candidates within the Bcl2 family that could mediate MYC-induced apoptosis, the recent identification of BIM as a direct target of MYC suggests that this BH3 only protein may directly mediate MYC-induced apoptosis (Campone et al., 2011; Lee et al., 2013). Myc induces accumulation of Bim protein in Burkitt's Lymphoma, and MYC point mutants (T58A, P57S) commonly found in human

cancer that fail to induce Bim, also fail to induce apoptosis. Notably, such mutants are still capable of inducing p19Arf, p53 and its downstream target p21 (Hemann et al., 2005). This suggests that the increased oncogenicity of MYC mutants is because of an abrogated apoptotic signal from MYC to Bim, rather than a failure of sensing MYC-induced hyper proliferative signals by the p19Arf-p53 pathway. Importantly, Bim loss also relieves selective pressure to inactivate p19Arf-Mdm2-p53, which is otherwise common in wild type E μ -Myc lymphoma (Egle et al., 2004; Eischen et al., 1999; Hemann et al., 2005). These conflicting observations from different research groups suggest that a better understanding of molecular players that mediate MYC induced apoptosis is required.

1.4.3 Synthetic lethality

Despite being involved in a wide variety of tumours, an effective therapeutic strategy for targeting MYC remains elusive. Exploiting selective dependencies imposed by oncogenes is a novel strategy, especially in the case of MYC, which remains undruggable until now.

MYC was reported to be synthetic lethal with inhibition of aurora-B kinase. Aurora-B kinase is a Ser/Thr protein kinase, which regulates a number of aspects of mitosis including spindle structure to completion of cytokinesis. Inhibition of Aurora-B kinase in MYC overexpressing cells resulted in apoptosis and autophagy, as cells fail to stop DNA replication during arrested cytokinesis. In contrast, control cells that do not overexpress MYC, stop proliferating upon inhibition and revert back to a normal cycle upon restoration of Aurora-B kinase function (Yang et al., 2010). Another group unravelled a synthetic lethal interaction between MYC and mTORC1 target 4EBP1. 4EBP1, a translational repressor, binds and blocks translation initiation factor eIF4E, thus inhibiting cap dependent translation initiation, and mTORC1 dependent phosphorylation of 4EBP1 blocks this function. Expressing mutant form of 4EBP1 that cannot be phosphorylated by mTORC1, in B cells of E μ Myc mice delayed lymphomagenesis. This underlines the possibility of using mTOR inhibitors in MYC overexpressing cancer (Pourdehnad et al., 2013). Also, the cell cycle kinase CDK1, Chk1 an essential kinase involved in DNA damage and SUMO-activating enzyme 1/2 (SAE1/2), have been reported to be critical for survival of MYC overexpressing cells (Horiuchi et al., 2014).

Similarly, an effort made by the Murphy group to identify kinases which are specifically required for the survival of MYC overexpressing cells identified AMPK and a related kinase ARK5 (Nuak1) as potential targets. Depletion of Nuak1 in the context of MYC

overexpression was found to be detrimental to cancer cells. Depletion of Nuak1 in MYC overexpressing cells lead to a plethora of effects including defective electron transport chain leading to loss of ATP, increased protein synthesis because of the unrestrained mTOR pathway, reactive oxygen (ROS) production and loss of viability. Most importantly, an intervention study using an orthotopic liver tumour model revealed that targeting Nuak1 is indeed an effective approach *in vivo* (Liu et al., 2012b).

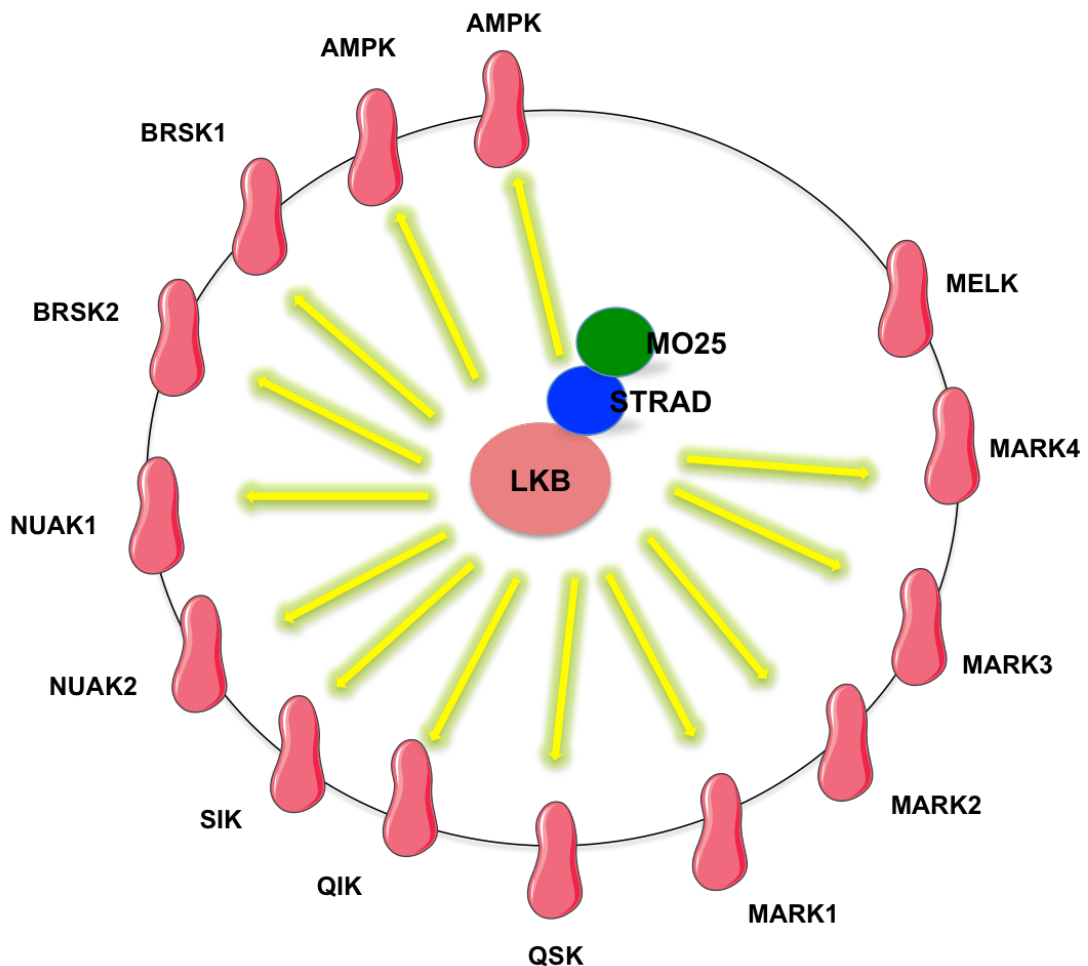


Figure 1-3 Activation of the AMPK-related kinases by LKB1.

LKB1 in complex with STRAD and MO25 phosphorylates and activates AMPK and 11 AMPK-related kinases including NUAK1, with the exception of MELK (modified from (Alessi et al., 2006))

1.5 ARK5/NUAK 1

AMPK, an energy sensor is activated in a variety of physiological or pathological stress conditions, when there is an increase in the AMP:ATP ratio. AMPK is a key regulator of cellular and whole-body energy homeostasis (Hardie, 2014). ARK5 otherwise known as NUAK1 was identified as a one of the AMPK- related kinases (AMPK-RK) (Suzuki et al., 2003b). Another member of NUAK family is NUAK2 (SNARK), which shares 55% sequence similarity with NUAK1 (Sun et al., 2013). There are 12 members in the AMPK-

related kinase family and all the members were identified based on their sequence homology with the kinase domain of AMPK. LKB1, a tumour suppressor kinase is a master kinase upstream of AMPK and other members including NUA1 (Fig. 1-3). LKB1 phosphorylates Nuak1 at Thr211 in the putative activation T loop and phosphorylation of this site is required for its kinase activity (Lizcano et al., 2004). In addition, other kinases such as Ca²⁺/Calmodulin-dependent kinase kinase β (CaMKK β) and Transforming growth factor- β activating kinase 1 (TAK1) have been reported as upstream kinases of AMPK and it is currently unclear if these kinases regulate all AMPK-RKs (Bright et al., 2009). However, there have been number of other upstream kinases identified for individual AMPK-RK subfamilies. For example, Suzuki et al., (Suzuki et al., 2006) showed that NDR2 could phosphorylate NUA1 at the same site as LKB1, during insulin-like growth factor-1 signalling (IGF-1). In addition, NUA1 can be phosphorylated on Ser600 in an AKT dependent manner (Suzuki et al., 2003a). However, it is not completely clear if this phosphorylation is absolutely required for all Nuak1 functions (Liu et al., 2012b).

1.5.1 Nuak1 functions

Nuak1 is required during development for closure of the ventral body wall as Nuak1 knockout mice displayed omphalocele, a defect in the abdominal wall closure (Hirano et al., 2006). Nuak1 is preferentially expressed in highly oxidative tissues like cerebrum, heart and muscle, and regulates glucose metabolism in skeletal muscle (Inazuka et al., 2012). NUA1 was reported to interact and phosphorylate p53 leading to p21 mediated cell cycle arrest (Hou et al., 2011). On the contrary, work done by Banerjee et al., (2014) and our own data suggests that NUA1 is positively required for cell proliferation. Both pharmacological inhibition and genetic depletion of NUA1 leads to reduced proliferation, likely by delaying cell cycle progression (Banerjee et al., 2014; Liu et al., 2012b). In addition, Nuak1 inhibits apoptosis triggered by certain stimuli such as glucose starvation and TRAIL by inhibiting activation of effector caspase-8 (Suzuki et al., 2003a).

Nuak1 has been closely associated with human malignancy. It is highly expressed in colon cancer, pancreatic ductal adenocarcinoma and hepatocellular carcinoma. NUA1 expression is also correlated with poor patient survival in hepatocellular carcinoma (Cui et al., 2013; Kusakai et al., 2004; Liu et al., 2012a). Gastric cancer patients with high NUA1 expression were found to have significantly shorter overall survival and recurrence-free survival (Ye et al., 2014). NUA1 has also been reported to mediate several tumour promoting processes. For example, NUA1 mediates tumour cell

migration and invasion in colon cancer, multiple myeloma and glioma cells *in vitro* (Kusakai et al., 2004; Lu et al., 2013; Suzuki et al., 2005). NUAK1 regulates tumour metastasis and invasion partly by regulating Matrix metalloproteases (MMP-2 and MMP9) (Chang et al., 2012). It has also been implicated in the regulation of cell adhesion. It does so by directly interacting and phosphorylating myosin phosphatase MYPT1, thereby suppressing dephosphorylation of the myosin light chain-2 (MLC2) (Zagorska et al., 2010). Recently, microRNA-211 was identified as a regulator of invasive gene clusters in melanoma cells and it was shown to inhibit loss of adhesion by directly down regulating Nuak1 expression (Bell et al., 2014).

1.5.1.1 Role of Nuak1 in mitochondrial respiration

As discussed earlier, NUAK1 depletion is lethal for MYC overexpressing cells. One of the reasons for cell death is the steady decline in ATP level (Liu et al., 2012b). The principle way by which a cell makes its energy currency (ATP) is through cellular respiration, which involves a series of metabolic reactions. Firstly, glucose in the cytosol is converted to pyruvate by glycolysis, next pyruvate enters the mitochondrion where it is oxidized by the citric acid cycle and finally ATP is generated by oxidative phosphorylation (Electron transport chain coupled with ATP synthesis). The mitochondria thus act as the powerhouse of the cells. They consist of an outer mitochondrial membrane, an intermembrane space, an inner mitochondrial membrane and the mitochondrial matrix. The electron transport system, which resides in the inner mitochondrial membrane, converts energy generated from TCA or citric acid cycle (NADH) into ATP. The inner mitochondrial membrane contains five complexes of integral membrane proteins that include NADH dehydrogenase (Complex I), succinate dehydrogenase (Complex II), cytochrome c reductase (Complex III), cytochrome c oxidase (complex IV) and ATP synthase (Complex V). The electrons generated during the TCA cycle in the mitochondrial matrix are pushed into the intermembrane space by complex I-IV, thereby creating a proton gradient. ATP synthase finally uses this force to phosphorylate ADP to generate ATP.

Proteomic analysis in a hepatocarcinoma cell line expressing inducible shRNA against NUAK1 revealed down regulation of multiple subunits of complex I, III and IV (Fig. 1-4). This explains the loss of ATP upon NUAK1 depletion and suggests that NUAK1 is required to maintain sufficient respiratory capacity.

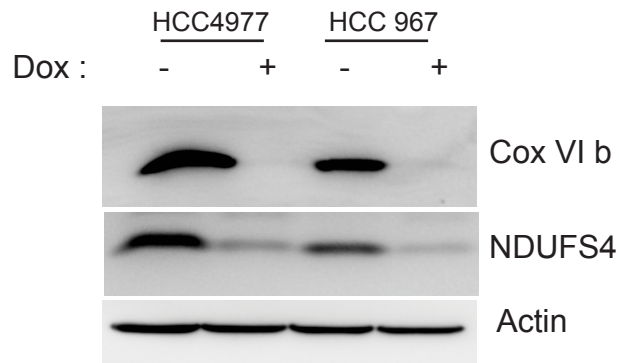


Figure 1-4 Decreased expression of ETC components upon NUAK1 depletion

Depletion of NUAK1 using two different doxycycline (dox) inducible shRNA (4977, 967) leads to decreased expression of electron transport chain components Cox VIb and NDUFS4.

1.5.2 Reactive oxygen species

Reactive oxygen species (ROS) are a variety of molecules and free radicals with one unpaired electron derived from molecular oxygen. Super oxide anion (O_2^-), the product of one-electron reduction of oxygen, is the precursor of most ROS generated in cells. It is important to maintain a minimum steady state level of ROS, as uncontrolled ROS can be deleterious. Free radical mediated chain reaction can be detrimental to cells as they indiscriminately target and thereby damage proteins, lipids, polysaccharides and DNA (Turrens, 2003).

The primary source of free radicals is the electron transport chain in most tissues. Electron transport chain complexes, while transferring electrons from the mitochondrial matrix and within themselves, can leak electrons to oxygen resulting in superoxide production. Initially, complex III was considered as the major source for ROS production, but later complex I and II were also shown to be involved in ROS production (Turrens, 2003)

Mitochondria have different defence mechanisms to tackle ROS. A family of metallo enzymes called superoxide dismutase (SOD) converts superoxide to hydrogen peroxide, which can be further reduced to water and oxygen by glutathione peroxidase. The mitochondrial matrix has a specific isoform of SOD called MnSOD, with manganese in the active site, and this detoxifies superoxide generated in the mitochondrial matrix and inner side of the inner mitochondrial membrane (Fridovich, 1995). The ROS generated in the intermembrane space is kept in check by three different mechanisms. Firstly, this compartment has another specific isoform of SOD called CuZnSOD with copper and zinc in the active site. Also, intermembrane protein cytochrome C can be reduced by the free

radicals and pumped back into the respiratory chain. Finally, superoxide can also be dismutated spontaneously which is facilitated by low pH of this compartment (Turrens, 2003).

1.6 Pancreatic cancer

1.6.1 Basic function of the pancreas

The pancreas is made up of glandular tissue and a system of ducts. It is both an exocrine and an endocrine gland. The exocrine part of pancreas mainly consists of acinar cells, which are responsible for the production of precursor digestive enzymes such as trypsinogen, chymotrypsinogen, pancreatic lipase and amylase. These enzymes are carried by pancreatic ducts that finally join the main bile duct and drain into the duodenum. The endocrine part is made of discrete cell clusters called Islet of Langerhans. Islets are made up of four different cell types, which differ in their secretion capacity. Alpha cells secrete glucagon, beta cells secrete insulin, delta cells secrete somatostatin and gamma cells secrete pancreatic polypeptide. Endocrine function of the pancreas is pivotal for maintaining blood glucose level. For example, when the blood glucose level is high, Insulin promotes absorption of glucose by skeletal muscle and fat tissues for storage. On the other hand, when the blood glucose level is low, glucagon released from the pancreas stimulates the liver to convert stored glycogen into glucose.

1.6.2 Pancreatic cancer: Statistics, causes and types

Pancreatic cancer is the 10th most common form of cancer in the UK and 12th most common cancer worldwide (Cancer Research UK). It has an estimated overall 5-year survival of less than 5%. This poor survival rate is mainly due to the fact that most pancreatic cases present themselves at late stage, when therapies are ineffective. Also, the anatomical location of the pancreas makes it very difficult to diagnose early stage disease. The risk factors for pancreatic cancer include tobacco smoking, long-standing diabetes mellitus, obesity, age and lifestyle. A small proportion (5-10%) of pancreatic cancer patients have been associated with hereditary factors, however the genetic basis of this familial aggregation is not very clear (Ryan et al., 2014).

Pancreatic cancer can be categorized into two main types, exocrine and endocrine tumours, based on their cell of origin. Pancreatic ductal adenocarcinoma (PDAC) is the most common form, accounting for more than 90% of all exocrine tumours. Other exocrine

tumours such as acinar cell carcinoma are very rare. Neuro endocrine tumours or islet cell tumours have an endocrine/hormone-producing cell of origin. These account for less than 5% of all pancreatic tumours. Endocrine tumours can be further subdivided based on the hormone they overproduce. For example, tumours that overproduce insulin are called insulinomas and those overproducing hormone glucagon are called glucagonomas (pancreaticcancer.org.uk).

1.6.2.1 Pancreatic ductal adenocarcinoma

Pancreatic ductal adenocarcinoma (PDAC) is the most common form of malignancy, accounting for more than 80% of all malignancies of the pancreas. Histological, genetic and clinical studies have identified three preneoplastic lesions as precursors for PDAC. They include pancreataic intraepithelial neoplasia (PanIN), intraductal papillary mucinous neoplasia (IPMN) and mucinous cystic neoplasia (MCN). Amongst these, PanINs are the best characterized at pathological and molecular level and acinar ductal metaplasia (ADM) structures have been proposed to be the precursors of PanIN lesions. PanINs can be classified into four grades, PanIN-1A, PanIN -1B, PanIN-2, and PanIN-3 based on increase in cellular and nuclear atypia and also the degree of desmoplasia (Hruban et al., 2004) (Fig. 1-5). Molecular studies have shown that PanIN stages strongly correlate with the accumulation of mutations in both oncogenes and tumour suppressor genes. The most common mutational event during PDAC development is the activating mutation of the oncogene *Kras*, via point mutation in codon 12, which renders the protein constitutively active. Indeed, 74% of human low grade PanINs harbour *Kras* mutations and this percentage increases up to 90% with the progression to invasive carcinoma (Shi et al., 2009). Another common mutation in PDAC is in the tumour suppressor *p16/CDKN2A*. This gene is found inactivated, deleted or epigenetically silenced in 30-70% of PanIN lesions and the percentage increases up to 95% in high grade tumours (Wilentz et al., 1998). Mutations in other tumour suppressor genes such as *Trp53* and *SMAD4*, a TGF- β pathway mediator, was found in 50-70% of the tumour and is often associated with progression from PanIN3 to invasive PDAC (Kern et al., 2002). Although mutations in the *MYC* gene are not commonly reported, screening for genetic alterations in PDAC using a comparative genomic hybridization technique, revealed high-copy number amplification of the 8q region, which includes the *MYC* gene (Schleger et al., 2000). Also, three different signalling pathways that are deregulated in PDAC namely, NFAT, Wnt/ β -catenin, and PI3K have been described to converge on *MYC* expression (Skoudy et al., 2011). Recent studies using genetically engineered mouse models (GEMMs) of pancreatic cancer showed

that either depletion of Myc expression by shRNA or genetic deletion of just one allele of *Myc* significantly delayed tumourigenesis (Saborowski et al., 2014; Walz et al., 2014). These studies suggest that MYC expression plays an important role in PDAC development however, the mechanism remains to be elucidated.

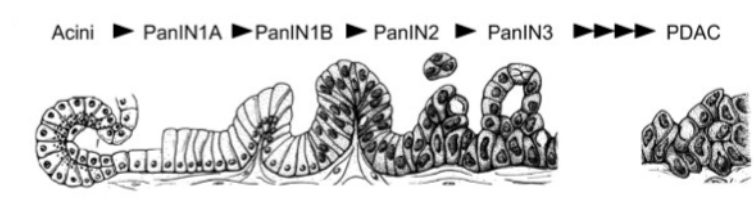


Figure 1-5- The progression model for PDAC

Normal duct epithelium progresses to infiltrating cancer through a series of histologically defined precursors (PanINs). Pancreatic intraepithelial neoplasia (PanIN) is graded based on the increase in cellular and nuclear atypia and also the degree of desmoplasia. [taken from (Guerra and Barbacid, 2013) with permission]

1.6.2.2 Current treatment of pancreatic cancer

Gemcitabine is used as the standard of care treatment for patients with advanced pancreatic cancer, although the response rate is very modest (24%) and the median overall survival is extended from 4.4 to 5.6 months (Burriss et al., 1997). Gemcitabine is a nucleoside analogue in which the hydrogen atom of 2' carbon deoxycytidine is replaced by a fluorine atom and incorporation of this analogue into nascent DNA blocks DNA replication. In recent years, a number of new therapeutic agents including cytotoxic agents oxaliplatin, capecitabine and inhibitors targeting specific molecular pathway like epidermal growth factor receptor (EGFR), vascular endothelial growth factor (VEGF), and platelet-derived growth factor (PDGF) receptors have been investigated with disappointing outcomes (Hidalgo, M., 2010). However, combination therapy has shown to be more effective than single agent therapy. For example, an early trial of patients with metastatic PDAC revealed that combination of gemcitabine with nab-paclitaxel, an albumin bound paclitaxel, prolonged median survival to 12.2 months. Also, the combination chemotherapy regime FOLFIRINOX (oxaliplatin, irinotecan, fluorouracil, and leucovorin) was more effective than gemcitabine alone, extending median survival of patients with metastatic disease from 6.8 to 11.1 months (Perez-Mancera et al., 2012).

1.7 Conditional transgenic techniques

Dr Mario R. Capecchi, Sir Martin J. Evans and Dr Oliver Smithies received the Nobel prize in Physiology or Medicine 2007 for their pioneering work in introducing gene modification in mice using embryonic stem cells. This technology is based on the homologous recombination between DNA sequences in the host genome and newly introduced DNA sequence. It is hard to overstate the importance of this technology in how we investigate gene function today. Specifically, an immeasurable amount of knowledge in relation to tumour biology has been obtained using gene targeting strategies. It exploits the targeted manipulation of mouse embryonic stem (ES) cells at desired loci by introducing loss or gain of function mutations, and cells bearing the appropriate insertion are then injected into a blastocyst of a foster mother to generate chimeras. Germ line transmission of the mutant allele is achieved by breeding the chimeras with the inbred mice. The genes required for carcinogenesis are often indispensable for embryonic or postnatal development. In such cases germ line mutation can result in embryonic, neonatal, or pre adult lethality hampering further studies. However, development of the Cre-loxP system, which allows gene modification in a spatially and temporally controlled manner, helps to circumvent this problem (Le and Sauer, 2001).

1.7.1 Site specific DNA recombination

Recombinase enzymes (e.g. Cre and Flp) are able to recognize and bind to short DNA sequences (sites), cleave the DNA backbone and re-ligate the DNA resulting in a deletion or inversion of a DNA sequence. Cre recombinase, a 38kDa enzyme from p1 bacteriophage, catalyzes DNA recombination between 34-bp sequences called LoxP sites. A LoxP site consists of an 8bp non-palindromic sequence at the centre flanked by 13bp inverted repeats. LoxP sites are not found endogenously in the mouse genome, hence genetic manipulation is restricted to the DNA sequence of interest. Generally, to delete a gene, two LoxP sites are introduced to flank either an entire gene or an essential region of the gene (called floxed allele). An animal expressing Cre recombinase can be bred with an animal bearing floxed allele to generate mice that have both. Cre recombinase recombine the DNA at the LoxP sites, leading to deletion of the intervening DNA sequences (Fig. 1-6) (Le and Sauer, 2001). Furthermore, spatial control of gene expression can be achieved using tissue specific promoters to drive Cre recombinase expression. For example, promoter of pancreatic and duodenal homeobox 1 gene (Pdx1), which encodes a transcriptional activator that plays an important role in the early development of the

pancreas, can be used to specifically express Cre recombinase in the pancreas (Hingorani et al., 2003; Offield et al., 1996). Also, temporal control of Cre recombinase can be achieved by using an inducible Cre recombinase (e.g. Cre-ER^{T2}). The Cre-ER^{T2} transgene encodes for a Cre recombinase-oestrogen receptor fusion protein, Cre recombinase is fused to the mutated ligand binding domain of the human oestrogen receptor (ER), which can be activated by synthetic ligands called tamoxifen and 4-hydroxytamoxifen but is unresponsive to endogenous oestrogen (estradiol). Thus alleles are activated only after administration of tamoxifen (Feil et al., 1996).

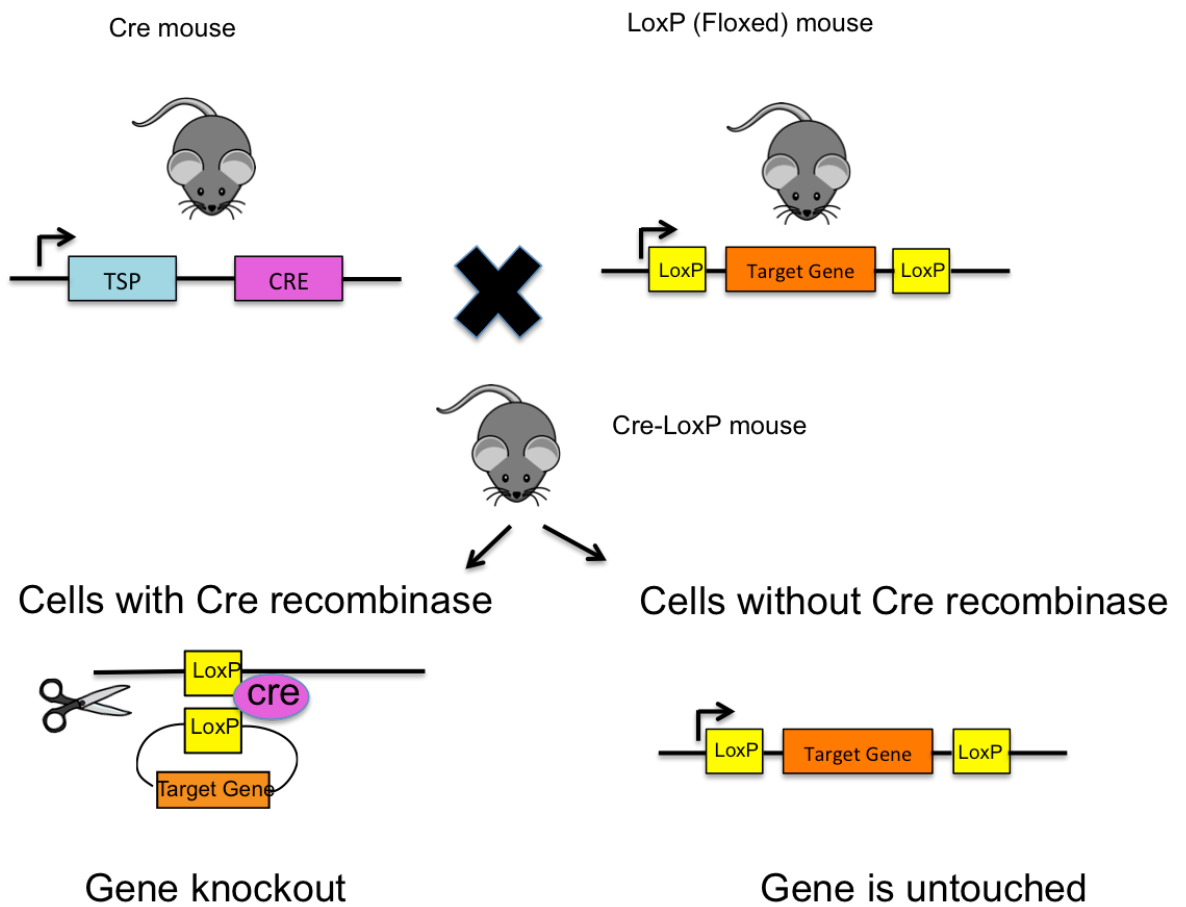


Figure 1-6- Outline of Cre-LoxP system for generating a gene knockout

Cre and LoxP (Floxed) strains are developed separately and bred to produce Cre-LoxP strain. In the LoxP strain, an entire gene or essential exons of the gene is flanked by 34-base LoxP sequence oriented in the same direction. In the cells that express Cre recombinase (using tissue specific promoter-TSP), Cre recombinase mediates a deletion of the floxed segment.

A similar approach is now widely used for systemic and tissue specific induction of different proteins. For example, Myc-ER^{T2} is frequently used *in vitro* and *in vivo* to study MYC function. Here, MYC is held inactive in the cytoplasm by ER^{T2} moiety and MYC activation is achieved by administration of tamoxifen. (Murphy et al., 2008).

In addition to gene deletion, the Cre-LoxP system can be used for gene activation and overexpression. Here, a synthetic STOP codon flanked by LoxP sites, is introduced in front of the coding region of an oncogenic mutant protein in the endogenous site for gene activation or in the exogenous site for overexpression of a protein (Fig. 1-6) (Hingorani et al., 2003; Murphy et al., 2008). Thus the protein of interest is expressed only after Cre mediated excision of the stop cassette.

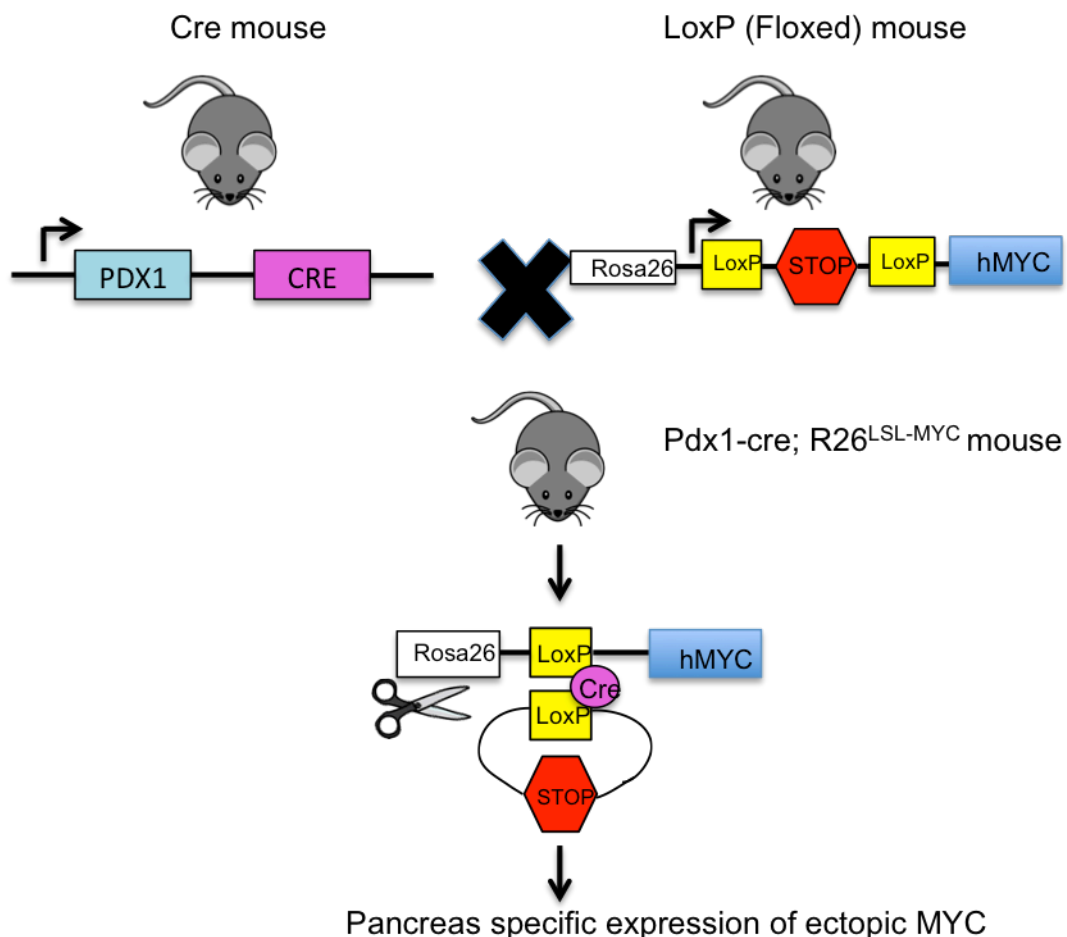


Figure 1-7- Outline of Cre-LoxP system for generating overexpression or Knockin strains.

Cre mediated excision of stop cassette and expression of ectopic MYC in the pancreas. A human MYC cDNA is expressed under the control of constitutive Rosa26 locus. A triple polyadenylation signal sequence flanked by LoxP sites is inserted upstream of MYC coding sequence (Lox-stop-Lox cassette). Pancreas specific expression of Cre recombinase (using Pdx1 promoter) leads to excision of the stop cassette and expression of MYC.

1.7.2 Modelling pancreatic cancer

Recent advances in understanding the molecular mechanisms of cancer initiation and progression have been possible because of mouse model systems and pancreatic cancer is not an exception. Currently, there are GEMMs and Xenograft models available to study pancreatic cancer that are valuable tools to understand the disease, evaluate therapeutic strategies experimentally, understand the mechanisms of resistance to therapy and finally, to improve treatment regimes.

1.7.2.1 Conditional *Kras* mouse models

Activating mutations of *KRAS* are universal events in human pancreatic cancer, hence most pancreatic GEMMs employ the expression of oncogenic *Kras*. In 2001, Jackson et al., made the first conditional *Kras* model, where a point mutation of G to A in codon 12 is introduced in the exon 1 of endogenous *Kras*. This mutation, commonly found in human PDAC, results in substitution of the amino acid glycine to aspartic acid, compromising its GTPase activity leading to constitutive Ras signalling. Conditional expression of the allele was achieved by inserting a stop codon flanked by LoxP sites upstream of the mutated exon [Lox-STOP-Lox (LSL)], thus mutant protein (*Kras*^{G12D}) is not expressed until activated by Cre recombinase (Jackson et al., 2001). Promoters of genes encoding Pdx1 and P48/pft1a, important transcription factors for pancreatic development, widely used to achieve pancreas-specific expression of Cre recombinase (Offield et al., 1996). *Pdx1-Cre; LSL-Kras*^{G12D} and *P48-Cre; LSL Kras*^{G12D} mice developed various grades of precursor lesions called PanINs and only a subset of older mice developed invasive ductal adenocarcinoma. However, PanINs developed in these mice resembled human PanINs in terms of histology and expression of markers such as mucins and cytokeratin-19 (Hingorani et al., 2003).

Human PanINs are believed to progress to invasive PDAC by acquiring additional genetic mutations. To model this several GEMMs incorporating additional mutations along with *Kras*^{G12D} have been developed. For example, oncogenic *Kras* in combination with monoallelic or biallelic loss of tumour suppressors *Cdkn2a*, which encodes p16 and p19Arf, and *Trp53* led to aggressive and metastatic PDAC (Aguirre et al., 2003; Bardeesy et al., 2006a; Hingorani et al., 2005; Morton et al., 2010). Also, compound mice with pancreas-specific ablation of type II TGF- β receptor (*Tgfr2*) together with oncogenic *Kras* developed invasive and metastatic pancreatic ductal adenocarcinoma. Loss of TGF- β -Smad signalling pathway is associated with uncontrolled and unregulated growth of epithelial cells. Smad4, a central signalling mediator downstream of TGF- β and type II TGF- β receptor is frequently mutated or deleted in human PDAC (Ijichi et al., 2006).

1.7.2.2 Other mouse models for pancreatic cancer

There are also GEMMs available for less common precursor lesions like intraductal papillary mucinous neoplasms (IPMNs) and mucinous cystic neoplasms (MCNs). For example, loss of Smad4 together with activation of mutant *Kras* in the pancreas leads to the development of IPMNs and MCNs (Bardeesy et al., 2006b; Izeradjene et al., 2007).

Similarly, concomitant expression of Tgf- α and Kras^{G12D} in pancreatic progenitor cells (using Pdx1-Cre) results in cystic papillary neoplasms, which resemble IPMNs (Siveke et al., 2007).

Although there are various mouse models available, poor 5-year survival rate and poor drug response of pancreatic cancer patients demands further understanding of the disease initiation, maintenance and progression.

1.8 Aim and Objectives

MYC is one of the most frequently deregulated oncogenes in a wide variety of human cancers. As discussed, there are many ways to target MYC directly and indirectly. However, an effective MYC centric therapy is still in its infancy. The central hypothesis of this thesis is that MYC in spite of its profound tumour promoting effects leaves the cells in a vulnerable state and such oncogene-induced vulnerabilities can be exploited to specifically target MYC overexpressing cells. The two main objectives of this thesis are to firstly understand the mechanism of MYC-induced apoptosis and secondly to exploit the MYC-induced dependence of AMPK related kinase Ark5 (Nuak1) in GEMM of pancreatic ductal adenocarcinoma.

To address the first objective, I used a previously described Rosa26MycER^{T2} mouse model (Murphy et al., 2008), where MycER^{T2} is expressed in all tissues. I will investigate the potential contribution of the pro-apoptotic BH3-only proteins Bim and Puma, and the tumour suppressor p19Arf in MYC-induced apoptosis and MYC-induced sensitization to pro-apoptotic stimuli *in vivo* and *in vitro*. Findings from these investigations are outlined in chapter 3.

The rationale for the second objective arises from the findings in Liu et al., (2012) study. Here, it was shown that MYC overexpressing cells selectively require NUA1 for their survival. To test this hypothesis in Pancreatic cancer as NUA1 was found to be overexpressed in human pancreatic cancer, I first characterize a new model for PDAC, which involves overexpression of MYC (*R26^{LSL-MYC}*) and oncogenic Kras^{G12D} (*LSL-Kras^{G12D}*). I will investigate the synergistic effect of MYC and Kras^{G12D} in pancreatic tumorigenesis, which is outlined in Chapter 4. Further, I will be using this model to evaluate the requirement of Nuak1 in PDAC. The effect of homozygous loss of *Nuak1*

(*Nuak1^{FL/FL}*) in MYC/ Kras^{G12D} induced pancreatic tumourigenesis will be tested. This study is described in Chapter 5.

2 Materials and Methods

2.1 Animal work

A number of transgenic mice were obtained from different laboratories (outlined in Table 2-1). All mice were housed on a 12hr light cycle, and fed and watered ad libitum. All the mouse procedures were performed in accordance with protocol numbers 55.2-2531.01-30/11 (University of Wuerzburg, Germany) and Home Office licence numbers 60/4183 and 70/7950 (CRUK BICR, UK).

Table 2-1- Outline of genetic models used in this study

Transgene and source	Tissue expression
<i>Pdx1-Cre</i> (Hingorani et al., 2003)	Pancreas; Constitutive
<i>LSL-KRAS^{G12D}</i> (Hingorani et al., 2003)	Mutated <i>Kras</i> Allele (G12D) bearing a LoxP flanking a Stop cassette in the 5'UTR replacing the endogenous allele.
<i>Rosa26^{LSL-MYC/LSL-MYC}</i> (Neidler and Murphy, unpublished)	Stop codon flanked by LoxP sites is inserted upstream of MYC transgene under the control of constitutive Rosa26 locus.
<i>Nuak1^{FL/FL}</i> (Inazuka et al., 2012)	Exon 3 of endogenous <i>Nuak1</i> is flanked by LoxP sequences.
Rosa26-MycER ^{T2} (Murphy et al., 2008)	Expresses tamoxifen inducible fusion protein (MycER ^{T2}) under the control of constitutive Rosa26 locus in all mouse tissues.
<i>Bcl2l1^{tm1.1Ast}</i> Jackson laboratory (Bouillet et al., 1999)	BH3 mutant of endogenous <i>Bim</i> is deleted and mutant protein expressed is highly unstable and behaves as a null mutation.
<i>Cdkn2a^{tm1(GFP)Cjs}</i> NCI mouse repository. (Zindy et al., 2003)	Exon1 β of endogenous <i>Cdkn2a</i> locus is replaced by GFP coding sequence abrogating p19Arf expression.
<i>Bbc3^{tm1Ast}</i> Jackson laboratory distributed by Charles River. (Villunger et al., 2003)	Exon1-3 of endogenous <i>Puma</i> is deleted.

2.1.1 Colony Maintenance

Some animals were used for breeding to generate experimental mice and to maintain the colony. This was carried out by setting up cages consisting of one male and one/two females. Pups were weaned at approximately 4 weeks of age and ear notched for identification and for DNA genotyping. All transgenic mice were maintained in positively pressured individually ventilated cages (IVCs) during mating and while they are kept as

stock animals. These mice were handled in a laminar flow changing station. After the mice were genotyped, cohort mice were identified and these mice were transferred to non-barrier cages. All mice were given irradiated standard diet (CRM (E) expanded diet from Special Diet Services; Cat: 801730) and sterilized water ad libitum.

2.1.2 Genotyping

Mice were ear notched for identification at 3-4 weeks of age and a piece of the ear tissue was sent to Transnetyx (Cordova, TN, USA). Transnetyx use a combination of quantitative PCR and DNA hybridization to determine the allelic presence in ear tissue.

2.1.3 Experimental cohorts

2.1.3.1 Spontaneous genetically-engineered mouse models (GEMM) of pancreatic tumourigenesis

Pdx1-Cre, LSL-Kras^{G12D} mice were first described by Hingorani et al (Hingorani et al., 2003) and were bred in house. Pdx1 is expressed from embryonic day 8.5-9.0. Cells expressing Pdx1 give rise to pancreatic buds and eventually cells of all lineages within the pancreas, namely, ductal, acinar and endocrine cells. Cre recombinase recognizes the 34 base pair LoxP sites, and excises the intervening region flanked by these sites, allowing expression or deletion of the transgenes described below in the pancreas.

By breeding the appropriate genotypes together *Pdx1-Cre; R26^{LSL-MYC/+}; LSL-Kras^{G12D/+}* (KMC), *Pdx1-Cre; R26^{LSL-MYC/+}* (MC), *Pdx1-Cre; R26^{LSL-MYC/LSL-MYC}*, *Pdx1-Cre; R26^{LSL-MYC/+}; Nuak1^{FL/FL}* cohorts were generated.

2.1.3.2 End points

Mice were monitored at least 3 times weekly and culled when any of the following symptoms were observed: Weight loss of >10%, abdominal distension, hunching or reduced mobility, subdued behaviour, paling of feet due to mild anaemia. Specific signs of pancreatic tumour development included abdominal distension, weight loss and reduced mobility. Pancreatic malignancy was confirmed by abdominal palpation.

Pdx1-cre; R26^{LSL-MYC/+}; LSL-KRAS^{G12D/+} mice rarely develop extrapancreatic health problems including, colonic intussusception, lymphoma and skin papillomagenesis. Animals were closely monitored for the signs of these illnesses and culled immediately when they become unwell. Mice were sacrificed if a skin papilloma exceeded 1.5cm in

size and papillomas greater than 1cm in size were measured three times weekly. The description of ill health is outlined in UK Home Office project license 4183 which was adhered to at all times.

All mice were sacrificed using schedule 1 methods. Mice were euthanized by exposure to carbon-dioxide gas in rising concentration followed by cervical dislocation.

2.1.3.3 Acute MYC activation model

The Rosa26^{MER/MER} transgenic mouse was described in Murphy et al., (2008). It expresses tamoxifen inducible fusion protein (MycER^{T2}), comprises of full length human c-Myc cDNA fused to modified ligand binding domain of human oestrogen receptor (ER^{T2}), downstream of constitutive and ubiquitously expressed Rosa26 locus (Murphy et al., 2008). This was crossed on to Bim null, p19Arf null or Puma null mice (see Table 2-1) to study the role of these proteins in MYC-induced apoptosis.

2.1.4 Administration of Tamoxifen

Activation of Rosa26 driven MYC is achieved by systemic injection of tamoxifen, which binds to the ER^{T2} moiety leading to the translocation of MYC from cytosol to nucleus. Tamoxifen (Sigma) was dissolved at a concentration of 10mg/ml in peanut oil (Sigma). A 50mg/kg dose of tamoxifen was administered to each experimental mouse via intraperitoneal (IP) injection daily, for three consecutive days.

2.1.5 Administration of Doxorubicin

Doxorubicin (LC laboratories) was dissolved at a concentration of 1mg/ml in 0.9% sodium chloride. A 10mg/kg dose of Doxorubicin was administered via intraperitoneal (IP) injection.

2.1.6 Tissue sample preparation

Tissues were isolated immediately after sacrificing the animals in order to prevent degradation of RNA, proteins and phospho-proteins. After euthanasia, mice were prepared for post-mortem by spraying 70% ethanol over the abdomen and the abdominal cavity was opened by first cutting through the skin and then through the smooth muscle wall. For the pancreatic tumour model, mice were examined carefully for the presence of tumour and metastasis (if any). Organs were dissected intact, with tumours being cut into pieces and fixed in zinc formalin.

For the acute MYC activation model, liver and pancreas were dissected intact and fixed separately. The intestines were removed by first cutting the attachment of the stomach to the oesophagus and then the intestine was removed by carefully removing all the attached connective tissue. The small intestine was separated by removing the stomach and cutting at the ileal-caecal junction. The colon was removed with the caecum and the caecum was then removed. The contents of the intestines were removed by flushing with 1X PBS.

All the tissues were fixed in Zinc-buffered formalin at 4°C overnight.

2.1.6.1 Processing the tissues

After fixation, all tissues were removed from the fixative and dehydrated with increasing gradient of alcohol (30%, 50%, 70%, 95%, 100%) for 30mins each. These tissues were then sent to BICR histology team for processing using an automated processor (Thermo scientific Excelsior ES). Finally tissues were embedded in a paraffin wax by hand and left to harden.

2.1.6.2 Sectioning of fixed tissues

Paraffin embedded tissues were then cut to 4µm sections using a microtome and were then placed on poly-L-Lysine (PLL) coated slides, and then baked at 58°C for 24hrs. The sections were then prepared either for Haematoxylin and Eosin (H&E) staining or immunohistochemistry (IHC) (see section 2.2 & 2.3). The sectioning and some of the stainings were done with the help of BICR histology team.

2.2 Cell specific staining

2.2.1 Preparation of sections for IHC or cell specific staining

Paraffin embedded tissue sections were first de-waxed by placing in a bath of xylene for 5mins and then transferred to two other xylene baths for 5mins each. The sections were now devoid of all paraffin wax and could be rehydrated down a gradient of alcohols. The sections were rehydrated in baths of descending gradients of ethanol (100%, 100%, 95%, 95%, 70%, 70%) for 2mins each and finally placed in deionised water (dH₂O) in preparation for immunohistochemistry (IHC) or cell specific staining.

2.2.2 Hematoxylin & Eosin staining

In order to visualize the morphological changes, tissue sections were stained with haematoxylin to mark nuclei and eosin to stain the cytoplasm of cells. Tissue sections were de-waxed and rehydrated as previously described in section 2.2.1 and were then stained by immersing the sections in a bath of Gli1Haematoxylin (Sigma) for 13mins, then washed in running tap water for 5mins followed by 20 dips in differentiation solution (Sigma). Sections were washed in running tap water for 30secs followed by 20 dips in Scotts tap water substitute (MgSO_4 + sodium bicarbonate). Slides were again washed in tap water for 30secs and then stained with an aqueous solution of 1% Eosin for 5mins followed by 2 washes in tap water. Tissues were then dehydrated, cleared and mounted as described in section 2.3.9.

2.2.3 Alcian blue/PAS staining

This is a combined method utilising the properties of both PAS (Periodic acid-Schiff) and Alcian blue staining to detect proteoglycans such as mucins. The rationale of the technique is that by first staining all the acidic mucins with Alcian blue, those remaining acidic mucins which are also PAS positive will be chemically blocked and will not react further during the technique. Neutral mucins that are solely PAS positive will subsequently be demonstrated in a contrasting manner. Where mixtures occur, the resultant colour will depend upon the dominant moiety. Tissue sections were de-waxed and rehydrated as previously described (section 2.2.1). The slides were then placed in a Coplin jar containing alcian blue solution for 30mins (1% Alcian blue in 3% acetic acid). The slides were rinsed completely in tap water and placed in a Coplin jar containing periodic acid for 10mins. After washing with tap water, slides were placed in a container with Schiffs reagent for 20mins. The slides were then washed thoroughly with water and dehydrated by placing in ethanol series (2x70%, 2x95%, 2x100%) for 2mins each followed by 2x Xylene for 5mins. Slides were then removed from xylene, mounted in DPX mounting medium (VWR), coverslipped and left to air dry in a fume hood. Acidic mucins were stained in blue, neutral mucins in magenta and the mixture of both mucins in blue/purple.

2.2.4 Picro-sirius red staining

Picro-Sirius red staining was used to visualize collagen I and III fibres. Tissue sections were de-waxed and rehydrated as previously described (section 2.2.1). The slides were then immersed in Picro-Sirius red solution for 2hrs and then rinsed in de-ionised water. The slides were dehydrated by placing in ethanol series (2x70%, 2x95%, 2x100%) for 2

mins each followed by 2x Xylene for 5 mins. Slides were then removed from Xylene, mounted in a DPX mounting medium, coverslipped and left to air dry in a fume hood.

2.3 Immunohistochemistry

IHC was used to visualize the distribution and localization of specific cellular proteins, general outline of the protocol is detailed in this section and specific conditions for individual protocols is outlined in table 2-2.

2.3.1 Preparation of sections for IHC

Formalin fixed, paraffin embedded tissues were sectioned onto PLL coated slides as described in section 2.1.6.2. They were then de-waxed and dehydrated as discussed in section 2.2.1.

2.3.2 Antigen retrieval

Fixation generates methylene bridges that crosslink proteins in tissue samples; these bridges can mask antigen presentation and prevent antibody binding. Thus formalin fixed, paraffin embedded tissues generally require a treatment to unmask the antibody epitopes. This typically involves heat mediated antigen retrieval carried out by boiling the tissue sections in citrate buffer (pH 6) or in antigen unmasking solution (Dako), in a microwave, pressure cooker, or a 100°C water bath for around 30mins and then slides were left to cool at room temperature for 30mins.

2.3.3 Blocking endogenous peroxidase

As the antibody visualization involves the enzymatic reaction of 3,3'-diaminobenzidine (DAB) catalyzed by horseradish peroxidase (HRP), quenching or masking endogenous form of peroxidase prevents false positive and high background detection. This can be achieved by incubating the slides in 3% hydrogen peroxide (in dH₂O) for 15mins, which irreversibly block endogenous peroxidase. After peroxidase blocking the slides were washed in deionized water.

2.3.4 Blocking of non-specific antibody binding

Although antibodies show high selective avidity for specific epitopes, antibodies may partially or weakly bind to sites on nonspecific proteins (called reactive sites), causing high background staining. To reduce the background staining, the samples were incubated with buffer that blocks the reactive sites to which primary or secondary antibodies may

otherwise bind. Commonly used blocking buffers are BSA and Normal goat serum. Tissue sections on PLL coated slides were first outlined using a hydrophobic barrier pen, Immedge pen (vector labs) before incubating with serum. Serum was diluted in wash buffer (PBS) in a concentration that adequately blocks non-specific binding. Serum block was removed and then tissue sections were incubated with primary antibody.

2.3.5 Primary antibody incubation

After blocking, tissue sections were incubated with a primary antibody at an optimized concentration. Antibodies were generally incubated overnight in a humidified chamber at 4°C, or at room temperature for 1hr. After incubation the slides were washed three times in PBS or TBST to remove residual unbound primary antibodies. Antibodies were diluted in the antibody diluent from Dako (see Table 2-2)

2.3.6 Secondary antibody incubation

Tissue sections were then incubated with the secondary antibody conjugated with HRP, diluted typically 1 in 200 in normal serum. Secondary antibodies are raised against antibodies from the animal in which the primary antibody was raised, so they bind to any primary antibodies that bind to the antigen of interest. Tissue section slides were incubated with secondary antibody for 30mins-1hr in a humidified chamber, the slides were then washed in wash buffer three times. Sometimes the secondary antibodies were biotinylated, therefore an additional signal amplification step was required in which HRP binds to the secondary antibody.

2.3.7 Signal amplification

When biotinylated secondary antibodies were used, a signal amplification step was required. This involved the formation of a complex between the biotin bound to the secondary antibody and a protein called avidin, which was bound to HRP. The Vectastain Avidin-Biotin Complex (ABC) kit (Vector labs) was used. The ABC reagent was prepared in 0.3M NaCl 30mins before use and left at room temperature, tissue sections were incubated with ABC reagent for 30mins and washed three times in wash buffer afterwards.

2.3.8 Visualizing the signal

The IHC antigens were visualized by chromogenic means. Chromogenic detection is based on the activities of the enzyme HRP, which forms coloured, insoluble products upon the addition of its substrate DAB (Sigma). Tissue sections were incubated with DAB reagent

until adequate staining is achieved by looking under the light microscope. Excess DAB was removed and washed in deionised water.

Table 2-2- IHC conditions

Primary antibody	Antigen Retrieval	Primary antibody dilution	Secondary antibody
Pan-Cytokeratin Thermo scientific MS-343	Sodium citrate (pH6); water bath method	1:100 in primary antibody diluent (Dako) @ RT for 35mins	EnVision; Mouse-HRP conjugated (Dako) @ RT for 30mins
Synaptophysin Abcam-ab80409	Sodium citrate (pH6); water bath method	1:75 in primary antibody diluent (Dako) @ RT for 35mins	EnVision; Mouse-HRP conjugated (Dako) @ RT for 30mins
pS6 (Ser240/244) Cell signalling- 5364	Sodium citrate (pH6); water bath method (30mins)	1:400 in 5% NGS @ 4°C over-night (O/N)	Vectastain, ABC kit- Rabbit-Biotinylated, 1:200 in 5% NGS @ RT for 1hr
p-P44/42 MAPK (Thr202/Tyr204) (p-ERK) Cell signalling- 4370	Sodium citrate (pH6); Microwave method (10mins)	1:500 in 5% NGS @ 4°C, O/N	Vectastain, ABC kit- Rabbit-Biotinylated, 1:200 in 5% NGS @ RT for 1hr
Ki67 Fisher scientific- RM-9106-SO	Sodium citrate (pH6); Microwave method (10mins)	1:200 in 1% BSA @ 4°C, O/N	Vectastain, ABC kit- Rabbit-Biotinylated, 1:200 in 1% BSA @ RT for 1hr

Key : HRP –Horse Radish Peroxidase, RT-Room temperature, O/N-over-night, NGS-Normal Goat serum, BSA-Bovine serum albumin

2.3.9 Counterstaining and slide mounting

The slides were dipped in hematoxylin (5 dips) to stain nuclei and washed in tap water for 5mins followed by 20 dips in differentiation solution. The slides were again washed in tap water for 30secs followed by 20 dips in Scotts tap water substitute. After washing in tap water for 30secs, slides were dehydrated through a gradient of alcohols (2 x 2mins 70% ethanol, 2 x 2mins 95% ethanol, 2 x 2mins 100% ethanol) and then cleared in 2 x 5mins xylene. Slides were then removed from xylene, mounted in DPX mounting medium (VWR), a coverslip was put on top and slides were left to air dry in a fume hood.

2.3.10 TUNEL staining

TUNEL staining was performed on paraffin-embedded sections (4 μ m thick) using the ApopTag peroxidase labeling kit (Millipore; S7100). It utilizes DNA fragmentation, a hallmark event of apoptosis, to detect apoptotic cells. Here, chemically labeled nucleotides (digoxigenin conjugated) were added to free 3'OH DNA termini by terminal deoxynucleotidyl transferase (TdT). TdT catalyzes template independent addition of nucleotide triphosphate to the 3'OH ends of double stranded or single stranded DNA. Incorporated nucleotide forms oligomers containing digoxigenin, which was then detected using an antibody against digoxigenin conjugated to HRP. Signal was detected using DAB as a substrate as described in section 2.3.8. Protocol was carried out according to the manufacturer's instructions and an additional blocking step (1% BSA for 1hr at room temperature) was incorporated prior to the addition of peroxidase-conjugated antidigoxigenin. Tissues were counterstained as described in section 2.3.9.

For quantification, the number of TUNEL-positive nuclei (pyknotic or intact) and the total number of cells per field were counted manually. Five representative fields per tissue sample from each mouse were scored, yielding a percent apoptosis value. Graphs represent the mean \pm SEM percent apoptosis across number ("n") of mice as indicated in the figure legends.

2.3.11 Epithelial cell extraction from the small intestine

The modified Weiser technique was used to isolate epithelial cells from the small intestine. The small intestine was dissected as described in section 2.1.7. Small intestine was flushed with ice cold PBS to empty the contents, split longitudinally and placed in a 30ml Weiser chelating solution (5.56mM Disodium hydrogen orthophosphate, 8mM Potassium dihydrogen orthophosphate, 96mM Sodium chloride, 1.5mM Potassium chloride, 27mM tri-Sodium citrate, 0.5mM dithiothreitol, 1.5% sucrose, 1% D-sorbitol, 6.07mM EDTA, 4mM EGTA [pH 7.3]). Intestines were washed with three changes of ice-cold Weiser solution (15ml) in a 50ml centrifuge tube. 15ml of ice-cold Weiser solution was added and vortexed for 15mins. The solution was transferred to the new 50ml centrifuge tube. This was repeated one more time to detach crypts and villi from the underlying muscle and mesenchyme. The supernatants were pooled and centrifuged at 2000rpm for 5mins. The pellet was resuspended in 20ml of 1xPBS (Dulbecco A) and centrifuged at 2000rpm for 5mins. The pellet was washed once again with 20ml of 1xPBS and resuspended in 3ml of ice-cold 1xPBS. This was aliquoted into three 1.5ml eppendorfs and centrifuged at 2000

rpm. The pellet represents epithelial cells from the intestine and was snap frozen using liquid nitrogen.

2.4 PCR-Genotyping

2.4.1.1 Genomic DNA isolation

Genomic DNA was isolated from the pancreatic tumour samples. The tissue samples were stored at -80°C prior to extraction. Tissue was digested in 500µl of lysis buffer (10mM Tris [pH 8], 100mM NaCl, 10mM EDTA [pH 8], 10% SDS) containing 10µg/ml of Proteinase K (Sigma), overnight at 37°C or at 55°C for 3hrs with agitation. Protein was precipitated by addition of 200µl protein precipitation solution (Flowgen), the solution was mixed by inversion and protein and any insoluble debris was pelleted by centrifugation at 14000rpm for 10mins. The supernatant was removed and added to a tube containing 500µl of isopropanol to precipitate the DNA. The tube was inverted to mix, and centrifuged at 14000rpm for 15mins. The supernatant was discarded and the pellet was left to air dry for 1hr. The DNA was then resuspended in 50µl of PCR grade water.

2.4.1.2 PCR genotyping

The DNA extracted from the pancreatic tumour tissue was used to detect the presence of transgene and/or recombined allele using polymerase chain reaction (PCR). The PCR reaction contains 1x Phusion high fidelity GC buffer (Thermo scientific), 200µM dNTPs, Phusion DNA polymerase, 0.5µM Gene specific primers and template DNA. The primers used were outlined in Table 2-3 and PCR conditions used were outlined in Table 2-4.

Table 2-3- Primers used for genotyping PCR

Gene	Sequence
1.KRAS WT F 2.KRAS WT R 3.KRAS 1lox	ctcttccccagcacagtgc ctcttgccctacgccaccagct agctagccaccatggcttgagtaagtctgca
1.Rosa WT F 2.Rosa WT R 3.Rosa modified R	cccaaagtgcctctgagttg ggagcgggagaaatggatatga gcgaagagtttgcctcaacc
1.Nuak1 Floxed F 2.Nuak1 Floxed R	ggtaggtggaggtcggctgagaagg tcggatcctagtgaacctcttc

2.4.1.3 Agarose gel electrophoresis

After the PCR reactions were carried out, PCR products were visualized by agarose-gel electrophoresis. 2% agarose gels were made by dissolving 2% (w/v) of agarose (sigma) in 1X Tris Acetate-EDTA buffer [TAE: 40mM Tris-acetate, 1mM EDTA (pH8.3)], and heated in a microwave until boiling, once boiled the solution was cooled quickly under cold running water and 4 μ l of ethidium bromide (Sigma) was added per 100ml of agarose solution. Gel as then poured into mould (BioRad) and combs were placed to create wells, after gels were set they were placed in a gel electrophoresis tank, which was filled with 1xTAE.

PCR products were prepared by adding 5 μ l of 5x loading dye (NEB). The PCR samples were then added to the well (10 μ l) and a 100bp molecular weight DNA ladder (NEB) was added to one of the well in order to assess the PCR product size. The gel was run at 120V for approximately 30mins and the products were visualized using a GelDoc Transilluminator.

	Rosa WT	Rosa-LSL MYC	KRAS	Nuak1
PCR Reaction (in µl)				
5x GC Buffer	4	4	4	4
10mM dNTP	0.5	0.5	0.5	0.5
Primer 1	0.5	0.5	0.5	0.5
Primer 2	0.5	-	0.5	0.5
Primer 3	-	0.5	0.5	-
Phusion DNA polymerase	0.2	0.2	0.2	0.2
Water	12.8	12.8	12.8	12.8
gDNA	2	2	2	2
PCR Cycling conditions				
Initial denaturation	94°C-30sec	94°C-30sec	94°C-30sec	94°C-30sec
Cycle number	35	35	35	35
Step 1 : Denaturation	94°C-30sec	94°C-30sec	94°C-30sec	94°C-30sec
Step 2 : Annealing	66°C-20sec	63°C-20sec	66°C-20sec	65°C-20sec
Step 3 : Extension	72°C-80sec	72°C-80sec	72°C-80sec	72°C-80sec
PCR product size	605bp	320bp	WT- 622bp Targeted- 500bp Recombined-	Floxed-1166bp Knockout-378bp

Table 2-4- Outline of PCR reactions, cycling conditions and product sizes

2.5 Cell Culture techniques

2.5.1 Fibroblast cell culture

Primary mouse embryonic fibroblasts (MEFs) were isolated from E13.5 embryos from respective genotypes. First, embryos were removed from pregnant female and placed in a dish of sterile PBS on ice. Sterile sharp forceps were used to remove uterine wall and each embryo was placed separately in a 6cm culture dish. “Red” tissue in body cavity was removed using a spatula. The head was removed and a portion of the head tissue was sent to Transnetyx (USA) for genotyping. The remainder of the embryo was homogenized using a scalpel in 1ml of PBS and transferred to a 15ml centrifuge tube. Another 1ml of PBS was used to collect remaining cells from the dish. 1ml of 1x trypsin was added and incubated for 15mins at room temperature. Cells were re-suspended by pipetting up and down; trypsin was quenched by adding 7ml of complete medium and then transferred to a 10 cm tissue culture dish. Medium was changed 24hrs after culture. The above protocol was carried out in a sterile laminar air flow hood and the forceps were sterilized in-between using 70% ethanol. The cells were cultured in DMEM supplemented with 10% FBS, 1% glutamine, Penicillin (50,000units) and Streptomycin (50,000 μ g), and grown at 37°C at 5% carbon dioxide (CO₂). The MEFs were cultured using the standard 3T3 protocol as follows: MEFs were passaged (see section 2.5.3) once in 3 days and 1.3×10^6 cells were seeded each time for maintaining the cells in culture, they were passaged for maximum of 5 passages.

2.5.2 Generation of primary pancreatic cells

Mice displaying signs of tumour burden were euthanized using a schedule 1 method. PDAC was dissected using aseptic techniques. A small piece of fresh tumour tissue was collected and transported in sterile PBS to the laboratory. In a laminar flow hood, the tumour tissue was washed in PBS twice and subjected to repeat passages of a scalpel blade through the tumour bulk until the cells were in suspension in culture medium. Cells were then transferred to a 6cm culture dish with the addition of 5mL culture medium plus an additional 0.5ml FBS (20% total). Cells were maintained at 37°C in a 5% CO₂ incubator. Thrice weekly changes of medium were required until cells were confluent, after which cells were split according to the requirement (see section 2.5.3 for passaging protocol). Once established, cells were maintained in 10cm culture dish in 10ml culture medium and passaged as required.

2.5.3 Passaging cells in culture

Once the cells were confluent, as determined by microscopy, they were passaged using standard techniques. The Medium was aspirated of the cells and were then washed using 5ml PBS. Cells were trypsinized using 1ml of 10% trypsin to break peptide crosslinking for 5-10 mins in the incubator. Cells were then washed off the plastic surface and suspended in culture medium and split into a requisite number of flasks or to the required dilution factor.

2.5.4 Freezing down cell lines

Medium was aspirated and the cells were washed using 5ml PBS. Cells were trypsinized using 1ml of 10% trypsin for 5-10 minutes in the incubator. Cells were then suspended in a solution of 90% FBS: 10% DMSO. Once cells were in suspension they were transferred to 1ml cryovials and placed in a freezing container (Mr.Frosty™), which allows cooling rate at -1°C/min in a -80°C freezer. The next day, cells were transferred to liquid nitrogen cold storage.

2.5.5 Thawing cells in culture

Frozen cells in 1ml cryovials were taken from cold storage and defrosted quickly in a 37°C water bath. Cells were resuspended gently in 10ml culture medium and plated into a 10cm culture dish. Cells were established in culture with medium being changed 24 hrs later.

2.5.6 siRNA transfection

Lipofectamine RNAiMAX (Life Technologies) reagent was used for the transfection. MEFs (0.6×10^6) were seeded in a 6cm culture dish day before the transfection. The next day, RNAiMAX (2.5µl) was diluted in Opti-MEM medium (250µl). siRNA against *Bad* (Dharmacon-LU-042966-00-00022) was diluted (40nM) in Opti-MEM medium (250µl). Both the transfection reagent and siRNA was incubated for 5mins. Diluted siRNA was added to the diluted RNAiMAX and incubated for 10mins. The siRNA-lipid complex was then added drop wise to the cells (in 10% serum, without antibiotics). After 6hrs, the medium was changed and the efficiency of knockdown was analysed by Q-RT PCR (see section 2.8). siRNA non-targeting pool (D-001206-13-05) was used as control.

2.6 Analysis of cell death

2.6.1 Annexin V/PI staining

Annexin V/PI staining was used to measure apoptosis *in vitro*. MEFs were seeded in 6-well plate (50,000 cells/well). After 24hrs, medium was changed to low serum medium (0.2% FBS) and MycER^{T2} was activated by 100nM 4-hydroxy tamoxifen, an equivalent volume of absolute ethanol was used as a vehicle control. Cells were prepared for Annexin V/PI staining 30hrs or 72hrs post induction. Alternatively, MEFs (in full serum conditions) were treated with 5 Grays gamma irradiation 24hrs after MycER^{T2} activation or treated with 1 μ M ABT-737 for indicated time periods in combination with MycER^{T2} activation. Cells were prepared for flow cytometry as follows; the culture medium of cells was collected in a 15ml centrifuge tube and kept on ice, then cells were trypsinized using 10% trypsin, 1% BSA was added to quench the trypsin and cells were collected in the same tube as the medium. Cells were centrifuged at 300g for 5mins. Supernatant was aspirated, 300 μ l of Annexin V binding buffer (10mM HEPES [pH7.4], 140mM NaCl, 2.5mM CaCl₂) and 2 μ l of Annexin V (conjugated with OG488 or APC, Biolegend) was added to the pellet and incubated in the dark for 15mins; Propidium iodide (1 μ g/ml) was added prior to the analysis.

2.6.2 SYTOX green cell death assay

Pancreatic cancer cells (KMC 1 and KMC 2) were seeded at 5×10^3 cells per well in a 96-well plate. Cells were treated with either ABT-737 (1 μ M) or HTH-01-015 (10 μ M) and dead cells were monitored in real time in the presence of 100nm of Sytox green (Invitrogen). SYTOX green labels the nucleic acid of dead cells yielding green fluorescence when excited at 488nm. Fluorescence intensities from the dead cells were acquired every 2hrs using IncuCyteTM Live-Cell imaging system (Essen bioscience) equipped with a 37°C incubator (5% CO₂). Additionally, phase-contrast and fluorescent images were automatically collected for each time point. The IncuCyte software was used to calculate the number of fluorescent events (dead cells) and the confluence factor, which is the indirect measure of cell number.

2.6.3 Crystal violet staining

MEFs were seeded in a 24 well tissue culture plate (3×10^4 cells/well). After 24hrs, cells were treated with either DMSO or varying concentration of Nuak1 inhibitor (HRH-01-015). After 72hrs, plates were removed from the incubator, medium was aspirated and

cells were washed with 1xPBS. Cells were fixed with ice-cold 100% methanol for 10mins. The fixed cells were stained with crystal violet (0.1% Crystal violet in 20% ethanol) for 20mins. After 20mins, stained cells were washed twice with distilled water and dried.

2.7 ROS detection

MitoSOXTM red mitochondrial superoxide indicator (Molecular probes) was used to detect ROS selectively in the mitochondria. U2OS cells were seeded at 1×10^5 cells per well in a 6-well plate. 24 hours later, cells were treated with 10 μ M of Nuak1 inhibitors (HTH-01-015,) for 2hrs. MitoSOXTM reagent was added to a final concentration of 5 μ M 10 mins before the measurement and incubated in dark at 37°C in 5% CO₂. Cells were removed from the incubator, the medium was aspirated and the cells were trypsinized after washing with PBS. The trypsin was quenched with 100 μ L of 1% BSA and cells were collected in a FACS tube. Cells were centrifuged at 300g for 5mins, the supernatant was aspirated and the pellet was dissolved in 200 μ L of 1XPBS. The cell suspension was analysed using the BD FACS Calibur and excited between 564-601nm allowing detection of the red fluorescence from MitoSOXTM. 10,000 cells were counted from each sample and data were corrected for background using the unstained samples. This was repeated till three replicates were obtained for each cell line.

2.8 RNA isolation and quantitative real-time PCR

2.8.1 RNA isolation by Trizol method

MEFs were seeded at a concentration of 1×10^5 cells per well in a 6 well cell culture plate. MycER^{T2} was activated with 4-OHT (100nm) for different time points. Cells were collected using 1ml of Trizol (Ambion) in a 1.5ml centrifuge tube and 200 μ L of chloroform (sigma) was added. Solutions were then mixed by gently inverting the tubes for 15secs. The mixture was then centrifuged at 14,000rpm for 15mins at 4°C. After centrifugation, the aqueous phase was carefully removed and collected in a fresh autoclaved 1.5ml centrifuge tube. An equal volume of isopropanol was added and incubated at -20°C overnight. The next day, tubes were centrifuged at 14,000 rpm for 15mins at 4°C. The supernatant was carefully removed and the pellet was washed twice with 500 μ L of 70% Ethanol at 8000rpm for 5mins. The pellet was air dried until it was translucent and dissolved in an appropriate volume of sterile water (usually 30 μ L). Finally, the sample was heated at 56°C for 10mins and stored at -80°C until further use.

In order to isolate RNA from tissues, the above protocol was applied with the following modification. A small amount of tissue was homogenized using a micropestle (Eppendorf) in 1ml of Trizol. An additional centrifugation step (14,000rpm for 10mins at 4°C) was performed prior to the chloroform addition to remove the debris.

2.8.2 cDNA synthesis

RNA quantity was measured using Nanodrop (Thermo scientific). 100-500ng of RNA was used to synthesize cDNA using QuantiTect Reverse transcriptase kit (Qiagen). In this method genomic DNA contamination was eliminated first by incubation with gDNA wipe out buffer at 42°C for 2mins (Table 2-5). RNA was incubated with reverse-transcription reaction components (Table 2-6) and incubated at 42°C for 15mins followed by 95°C for 3mins. The cDNA generated was later used for SYBR green based real-time PCR analysis. The RT-Primer mix includes both oligo-dT and random primers that enable cDNA synthesis from all regions of RNA transcripts.

Table 2-5- Genomic DNA elimination components

Components	Volume/reaction
gDNA wipeout buffer, 7x	2µl
Template RNA, up to 1µg	Variable
RNase free water	Variable
Total reaction volume	14µl

Table 2-6- Reverse-transcription reaction components

Components	Volume/reaction
Reverse-transcription (RT) master mix	
Quantiscript Reverse Transcriptase	1µl
Quantiscript RT Buffer	4µl
RT primer mix	1µl
Template RNA	
Entire genomic DNA elimination reaction	14µl
Total reaction volume	20µl

2.8.3 Primer Design

SYBR green quantitative real time PCR was employed. Intron spanning primers were designed for *BIM*, *BAD*, *TFAM* using Universal Probe Library Assay Design Centre, a publically available website run by Roche (Table-2-7).

Table 2-7- Primers used for Q-RT PCR

Protein	Primer sequence
---------	-----------------

<i>BIM</i> (mouse)	F: aacagttgtaagataaccatt R: ggagacgagttcaaggaaact
<i>BAD</i> (mouse)	F: ggagcaacattcatcagcag R: tacgaactgtggcgactcc
<i>TFAM</i> (human)	F: aagattccaagaagctaagggtga R: cagagtcagacagattttccagtt

2.8.4 qRT-PCR

SYBR Green mix from Quanta Biosciences (QUNT95072-012) was used. A PCR mix was formulated for each reaction (10 μ L) as follows.

Table 2-8- Q-RT PCR reaction components

Components	Volume/reaction
Master mix, 2x	5 μ l
Primer-F (10mM)	0.1 μ l
Primer-R (10mM)	0.1 μ l
Water	4.3 μ l
cDNA	0.5 μ l
Total reaction volume	10 μ l

The following cycling protocol was followed

Table 2-9- Q-RT PCR cycling condition

Q-PCR cycling condition
1. 95°C for 5mins
2. 95°C for 30secs
3. 60°C for 20secs
Go to step 2 x35 cycle
4. 72°C for 10mins
5. 65°C for 10secs
6. 95°C for 30secs

2.9 Protein Extraction and Western Blot Analysis

2.9.1 Protein Extraction

Whole cell lysates were prepared in RIPA buffer (150mM NaCl, 50mM Tris [pH 7.5], 1% NP-40, 0.5% sodium deoxycholate, 0.1% SDS plus complete protease inhibitor cocktail [Roche, 4693124001]). The cells were seeded and treated according to the respective experimental set up. The plate was removed from the incubator and placed on ice. The medium was aspirated and cells were washed 1X with PBS and scraped in 300 μ L RIPA buffer. The cells were collected in a 1.5ml centrifuge tube and incubated on ice for 15mins

with repeated mixing followed by centrifugation at 12,000 rpm at 4°C to remove cell debris.

Nuclear fractions were prepared in low salt buffer (20mM KCL, 10mM HEPES [pH 7.5], 1mM MgCl₂, 1mM CaCl₂, 0.1% Triton X-100) as follows. The cells were seeded and treated according to the respective experimental set up. The plate was removed from the incubator and placed on ice. The medium was aspirated and the cells were washed in 1x PBS and scraped in 300µL of low salt buffer. The cells were collected in a 1.5ml centrifuge tube and centrifuged at 3300 rpm at 4°C and the pellet was used as nuclear extract.

To isolate proteins from the small intestine, epithelial cell pellet obtained from epithelial cell extraction (described in section 2.3.11) was used. Whole cell lysates were prepared in RIPA buffer as described above.

2.9.2 Protein quantification

Proteins were quantified using the bicinchoninic acid (BCA) method. The BCA method utilizes the biuret reaction in which Cu²⁺ ions are reduced to Cu⁺ ions to produce a purple colour. The reaction is facilitated by the presence of the amino acids cysteine, tyrosine and tryptophan in the proteins. The amount of Cu²⁺ reduced is proportional to the protein concentration. The extent to which the copper ions are reduced can be quantified by the colorimetric detection as the BCA reagent strongly absorbs light at 562nm, a high absorbance reading therefore indicates a high protein concentration. Protein samples were measured in duplicate, 2µl of protein sample was added to 98µl of PBS and mixed. Bovine serum albumin (BSA) was used as a standard and diluted from stock in PBS to generate a concentration range of 5-25µg/ml. 2µl of lysis buffer was added to the blank and all the standards to account for the sample buffer in the protein samples. All samples were diluted in a colourless, flat bottom 96-well plate. BCA reagents were made up according to manufacturer's instructions (Pierce) and 100µl was added to each sample. The plate was then incubated at 37°C for 1-2 hours. The absorbance of each sample was read on a plate reading spectrophotometer at 562nm (Molecular devices). The concentration of each diluted protein sample was calculated using the standard curve.

2.9.3 Preparation of protein samples

Protein samples were removed from the -80°C freezer and thawed on ice. 50µg of protein was used for each condition. The proteins were denatured by the addition of 5X Lamelli Buffer (300mM Tris [pH 6.8], 50% Glycerol, 10% SDS, 4% β-Mercapto ethanol, 0.5% Bromophenol blue) to the final concentration of 1X and then heated at 95°C for 5mins.

2.9.4 SDS-PAGE

Cell lysates were resolved using SDS-PAGE. The mini-protean (Biorad) gel apparatus was used to prepare polyacrylamide gels. Separating gels were poured using either 10% or 15% acrylamide (dependent upon the molecular weight of the protein to be detected), and allowed to set with a layer of isopropanol to prevent the desiccation of the gel and to ensure that the gel surface was flat. Once the gel is set, the isopropanol was removed and 4% stacking gel poured on top and the gel comb (10 well) was inserted. Once the stacking gel had set the entire gel was transferred into the gel tank, which was filled with 1xSDS-PAGE running buffer (Table 2-10). The comb was then removed and 5µl of protein molecular weight marker (Full range rainbow molecular weight marker GE healthcare Life sciences) was added to the first well of the gel. The protein samples were added to the other wells. Each gel was run at 100V continuously until the required degree of separation was achieved.

Table 2-10- SDS-PAGE gel composition

Components	Separating gel (10%)	Separating gel (12.5%)	Stacking gel (4%)
Acrylamide	5.1ml	6.35ml	650µl
Tris 1M pH 8.9	5.6ml	5.6ml	-
Tris 1M pH 6.8	-	-	600µl
Water	4.2ml	2.95ml	3.6ml
SDS 10%	150µl	150µl	150µl
APS 20%	75µl	75µl	25µl
TEMED	15µl	15µl	5µl

Key: SDS- Sodium dodecyl sulphate, APS- Ammonium persulfate, TEMED- Tetramethylethylenediamine

2.9.5 Western blot

Following protein resolution by SDS-PAGE, proteins were transferred from the gel to a nitrocellulose membrane (Protran) using the Hoefer transfer module (TE22), as per manufacturer's instructions. Once the gel, membrane and sponges had been placed inside the cassettes, it was placed inside the Mini-transfer tank and locked in place. The chamber was then filled with 1x transfer buffer (Table 5). The transfer was performed at 230mA for 2hrs in

a cold room maintained at 4°C. The membrane was incubated briefly in Ponceau S solution (0.1% Ponceau S in 5% acetic acid) to determine if the transfer was successful, followed by incubation in 5% milk (Marvel milk powder) in TBS-T for 1hr to block the membrane. The membrane was then incubated in primary antibody (Table 2-12) overnight in 5% milk (and 0.1% sodium azide) at 4°C. The following day the membrane was washed three times in TBST for 5mins each, and then incubated with appropriate HRP linked-secondary antibody in 5% milk solution for 1hr at room temperature. The membrane was then washed again three times in TBST and proteins were visualized using ECL western blotting detection reagent from GE healthcare Life Science. This reagent utilizes a chemiluminiscent reaction catalyzed by HRP to expose X-ray film (Fuji film super RX) and the films were developed using an automated X-ray processor (AGFA, Classic EOS). A number of different exposures of X-ray film were generated to produce clear images. The films were overlaid against the nitrocellulose membrane in order to confirm the protein band size according to the molecular weight marker.

Table 2-11- Buffers used during Protein analysis

10X SDS-PAGE Running Buffer	1X SDS-PAGE Transfer Buffer
10% SDS 250mM Tris 1.92M Glycine	0.1% SDS 25mM Tris 0.192M Glycine 20% Methanol
10X Tris buffered saline with Tween20 (TBST)	
200mM Tris 1.37M Sodium Chloride 1% Tween20 pH adjusted to 7.5	

Table 2-12- Antibody conditions for western blot analysis

Primary antibody	Primary antibody conditions	Secondary antibody	Secondary antibody condition
Bim (cell signaling, 2933)	1:800 in 5% Milk, O/N @4°C	ECL anti-rabbit (GE healthcare NA934V)	1:2500 in 5% Milk, 1hr at RT
P19Arf (Novus, N200-174)	1:800 in 5% Milk, O/N @4°C	ECL anti-rat (GE healthcare NA935V)	1:5000 in 5% Milk, 1hr at RT
Histone H2B (Abcam, ab1790)	1:5000 in 5% Milk, O/N @4°C	ECL anti-rabbit (GE healthcare NA934V)	1:5000 in 5% Milk, 1hr at RT
Ark5 (cell signalling, 4458)	1:800 in 5% Milk, O/N @4°C	ECL anti-rabbit (GE healthcare NA934V)	1:5000 in 5% Milk, 1hr at RT

β -actin (Sigma, A5441)	1:10000 in 5% Milk, O/N @4°C	ECL anti-mouse (GE healthcare NA931V)	1:5000 in 5% Milk, 1hr at RT
-------------------------------	------------------------------	---------------------------------------	------------------------------

2.10 Chromatin immunoprecipitation

For ChIP, Rosa26-MYCER MEFs were plated in a 15cm culture dish and induced with 100nM 4-hydroxy tamoxifen for 1hr. Cells were cross-linked with formaldehyde (1% final) for 10mins at 37°C. The medium was aspirated and washed with ice-cold PBS. Cells were scraped in PBS containing complete protease inhibitors and centrifuged at 300xG for 5mins at 4°C. Cells were resuspended in 3ml of lysis buffer I (5mM PIPES pH8, 85mM KCl, 0.5%NP40) and incubated on ice for 20mins. After lysis, cells were centrifuged at 300xG for 5mins at 4°C and the pellets were resuspended in 3ml lysis buffer II (RIPA as described above). After 10mins incubation, lysates were sonicated to fragment DNA. Chromatin was precleared using 60 μ l of saturated Sepharose protein A/G beads (120 μ l of sepharose+1mg/ml BSA+400 μ g/ml of salmon sperm DNA in 5ml of RIPA O/N) for 3hrs at 4°C with rotation. Pre-cleared chromatin was centrifuged at 2000rpm for 5mins (4°C) and the supernatant was immunoprecipitated with c-MYC antibody (N-262, Santa Cruz SC-764) overnight at 4°C. The chromatin-antibody complex was pulled down by saturated Protein A/G slurry for 6hrs at 4°C. DNA. The beads were pelleted by centrifugation at 3000rpm for 5mins at 4°C and washed with wash buffer as follows: 2x washing buffer I, 3x washing buffer II, 4x washing buffer III (see Table 2-13). The beads were centrifuged at 3000rpm for 5mins in between washes. DNA was eluted using elution buffer (1%SDS, 0.1M NaHCO₃), crosslinks were reversed by incubating 3hrs at 37°C followed by an overnight incubation at 65°C using buffer IV (see Table 2-13). DNA was purified using Qiaquick PCR purification kit for Q-PCR analysis. The following primer sets were used: *BIM* promoter (human) F: catggctactagaaaaatgcaca, R: tgaggccagcctgttagat. *BIM* promoter (mouse) F: catcgtcgccgtcaccgat, R: accagcggaggtggtggaat. *BIM* negative control fragment (mouse) F: gttcggctgattcaacacag, R: aaatagaacaagttacgtgggaagt.

Table 2-13- Buffers used for Chromatin immunoprecipitation

Wash Buffer I	Wash Buffer II
20mM Tris pH8.1	20mM Trs pH8.1
150mM NaCl	500mM NaCl
0.1% SDS	2mM EDTA
1% TritonX-100	0.1% SDS
	1% TritonX-100

2.11 Data Analysis

2.11.1 Graphical representation of the data

Raw data obtained from apoptosis scoring, quantitative RT-PCR, Flow cytometry, and SYTOX green assay were inputted into Excel (Microsoft) spreadsheets. All means, standard deviation, standard error of mean were calculated using the calculator function. Graphical representation of all data was also produced in Excel (Microsoft)

2.11.2 Comparison of Means

The Prism online software was used to carry out unpaired T-tests to compare means. Comparison of means analysis was carried out on all results with $n \leq 3$.

2.11.3 Survival analysis

Survival data were analysed using SPSS software. Kaplan-Meier plots were used to present the data, and significance was measured using Log-Rank test.

3 Evaluating the relative contribution of p19Arf and BIM in MYC-induced apoptosis

3.1 Introduction

The tumourigenic properties of some oncogenes are constrained by intrinsic tumour suppressive functions such as apoptosis, and MYC is a paradigm for this phenomenon. The Myc family of oncogenes are amongst the most frequently deregulated oncogenes in a wide variety of human cancers. An effective MYC centric therapy could therefore have a great impact on cancer survival rates. Currently several efforts are being actively pursued to target MYC, such as targeting transcriptional function of MYC, destabilizing MYC protein, suppressing MYC expression itself, synthetic lethality etc. (Horiuchi et al., 2014). In addition, exploiting MYC-induced apoptosis will complement these efforts. To pursue this as a therapeutic strategy, a clear understanding of the mechanism of MYC-induced apoptosis is important.

The Arf-Mdm2-p53 pathway has been reported to be required for MYC-induced apoptosis. The tumour suppressor p19Arf, encoded by alternative splicing of the *Cdkn2a* locus, interacts with and inhibits Mdm2, a negative regulator of p53, thereby stabilizing p53 protein (Kamijo et al., 1998). Loss of p19Arf or p53 has been shown to suppress MYC-induced apoptosis and loss of either of these proteins cooperates with Myc to accelerate lymphomagenesis (Schmitt et al., 1999; Zindy et al., 1998). Moreover, polycomb transcriptional repressor Bmi-1 and the Foxo4 transcriptional factor are both reported to cooperate with Myc in lymphomagenesis by downregulating p19Arf, thereby blocking Myc-induced apoptosis (Bouchard et al., 2007; Jacobs et al., 1999).

Similarly, several reports suggest a central role for the mitochondrial pathway of apoptosis in MYC-induced apoptosis. The main components regulating the mitochondrial pathway are Bcl2 proteins, which can be classified into three groups based on their action: anti-apoptotic proteins (e.g. Bcl2, Bcl-x_L); pro-apoptotic executioner protein (e.g. Bax, Bak); pro-apoptotic BH3-only proteins (e.g. Bim, Puma). The executioner proteins are critical for mitochondrial membrane permeabilization (MOMP), which leads to a sequence of events that activate cysteine proteases called caspases resulting in cell death. The anti-apoptotic proteins keep Bax and Bak in check, thus maintaining the integrity of the mitochondrial outer membrane. BH3-only proteins sequester the anti-apoptotic members so that Bax and Bak are free to oligomerize and form pores in the outer mitochondria membrane (MOMP)

(Czabotar et al., 2014; Tait and Green, 2013). A ‘direct activation’ model proposes that some BH3-only proteins such as Bim and Puma can activate Bax and Bak directly (Kuwana et al., 2005; Letai et al., 2002; Llambi et al., 2011). The fine balance of Bcl2 proteins is therefore important for the survival of the cells. Several studies have shown that MYC can alter the balance of anti- and pro-apoptotic Bcl2 family members (Hoffman and Liebermann, 2008). In particular, a recent study has demonstrated direct binding of MYC to *BCL2L11* locus, which encodes BIM, in human breast cancer cells (Campone et al., 2011). Bim was previously shown to be required for MYC-induced apoptosis and disruption of the *Bcl2l11* locus accelerates Myc-induced lymphomagenesis, even in the heterozygous state (Egle et al., 2004).

Although there is evidence supporting the role of both p19Arf and Bim in driving MYC-induced apoptosis, many of the observations are inferences from lymphoma studies. However, it is likely that different tissues exhibit different level of apoptosis priming, in other words, differential expression of apoptosis regulators might determine their sensitivity and therefore results obtained in one context might not be applicable to other. Moreover, the level of MYC deregulation is a determinant of its biological output and different levels of MYC activate and repress different gene sets (Murphy et al., 2008; Walz et al., 2014). Therefore, there is a need to evaluate the molecular players involved in MYC-induced apoptosis in multiple tissues using a single genetic system. In this chapter, I aimed to compare the relative contribution of both p19Arf and Bim in MYC-induced apoptosis using a single transgenic model under various settings and to determine whether Bim is regulated by MYC.

3.1.1 Mouse models used to address the aims

To investigate the mechanism of MYC-induced apoptosis, I have used a previously described *Rosa26-MycER^{T2}* mouse model (*R26^{MER/MER}*), which expresses a tamoxifen inducible fusion protein (MycER^{T2}), comprising of full length human c-Myc cDNA fused to the modified ligand binding domain of the human oestrogen receptor (ER^{T2}), downstream of the constitutive and ubiquitously expressed *Rosa26* locus (Murphy et al., 2008). Constitutively expressed MYC is held inactive in the cytoplasm by the ER^{T2} moiety and MYC activation is achieved by administration of tamoxifen (Fig. 3-1). Owing to the relatively weak activity of the *Rosa26* promoter, the level of MycER^{T2} expressed in most adult *R26^{MER/MER}* tissues is sufficient to drive ectopic proliferation but unable to breach the apoptotic threshold, with the exception of the small intestine and colon, wherein MycER^{T2}

is expressed at higher levels compared to other tissues. Consequently, the continuous activation of MycER^{T2} (3 days with 50mg/kg Tamoxifen) breaches the threshold of MYC required to drive apoptosis in the intestine, whereas in tissues such as liver and pancreatic islets of Langerhans, MYC requires additional pro-apoptotic stimuli (e.g. Doxorubicin) to drive apoptosis.

To evaluate the contribution of p19Arf to MYC-induced apoptosis, I bred $R26^{MER/MER}$ mice with $Cdkn2a^{tm1(GFP)Cjs}$ (*p19Arf* null), wherein exon1 β of the endogenous *Cdkn2a* locus is replaced by GFP coding sequence abrogating p19Arf expression (Zindy et al., 2003). To investigate the role of Bim in MYC-induced apoptosis, I bred $R26^{MER/MER}$ mice with $Bcl2l1^{tm1.1Ast}$ (*Bim* null), wherein the BH3 only domain is deleted and the resultant mutant protein behaves as a null mutation (Bouillet et al., 1999). To investigate the requirement of Puma for MYC-induced apoptosis, I bred $R26^{MER/MER}$ mice with $Bbc3^{tm1Ast}$ (*Puma* null) mice (Villunger et al., 2003) (Fig. 3-1).

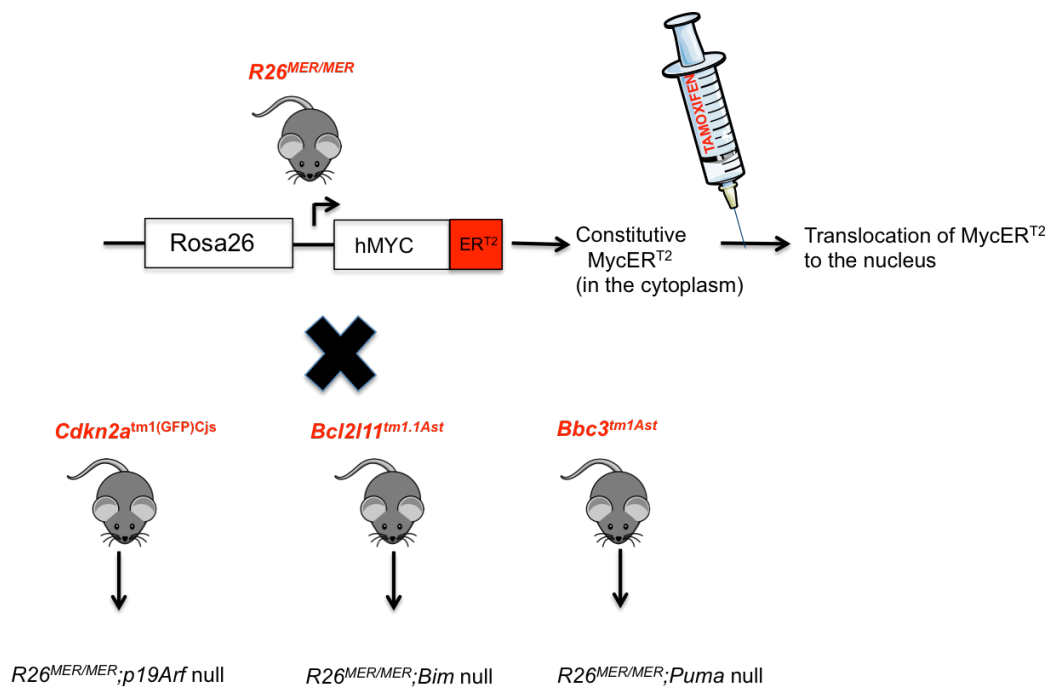


Figure 3-1- Mouse models used to study MYC-induced apoptosis

$R26^{MER/MER}$ mice express tamoxifen inducible fusion protein MycER^{T2} under the control of constitutive *Rosa26* locus. This model was bred on to *p19Arf* null, *Bim* null, and *Puma* null mice to study the role of respective proteins in MYC-induced apoptosis.

3.2 Results

3.2.1 Bim is required for MYC-induced apoptosis

MycER^{T2} was activated by intraperitoneal (IP) injection of tamoxifen for 3 days in $R26^{WT/WT}$, $R26^{MER/MER}$ (WT for both *Bim* and *p19Arf*), $R26^{MER/MER};p19Arf$ null,

$R26^{MER/MER};Bim$ null cohorts and the tissues were harvested 24hrs after the final induction. Apoptosis was measured by a terminal deoxynucleotidyl transferase dUTP nick end labelling (TUNEL) assay (as described in section 2.3.10), which detects fragmented DNA a hallmark of apoptosis. Apoptosis scoring as described in section 2.3.10, revealed that MycER^{T2} activation in $R26^{MER/MER}$ mice induces a significant amount of apoptosis in the crypt region of the small intestine (5.7%) compared to the tamoxifen treated wild type controls (0.6%) (Fig. 3-2A [upper panel] and B). Loss of *p19Arf* did not reduce the MYC-induced apoptosis significantly (4.5%), whereas deletion of *Bim* abrogated MYC-induced apoptosis (0.7%) in the small intestine of $R26^{MER/MER}$ mice (Fig. 3-2).

MycER^{T2} activation in $R26^{MER/MER}$ mice drives a significant amount of apoptosis in the colon as well. MycER^{T2} activation in $R26^{MER/MER}$ mice resulted in a modest 0.7% of apoptosis in the colonic epithelium compared to the 0.2% in tamoxifen treated wild type controls. Again, as shown in Fig. 3-2C deletion of *Bim* abrogated MYC induced apoptosis (0.2%) but deletion of *p19Arf* had no effect (0.9%) (Fig. 3-2A lower panel and C).

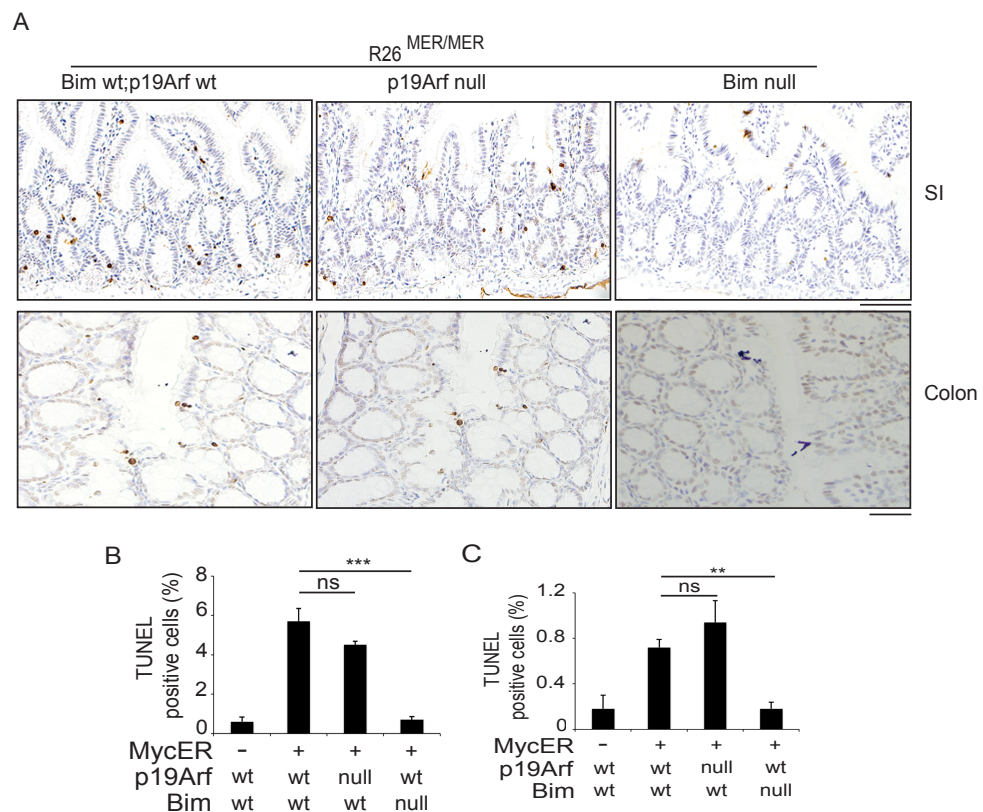


Figure 3-2- Bim is required for MYC-induced apoptosis in the intestine.

(A) Representative images of TUNEL staining of apoptotic cell in small (SI) intestine and colon, of mice of the indicated genotypes, treated consecutively for 3 days with tamoxifen (50mg/kg). Scale bar represents 100µm. Quantification (Mean ± SEM) of TUNEL staining (percentage of total) in the small intestine (B) and colon (C) of Tam-treated wild type (wt) controls (n=3), $R26^{MER/MER}$ (n=3), $R26^{MER/MER};Bim$ null (n=4), $R26^{MER/MER};p19Arf$ null (n=3). Two-tailed, unpaired T tests were used to calculate the statistical significance. ** P< 0.01; *** P< 0.001; ns, not-significant P>0.05. This figure is taken from (Muthalagu et al., 2014)

It has previously been reported that MYC drives apoptosis in fibroblasts when cells are deprived of serum (Evan et al., 1992). Mouse embryonic fibroblasts (MEFs) from E 13.5 embryos of $R26^{MER/WT}$ mice were generated. Here, MycER^{T2} can be activated by treating the cells with 4-hydroxy tamoxifen (4-OHT). Annexin V/PI staining followed by flow cytometry was used as a measure of apoptosis. In line with previous reports, activation of MycER^{T2} with 4-OHT for 30hrs in MEFs cultured in low serum resulted in a significant amount of apoptosis compared to vehicle (Ethanol) treated control cells (Fig. 3-3). To investigate the role of Bim and p19Arf in MYC-induced apoptosis *in vitro*, MEFs from multiple embryos of $R26^{MER/WT};Bim$ null and $R26^{MER/WT};p19Arf$ null mice were generated. The western blots confirmed the nullizygoty of the MEFs (Fig. 3-3C, D). Activation of MycER^{T2} with 4-OHT for 30hrs in *Bim* null MEFs cultured in low serum did not induce apoptosis (Fig. 3-3A), whereas MycER^{T2} activation drives apoptosis in *p19Arf* null cells comparable to *p19Arf* wild type cells (Fig.3-3 B).

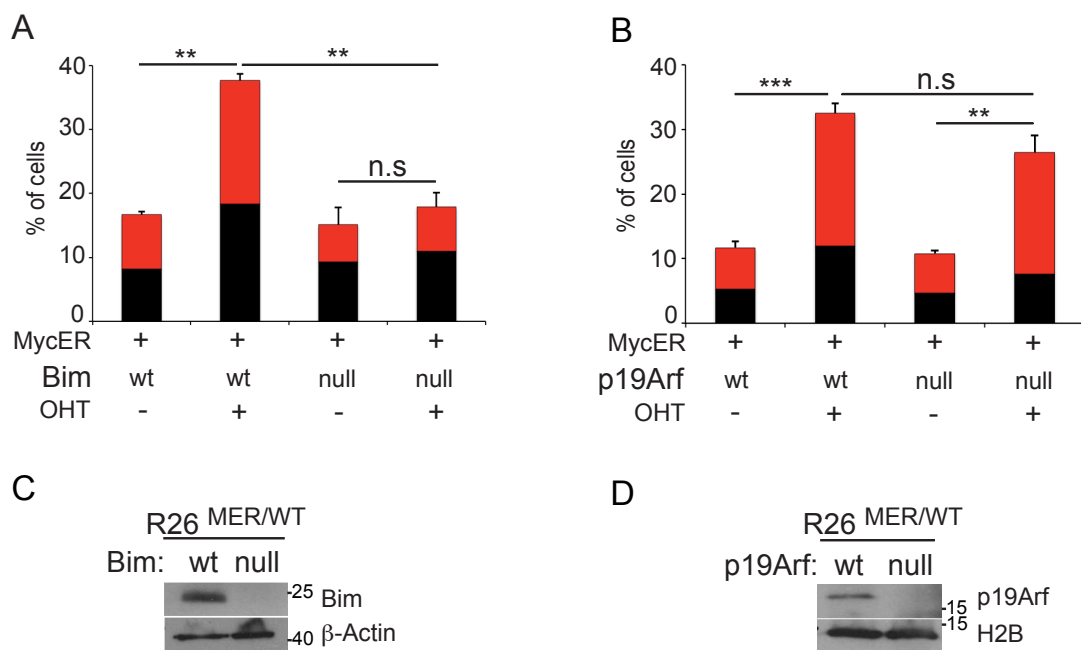


Figure 3-3- Bim is required for MYC-induced apoptosis in MEFs

(A & B) Early passage MEFs ($P < 5$) from E13.5 embryos of $R26^{MER/WT}$ mice, wild type or nullizygous for *Bim* or *p19Arf*, were treated with 100nM 4-OHT for 30hrs in low serum conditions (0.2%). The graph represents percentage of cells stained only for Annexin V (black) and the cells stained for both Annexin V/PI (red). Mean \pm SEM from a representative experiments performed in biological triplicates were shown. Consistent results were obtained in MEFs derived from at least 2 different embryos for each genotype. (C & D) Immunoblots confirming the *Bim* and *p19Arf* nullizygoty of MEFs. Two-tailed, unpaired T tests were used to calculate the statistical significance. ** $P < 0.01$, *** $P < 0.001$; ns, not significant $P > 0.05$. This figure is taken from (Muthalagu et al., 2014)

To verify if deletion of *Bim* delays the apoptotic response to MYC or suppress MYC-induced apoptosis, MycER^{T2} was activated for 72hrs in MEFs cultured in low serum (0.2%). As shown in Fig.3-4A, *Bim* null cells failed to undergo apoptosis to the same extent as *Bim* wild type, whereas apoptosis induced by MycER^{T2} in *p19Arf* wt or *p19Arf* null cells were indistinguishable (Fig.3-3 B). These data clearly indicate that Bim is required for MYC-induced apoptosis in the intestinal compartment *in vivo* and in MEFs *in vitro*.

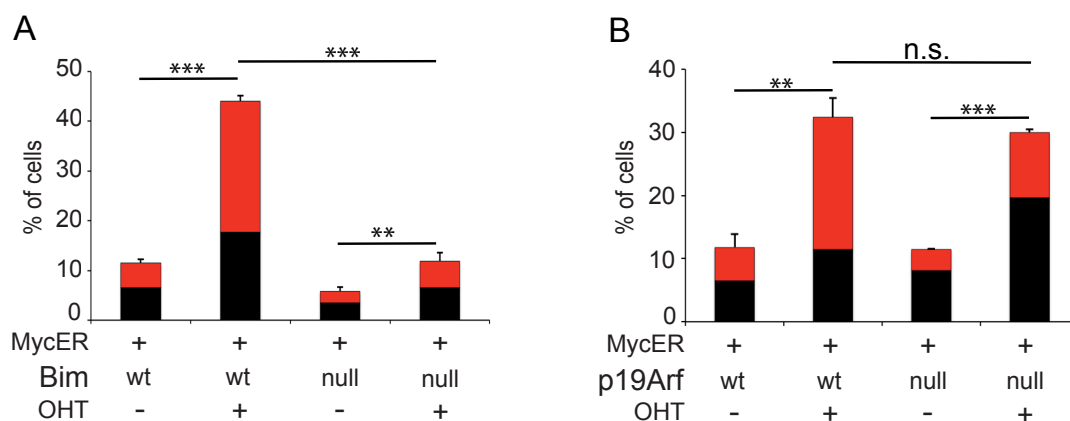


Figure 3-4- *Bim* null cells are resistant to MYC-induced apoptosis after 72hrs of MYC activation

(A) $R26^{MER/WT}$ MEFs, wild type or nullizygous for *Bim* or *p19Arf*, were treated with 100nM 4-OHT for 72hrs in low serum conditions (0.2%). The graph represents percentage of cells stained only for Annexin V (black) and the cells stained for both Annexin V and PI (red). Mean \pm SEM from a representative experiment performed in biological triplicates was shown. Two-tailed, unpaired T tests were used to calculate the statistical significance. ** $P < 0.01$, *** $P < 0.001$; ns, not significant $P > 0.05$. This figure is taken from (Muthalagu et al., 2014)

3.2.2 Bim mediates the pro-apoptotic signalling by MYC

As pointed out earlier, in the model used the level of MYC expressed in tissues other than intestine is below the apoptotic threshold. Nonetheless, MYC does elicit pro-apoptotic signalling, thereby sensitizing the cells to additional pro-apoptotic stimuli, such as Doxorubicin, a DNA damaging agent (Murphy et al., 2008). MycER^{T2} was activated by administration of tamoxifen (IP) for 3 days in $R26^{MER/MER}$ mice and when the MYC-induced proliferation is at its peak (on day 3), a sub-apoptotic dose of Doxorubicin, which alone fails to drive apoptosis in most tissues (except small intestine), was administered (3day Tam+Dox). The tissues were harvested 24hrs after Doxorubicin treatment and analysed for apoptosis using TUNEL assay. The combination of MYC activation and Doxorubicin treatment resulted in a clear induction of apoptosis in liver and pancreatic

islets of Langerhans and enhanced MYC-induced killing in colonic epithelium, compared to respective wild type controls treated with 3day Tam+Dox (Fig 3-5A first and second panel). To analyse the requirement of Bim and/or p19Arf for MYC induced pro-apoptotic signalling, the same treatment (3day Tam+Dox) was performed in $R26^{MER/MER}$, Bim null and $p19Arf$ null cohorts. Again, deletion of Bim abrogated the apoptotic response in all the three tissues and deletion of $p19Arf$ did not (Fig. 3-5 A&B).

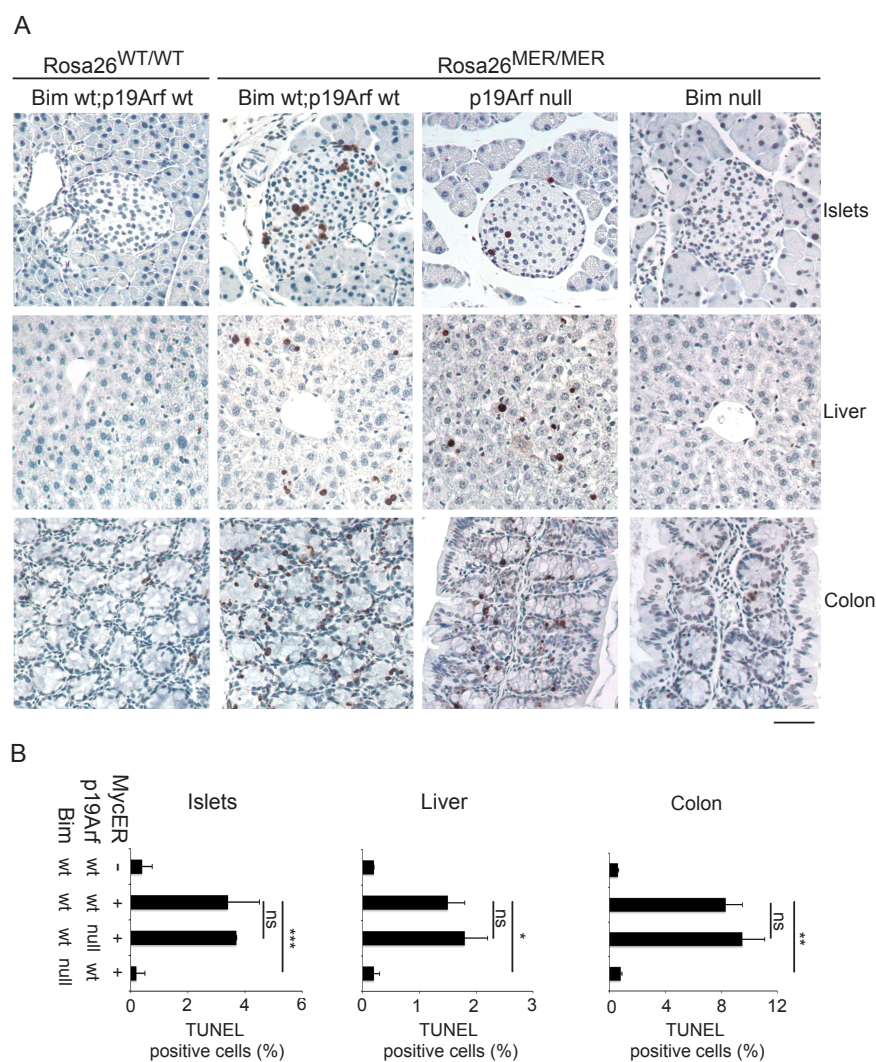


Figure 3-5- Bim is required for MYC-induced sensitization to Doxorubicin

(A) Representative images of TUNEL staining in pancreatic islets, liver and colon of the respective genotypes, treated with Tam (50mg/kg) + Doxorubicin (10mg/kg). Scale bar represents 50 μ m. (B) Quantification (Mean \pm SEM) of TUNEL staining (percentage of total) in the indicated tissues of 3 day Tam+Dox- treated $R26^{WT/WT}$ controls (n=3), $R26^{MER/MER}$ (n=3), $R26^{MER/MER};Bim$ null (n=3), $R26^{MER/MER};p19Arf$ null (n=5). Two-tailed, unpaired T tests (from prism software) were used to calculate the statistical significance. ** P < 0.01; *** P < 0.001; ns, not-significant P > 0.05. The data to generate this figure was collected by Melissa R.Junttila. This figure is taken from (Muthalagu et al., 2014)

In order to understand the cooperation between MYC and Doxorubicin, $R26^{MER/WT}$ MEFs were treated with Doxorubicin (1 μ g/ml) with or without MycER^{T2} activation for 8hrs. As shown in figure 3-6, Doxorubicin treatment does not induce Bim protein expression in MEFs and neither does it augment MYC-induced Bim expression. This hints that MYC and Doxorubicin act independently, possibly via induction of different pro-apoptotic proteins (see section 3.2.3). Phosphorylation of H2AX at ser139 is a rapid event following DNA damage and this was used as a marker for DNA damage response activated by Doxorubicin (Fig.3-6).

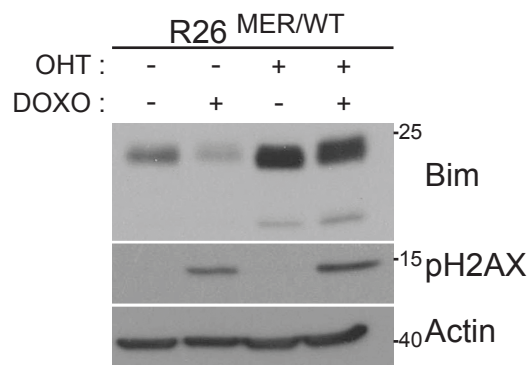


Figure 3-6- Bim is not induced by Doxorubicin

Immunoblots showing the induction of Bim and pH2AX by MYC activation and Doxorubicin treatment (8hrs), respectively. This figure is taken from (Muthalagu et al., 2014)

To analyse the requirement of Bim for MYC-induced sensitization *in vitro*, I used two different sub-apoptotic stimuli: γ -Irradiation (γ -IR) and ABT-737. MycER^{T2} activation in $R26^{MER/WT}$ MEFs cultured in full serum conditions or a single dose of γ -IR (5Gy) failed to drive apoptosis (Fig 3-7 A). Consistent with previous results, the combination of MycER^{T2} activation and a single dose of γ -IR (5Gy) resulted in a clear accumulation of dead cells as revealed by Annexin/PI staining (Maclean et al., 2003). However, in the absence of Bim, MYC-induced sensitization to γ -IR is attenuated (Fig.3-6 A). Similarly, 1 μ M of ABT-737 (BH3 mimetic) did not induce apoptosis in $R26^{MER/WT}$ MEFs after 48hrs, but concomitant MycER^{T2} activation and ABT-737 treatment resulted in a clear accumulation of dead cells as revealed by Annexin/PI staining and again this is Bim dependent (Fig.3-6 B). All these data suggest that Bim mediates pro-apoptotic signalling downstream of MYC.

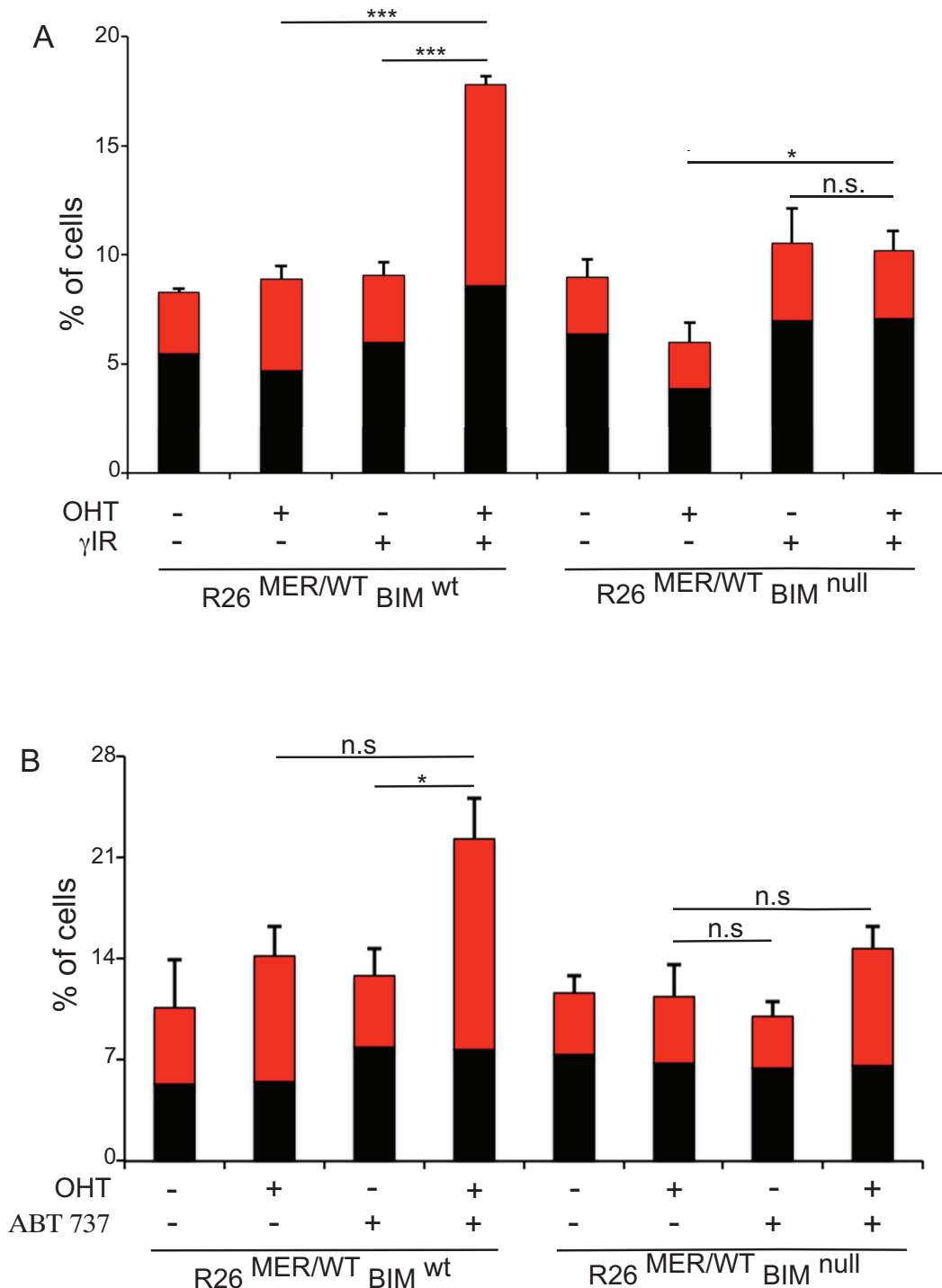


Figure 3-7- Bim is required for MYC-induced sensitization to irradiation and ABT-737

(A) Early passage $R26^{MER/WT}$ MEFs ($P < 5$) that are wt or null for *Bim* allele, were pre-treated with 100nm 4-OHT overnight, then irradiated with 5Gy and analyzed by Annexin V/PI staining 30hrs later. The graph represents the percentage of cells stained only for Annexin V (in black) and the cells stained for both Annexin V/PI (in red). Mean \pm SEM from representative experiments performed in biological triplicates. Similar results were obtained in at least 3 independent experiments (B) Early passage $R26^{MER/WT}$ MEFs ($P < 5$) that are WT or null for *Bim* allele, were co-treated with 100nM 4-OHT and +/- 1 μ M ABT-737 and stained for Annexin V/PI 48hrs later. The graph represents the percentage of cells stained only for Annexin V (in black) and the cells stained for both Annexin V/PI (in red). Mean \pm SEM from representative experiments performed in biological triplicates were shown. Similar results were obtained in at least 3 independent experiments. Two-tailed, unpaired T tests (from prism software) were used to calculate the statistical significance. ** $P < 0.01$; *** $P < 0.001$; ns, not-significant $P > 0.05$. This figure is taken from (Muthalagu et al., 2014)

3.2.3 Bim is a specific BH3-only protein required for MYC-induced apoptosis

BH3-only proteins act primarily by binding and neutralizing the pro-survival (anti-apoptotic) proteins (Czabotar et al., 2014). To determine whether Bim is a specific BH3-only protein required for MYC-induced apoptosis, I investigated the role of another BH3-only protein, Puma, in MYC-induced apoptosis. Puma and Bim share similar specificity towards the survival proteins. Both Bim and Puma are capable of binding with high affinity to all pro-survival proteins including Bcl2, Bcl-x_L and Mcl1. In addition, Bim and Puma have been proposed to activate effector Bcl2 proteins Bax and Bak directly (Happo et al., 2012). Moreover, loss of *Puma*, similar to loss of *Bim*, cooperates with Myc and accelerates B cell lymphomagenesis (Egle et al., 2004; Michalak et al., 2009). Therefore, the role of Puma in MYC-induced apoptosis in the intestine was tested. Activation of MycER^{T2} in *R26^{MER/MER};Puma* null mice (3day Tam) revealed that deletion of *Puma* modestly, but not significantly, reduced MYC-induced apoptosis in the small intestine compared to *Puma* replete controls (Fig. 3-8A top panel and B), whereas deletion of *Puma* had no effect on MYC-induced apoptosis in the colon (Fig.3-8A lower panel and C).

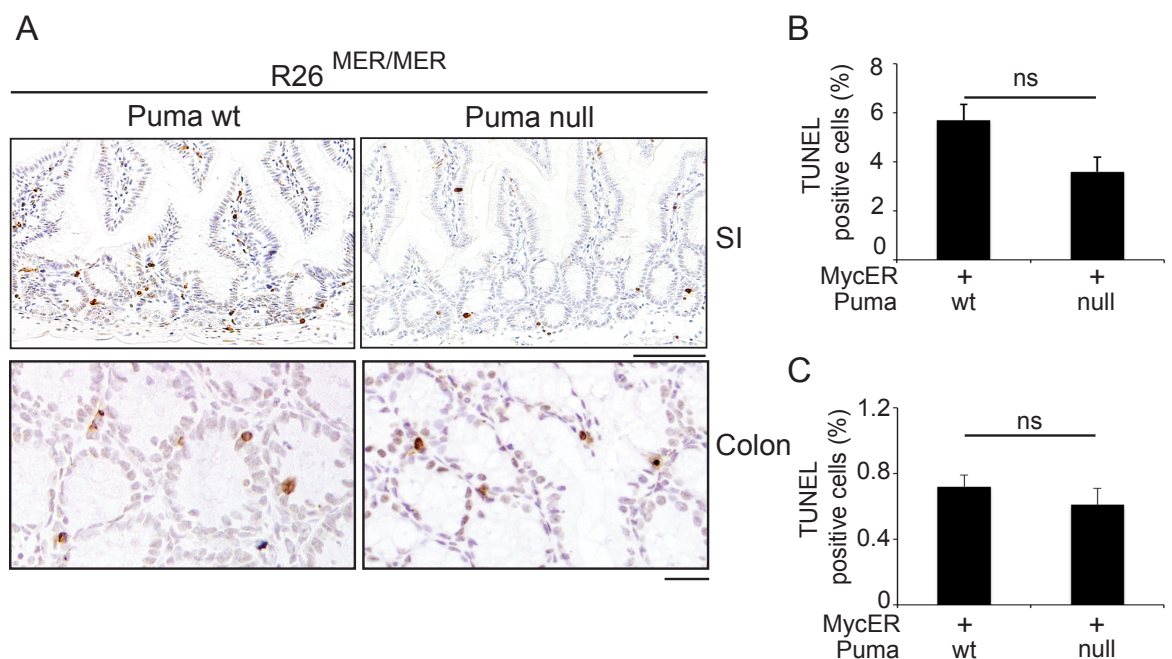


Figure 3-8- Puma is not required for MYC-induced apoptosis in the intestine

(A) Representative images of TUNEL staining of the small (SI) intestine and colon, of mice of the indicated genotypes (3day Tam). Scale bar represents 100 μ m. (B&C) Quantification (Mean \pm SEM) of TUNEL staining (percentage of total) in the small and colon respectively, of Tam-treated *R26^{MER/MER}* (n=3), *R26^{MER/MER};Puma* null (n=4). This figure is taken from (Muthalagu et al., 2014)

To investigate the role of Puma in MYC induced sensitization to Doxorubicin, $R26^{MER/MER};Puma$ null cohorts were treated with 3days of tamoxifen followed by Doxorubicin as discussed before (Section 3.2.2). Quantification of apoptotic cells in the liver, pancreatic islets and colon from 3dayTam+Dox treated $R26^{MER/MER};Puma$ wild type and $R26^{MER/MER};Puma$ null cohorts revealed that the deletion of *Puma* suppressed MYC and Doxorubicin induced apoptosis in all the three tissues (Fig 3-9A and B). This is not surprising because Puma is a downstream target of p53 and is required for p53 mediated DNA damage response and deletion of *Puma* abrogated Doxorubicin induced apoptosis in the small intestine (Fig. 3-10 A).

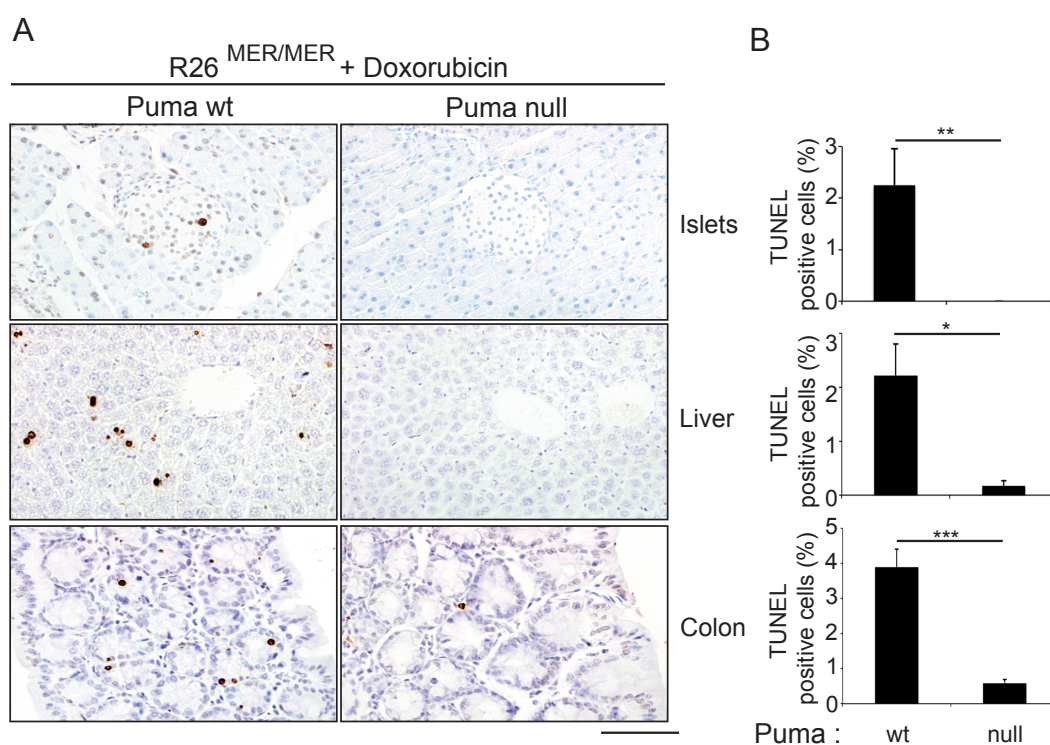


Figure 3-9- Puma is required for MYC induced sensitization to Doxorubicin

(A) Representative images of TUNEL staining of the pancreatic islets, liver and large intestine (LI) of the indicated genotypes treated with 3day Tam and Doxorubicin. The original magnification of the image is 20X and the scale bar represents 50 μ m (B) Quantification (Mean \pm SEM) of TUNEL staining (percentage of total) in the indicated tissues of Tam+Doxorubicin- treated $R26^{MER/MER}$ (n=3), $R26^{MER/MER};Puma$ null (n=3). Two-tailed, unpaired T tests (from prism software) were used to calculate the statistical significance. ** P< 0.01; *** P< 0.001; ns, not-significant P>0.05. This figure is taken from (Muthalagu et al., 2014)

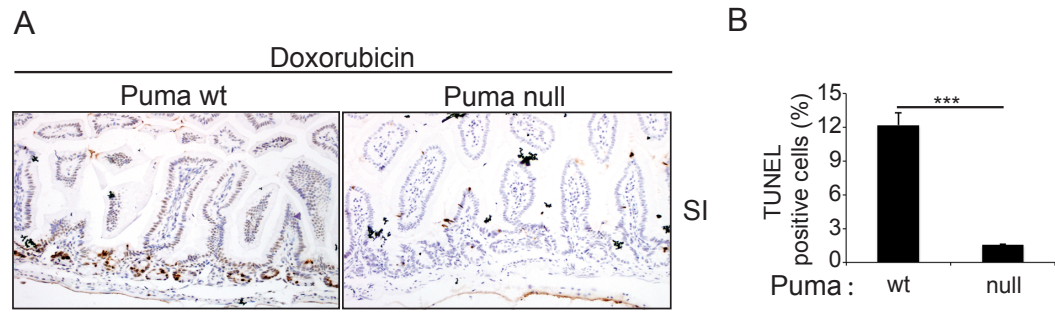


Figure 3-10- Puma is required for Doxorubicin induced apoptosis in the small intestine

(A) Representative images of TUNEL staining in the small (SI) intestine of mice of the indicated genotypes, treated with Doxorubicin (10mg/kg) for 24hrs. Scale bar represents 100 μ m (B&C) Quantification (Mean \pm SEM) of TUNEL staining (percentage of total) in the small intestine of doxorubicin-treated (n=3) mice of the indicated genotypes. This figure is taken from (Muthalagu et al., 2014)

The survival signalling pathway triggered by cytokines such as IGF-1 can effectively suppress MYC-induced apoptosis (Harrington et al., 1994a). One of the downstream effects of IGF-1-PI3K-AKT pathway is the phosphorylation-mediated inhibition of BH3-only protein Bad (Datta et al., 1997). To evaluate the role of Bad in MYC-induced apoptosis, a siRNA approach was employed. Two different siRNAs were used to deplete Bad in $R26^{MER/WT}$ MEFs and knockdown of the gene was confirmed by Q-RT PCR after 48hrs of transfection (Fig. 3-11 B). As shown in Figure 3-11A, activation of MycER^{T2} in cells cultured in 0.2% serum for 30hrs induced the same amount of apoptosis both in siControl and siBad cells, suggesting that Bad is not required for MYC-induced apoptosis *in vitro* (Fig.3-9). Thus, among the different pro-apoptotic BH3-only proteins investigated, Bim is specifically required for MYC-induced apoptosis.

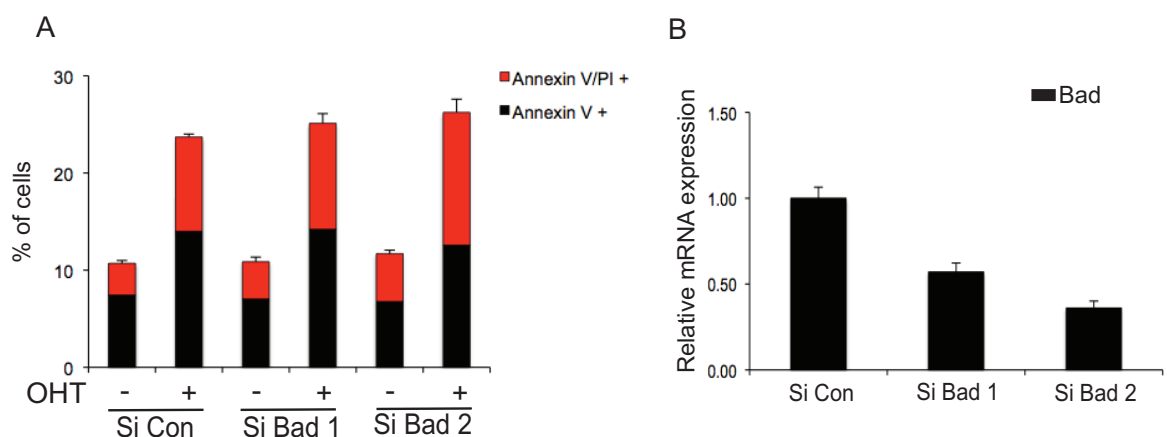


Figure 3-11- Bad is not required for MYC-induced apoptosis *In vitro*.

(A) Early passage MEFs (P<5) from E13.5 embryos of $R26^{MER/WT}$ mice were used for siRNA mediated depletion of Bad and siRNA against non-targeting region was used as a control. 48hrs after the depletion, cells were treated with 100nm 4-OHT for 30hrs under low serum conditions (0.2%). The graph represents percentage of cells stained only for Annexin V (in black) and the cells stained for both Annexin V/PI (in red). Mean \pm SEM from representative experiments performed in biological triplicates were shown. Consistent results were obtained in two independent experiments. (B) Q-RT PCR confirming the knock-down of Bad after 48hrs.

3.2.4 Bim is required specifically downstream of MYC

Bim is one of the potent BH3-only proteins with strong affinity to all survival proteins and is involved in apoptosis induced by various apoptotic stimuli (Akiyama et al., 2009; Chen et al., 2005). Therefore, it is important to determine the specificity of Bim requirement. To answer this question, I looked at the Doxorubicin induced apoptosis in the small intestine. The *Bim* Wt and *Bim* null cohorts were treated with one dose of Doxorubicin (10mg/kg), tissues were harvested 24hrs after the treatment and the small intestine was analysed for apoptosis using TUNEL as a marker. From fig 3-12, it is clear that there is no significant difference between Doxorubicin induced apoptosis in the *Bim* wt and *Bim* null cohorts. (Fig.3-12A and B), indicating that Bim is not required for Doxorubicin mediated apoptosis in the small intestine.



Figure 3-12- Bim is not required for Doxorubicin induced apoptosis in the small intestine

(A) Representative images of TUNEL staining in the small (SI) intestine of mice of the indicated genotypes, treated with Doxorubicin (10mg/kg) for 24hrs. The scale bar represents 100 μ m (B&C) Quantification (Mean \pm SEM) of TUNEL staining (percentage of total) in the small intestine of doxorubicin-treated (n=3) mice of the indicated genotypes. Two-tailed, unpaired T test was used to calculate the statistical significance. ns represents not-significant. This figure is taken from (Muthalagu et al., 2014)

To investigate the role of Bim in Doxorubicin mediated apoptosis *in vitro*, I treated the primary MEFs, wild type or null for *Bim* with Doxorubicin (1 μ g/ml) and the apoptosis was measured 48hrs later by Annexin V/PI flow cytometry. Again, *Bim* deletion had no effect on Doxorubicin-induced killing in MEFs (Fig.3-12), indicating a specific requirement of Bim for MYC-induced apoptosis but not in response to other pro-apoptotic stimuli such as doxorubicin.

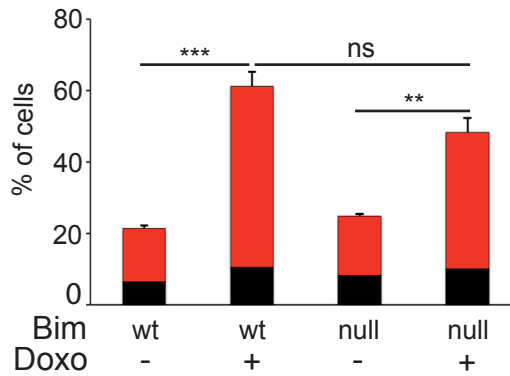


Figure 3-13- Bim is not required for Doxorubicin induced apoptosis in MEFs

Bim wt and null cells cultured in full serum conditions were treated with Doxorubicin (1 μ g/ml) and apoptosis was measured 48hrs after the treatment. The graph represents percentage of cells stained only for Annexin V (in black) and the cells stained for both Annexin V/PI (in red). Mean \pm SEM from the representative experiment performed in biological triplicates was shown. Consistent results were obtained in 3 independent experiments. Two-tailed, unpaired T tests (from prism software) were used to calculate the statistical significance. ** $P < 0.01$; *** $P < 0.001$; ns, not-significant $P > 0.05$. This figure is taken from (Muthalagu et al., 2014)

3.2.5 Bim is directly regulated by MYC

To examine the expression level of Bim upon MycER^{T2} activation, *R26^{MER/MER}* mice were treated with Tamoxifen for 2 days or 3 days. RNA was extracted from the small intestine of these experimental cohorts and Q-RT PCR for Bim-EL, a predominant isoform of Bim was carried out. As shown in Fig 3-14A, there was a modest but not statistically significant increase in the expression of Bim-EL in the small intestine of Tam treated mice compared to its untreated controls. Also, the increase in Bim-EL protein expression was evident in the 3 day Tam treated small intestines of the *R26^{MER/MER}* mice (Fig. 3-13B). Epithelial cells (see section 2.3.11) were extracted from the small intestine of the respective mice and used for protein detection.

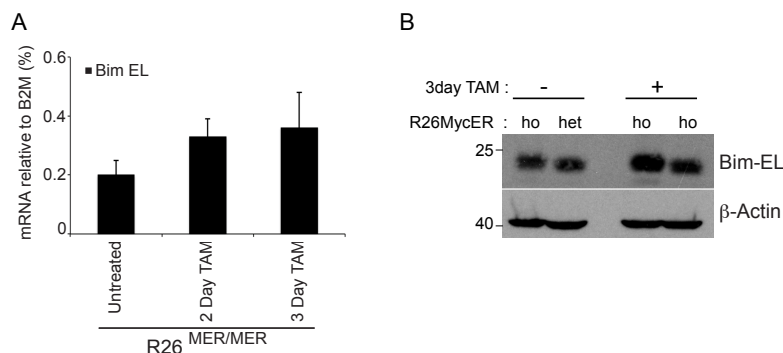


Figure 3-14- MYC activation results in increase in Bim expression in the small intestine

(A) Quantitative real-time PCR analysis of Bim-EL mRNA expression in the small intestine of *R26^{MER/MER}* mice treated with tamoxifen (50mg/kg) for indicated timepoints (n=3), β 2-microglobulin was used as housekeeping gene. (B) Immunoblot of Bim expression in the epithelial cells from the small intestine of mice with indicated genotypes that are vehicle treated (-) or Tam treated(+) for 3 days (n=3). This figure is taken from (Muthalagu et al., 2014)

I used $R26^{MER/WT}$ MEFs, to determine if MYC regulates Bim expression directly. MycER^{T2} was activated by the addition of 4-OHT for different time points and RNA was isolated to analyse the expression of Bim by Q-RT PCR. As shown in Fig 3-15A, activation of MycER^{T2} resulted in an increase in Bim-EL RNA level even after 6hrs and returned to basal level after 24hrs. Ornithine decarboxylase1(Odc1), a known MYC target was used as a positive control, although the kinetics of activation were different for Bim and Odc1, the strength of the increase was comparable. Similarly, MycER^{T2} was activated by the addition of 4-OHT for similar time points and protein was isolated to analyse the expression of Bim by western blot. The increase in RNA level was followed by accumulation of Bim-EL protein (Fig.3-15 B).

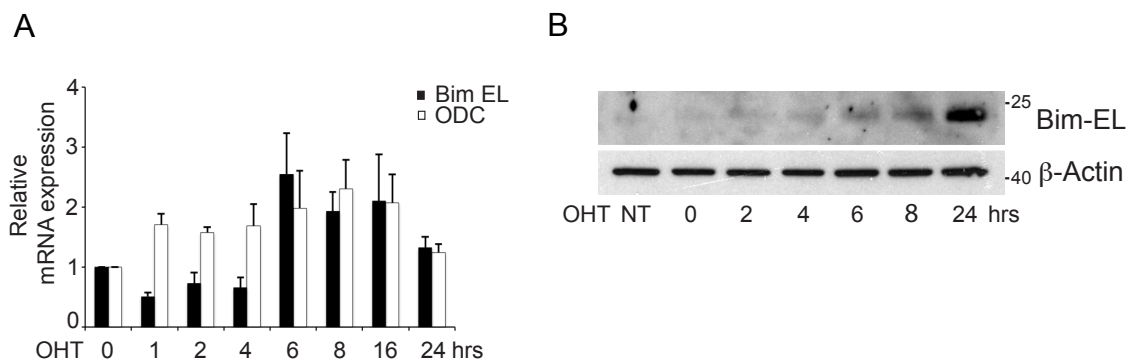


Figure 3-15- MYC activation induces Bim expression *in vitro*

(A) Q-RT PCR analysis of Bim-EL mRNA expression after 4-OHT (100nM) treatment for indicated time points in $R26^{MER/WT}$ MEFs, β 2-microglobulin was used as the housekeeping gene control (n=3). (D) Immunoblot showing Bim expression after 4-OHT (100nM) treatments for indicated time points in $R26^{MER/WT}$ MEFs. This figure is taken from (Muthalagu et al., 2014)

Furthermore, to determine if Bim is a direct MYC target I employed a gene specific chromatin immunoprecipitation (CHIP) assay using N262 antibody, which recognizes both endogenous murine MYC and exogenous MycER^{T2}. Following CHIP, Q-PCR was used to amplify the bound DNA region using specific primers corresponding to the Bim promoter region and the control region (see section 2-10). CHIP analysis in $R26^{MER/WT}$ MEFs revealed that endogenous MYC binds to the *Bim* promoter region and that there is an increase in *Bim* promoter occupancy by MYC, in response to 4-OHT (Fig. 3-16A). The control region, located several hundred base pairs downstream of the coding region was used to test the specificity of MYC binding and as expected there was no clear MYC binding (Fig. 3-16A white bars). CHIP analysis in HeLa cells confirmed the binding of MYC to the human *BIM* promoter region (Fig.3-16B).

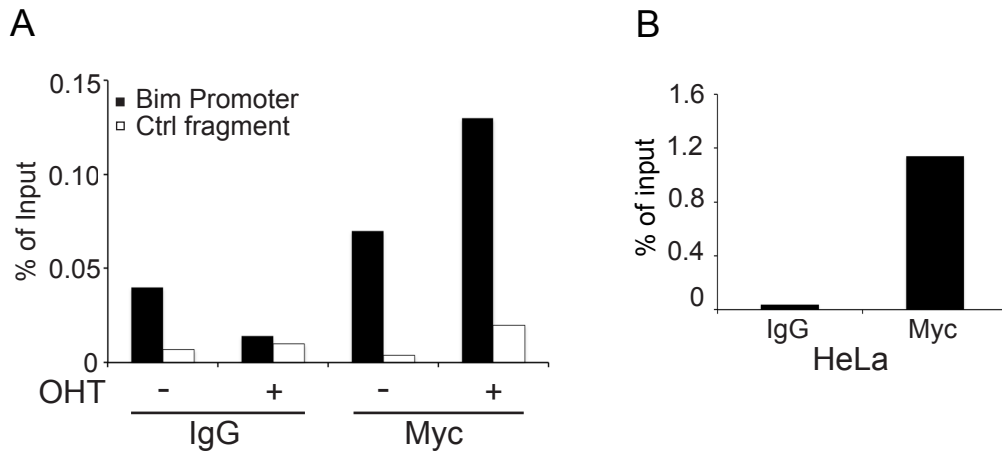


Figure 3-16- MYC binds to the Bim promoter region

(A) Chromatin immunoprecipitation on $R26^{M^{ER}/WT}$ MEFs treated with or without 4-OHT (100nM for 1hr) using IgG or MYC (N262) antibody, followed by Q-RT PCR with primers amplifying *Bim* promoter region or control fragment (n=2). (B) Chromatin immunoprecipitation on HeLa cells using IgG or MYC (N262) antibody, followed by Q-RT PCR with primers amplifying *BIM* promoter region (n=2). This figure is taken from (Muthalagu et al., 2014)

3.2.6 A threshold level of BIM is required for MYC induced-apoptosis

Activation of MycER^{T2} in a heterozygous $R26^{M^{ER}/WT}$ setting failed to induce apoptosis in the small intestine, whereas apoptosis was evident in the same tissue of homozygous $R26^{M^{ER}/M^{ER}}$ mice after MycER^{T2} activation, indicating that a threshold level of MYC deregulation is required to induce apoptosis (Murphy et al., 2008). Therefore, I asked if a threshold level of Bim is required to mediate MYC-induced apoptosis. MycER^{T2} was activated by administration of tamoxifen (IP) for 3 days in $R26^{M^{ER}/M^{ER}};Bim$ null, and $R26^{M^{ER}/M^{ER}};Bim$ heterozygous cohorts and tissues were harvested 24hrs after the final induction. Apoptosis analysis using TUNEL staining revealed that the MycER^{T2} activation did not induce apoptosis in either the small intestine or colon of *Bim* null and *Bim* heterozygous cohorts (Fig. 3-17). Thus, haploinsufficiency for *Bim* rescues the $R26^{M^{ER}/M^{ER}}$ intestines from MYC-induced apoptosis. This is in agreement with a previous report that haploinsufficiency of *Bim* accelerates Myc induced lymphomagenesis (Egle et al., 2004).

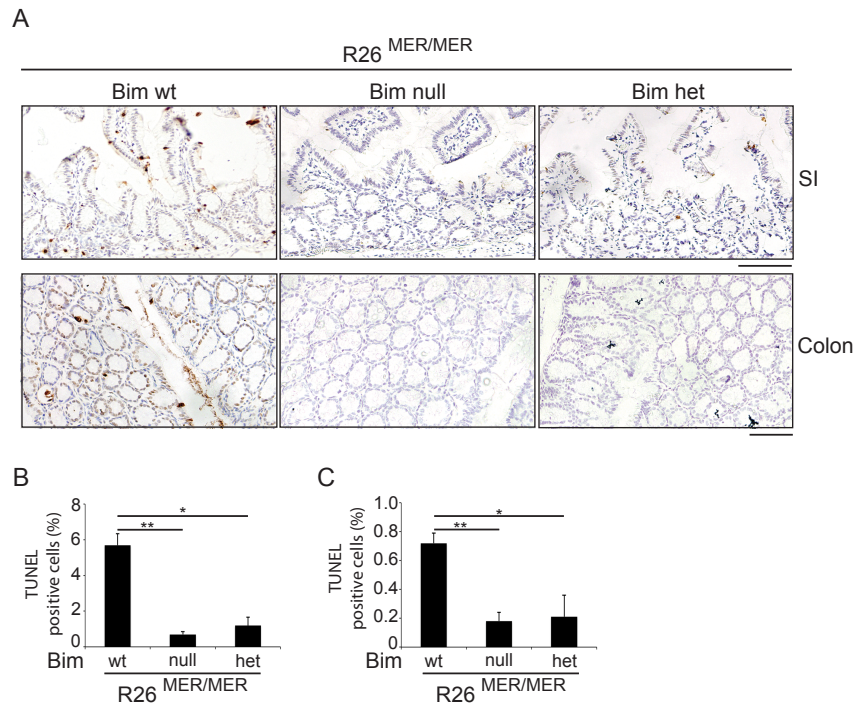


Figure 3-17- A threshold level of Bim is required for MYC induced apoptosis.

(A) Representative images of TUNEL staining of apoptotic cell in small (SI) intestine and colon, of mice of the indicated genotypes, treated consecutively with tamoxifen (50mg/kg) to activate MycER^{T2} for 3 days. Scale bar represents 100µm. Quantification (Mean ± SEM) of TUNEL staining (percentage of total) in the small intestine (B) and in the Colon (C) of Tam-treated R26^{MER/MER} (n=3), R26^{MER/MER}; Bim null (n=4), R26^{MER/MER}; Bim het (n=3). Two-tailed, unpaired T tests (from prism software) were used to calculate the statistical significance. ** P< 0.01; *** P< 0.001; ns, not-significant P>0.05. This figure is taken from (Muthalagu et al., 2014)

3.3 Discussion

In addition to its tumour promoting role, MYC is also a potent inducer of programmed cell death. This is seen as a built-in failsafe mechanism to protect against uncontrolled proliferation. Indeed, apoptosis is a barrier for MYC-induced tumourigenesis, as impairment of apoptotic pathways accelerates Myc-induced lymphomagenesis (Egle et al., 2004; Strasser et al., 1990) and apoptosis regulators are often modulated in MYC tumours (Eischen et al., 2001). There is evidence linking Bcl2 family members to MYC-induced apoptosis (Hoffman and Liebermann, 2008; Meyer et al., 2006). Here, I show that the BH3-only protein Bim is the primary mediator of MYC-induced apoptosis *in vitro* and *in vivo*. Bim is required for MYC induced apoptosis under various settings and in multiple solid tissues tested. In line with previous reports, I also show that Bim is a direct transcriptional target of MYC (Campone et al., 2011). Chip-sequencing analysis performed by our collaborators revealed strong binding of MYC to *BCL2L11* (encoding Bim) promoter region in non-transformed MCF10A human epithelial cells, strikingly in these cells no MYC binding was observed at other Bcl2 family genes, including *BCL2*, *BCLX*,

BBC3 (encoding Puma), *PMAIP1* (encoding Noxa), *BID*, *BAD*, *BAX*, or *BAK*. In contrast, profiling of Bcl2 family proteins promoter occupancy in tumour cells derived from a genetically engineered mouse model of pancreatic cancer (driven by *KRAS*^{G12D} and *p53*^{R172H}), which express high levels of MYC, revealed MYC binding to all the above promoters, except for Noxa and Bak (Muthalagu et al., 2014). Differences in chromatin occupancy could be explained by many factors including, tissue specific chromatin configuration or differences in species. However, a recent report studying the promoter occupancy by different level of MYC suggests that target genes can be classified based on the presence of low-affinity or high-affinity MYC binding sites (Walz et al., 2014). Hence, it can be hypothesized that Bim (*BCL2L11*) has a high-affinity binding site and even low-level of MYC deregulation can regulate its expression. On the other hand, other Bcl2 proteins have low-affinity binding sites and thus require high (tumourigenic) level of MYC for binding. Thus higher levels of MYC may elicit stronger pro-apoptotic signalling by engaging more pro-apoptotic Bcl2 family members.

Surprisingly, loss of Puma, a closely related BH3-only protein, failed to phenocopy loss of Bim as deletion of *Puma* did not affect MYC-induced apoptosis *in vivo*. Conversely, Puma is required for Doxorubicin induced apoptosis in the small intestine and Bim is not. However, both are required for apoptosis driven by the combination of MYC activation and Doxorubicin. This suggests a specific requirement for BH3-only proteins to transduce specific pro-apoptotic signals, despite their shared similarity in anti-apoptotic buffering.

There is also evidence suggesting a potential involvement of Arf-p53 pathway in MYC-induced apoptosis. Loss of p19Arf or p53 cooperates with Myc to accelerate lymphomagenesis in the E μ Myc lymphoma model and both have been previously linked to suppress MYC-induced apoptosis (Bertwistle and Sherr, 2007; Schmitt et al., 1999). In contrast, my attempt to identify a role for p19Arf in MYC-induced apoptosis and MYC-induced sensitization in several mouse tissues failed to reveal any requirement for p19Arf, despite the fact that MycER^{T2} activation is able to induce p19Arf expression (Murphy et al., 2008). In a different study, two MYC mutants (P57S and T58A), commonly found in Burkitt's lymphoma, were transfected to murine haematopoietic stem cells, which were then used to reconstitute the haematopoietic system of lethally irradiated recipient animals showed that the recipients of stem cells infected with MYC mutants developed tumours with high penetrance and short latency. Importantly, the mutant MYC proteins retained their ability to promote proliferation and activate p53, but are defective in engaging apoptosis due to their failure to induce Bim (Hemann et al., 2005) suggesting that p53 is

not sufficient to drive MYC induced apoptosis. However, because the level of MYC expressed from the *Rosa26* locus is not sufficient to drive apoptosis in B cells, I was unable to compare our model with E μ Myc and therefore one cannot exclude the possibility of tissue specific requirement of p19Arf for MYC induced apoptosis.

Disruption of the Arf-Mdm2-p53 tumour suppressor has been reported in MYC-induced lymphoma with tumours sustaining either p53 or p19Arf loss of function and this was believed to be selective pressure imposed by tumour cells to suppress MYC-induced apoptosis via mutating Arf-p53 pathway (Eischen et al., 1999). However, apoptosis is not the only outcome of Arf-p53 pathway and it can restrain tumourigenesis through alternate mechanisms such as cell cycle arrest and senescence. An elegant study compared Bcl-x_L gain of function and p19Arf loss of function for Myc oncogenesis in a pIns-MycER^{TAM} β cell model (MycER is expressed under the control of Insulin promoter) and found that both lesions cooperate with MYC via distinct mechanisms. Bcl-x_L overexpression cooperates with MYC by specifically blocking MYC induced apoptosis, whereas loss of p19Arf cooperates by facilitating MYC induced proliferation (Finch et al., 2006).

In conclusion, I have shown that Bim is required and p19Arf is dispensable for MYC-induced apoptosis in multiple solid tissues. Prophylactic treatments of ABT-737, a BH3-mimetic that acts primarily by blocking anti-apoptotic Bcl-2 proteins, suppresses lymphomagenesis in E μ Myc mice (Kelly et al., 2013). Given the prevalence of MYC overexpression in human cancers, my data suggests that augmenting intrinsic apoptotic response of MYC through the use of a BH3 mimetic might be a successful therapeutic strategy.

3.4 Future work

Although MYC induces BH3-only protein Bim to promote apoptosis, I propose that it is expressed below the apoptotic threshold in cancer cells and is therefore unable to buffer the anti-apoptotic proteins. Hence, augmenting the intrinsic apoptotic response of MYC could be a successful therapeutic strategy. To prove this, it would be useful to treat MYC dependent cancer cells with a BH3-mimetic. BH3-mimetics are small molecule inhibitors, which resemble BH3-only proteins in their mode of action. For example, BH3-mimetic ABT-737 inhibits anti-apoptotic proteins Bcl2 and Bcl-x_L by binding to the hydrophobic groove of these proteins similar to BH3-only proteins. Although, I tested the efficacy of

ABT-737 against a primary MYC driven murine pancreatic cancer cells (chapter 4), it would be insightful to use such drugs in MYC driven cancer models (GEMM).

4 Investigating the synergy between *MYC* and *Kras*^{G12D} in pancreatic tumourigenesis

4.1 Introduction

Pancreatic ductal adenocarcinoma (PDAC) ranks amongst the most lethal of human malignancies with poor prognosis, median survival of just 6 months and the lowest five-year survival rate (<5%) (www.cancerresearch.org/cancer-info/cancerstat/types/pancreas). Clinical and histopathological analyses have identified and classified precursor lesions for PDAC. They include pancreatic intraepithelial neoplasias (PanINs), intraductal papillary mucinous neoplasms (IPMNs) and mucinous cystic neoplasm (MCN). Furthermore, molecular analyses of evolving PDAC has identified a number of genetic and molecular events accompanying these histopathological phenotypes (Hezel et al., 2006). Amongst these mutations, the most common and earliest genetic mutation found in human cancer is the activating mutation of the oncogene KRAS. KRAS belongs to the Ras family of GTPase proteins, which cycle between 'on' and 'off' states that are conferred by the binding of GTP and GDP respectively. Under physiological conditions, GTPase-activating proteins (GAPs) attenuate Ras signalling by accelerating Ras mediated GTP hydrolysis. Activating point mutations at codon 12 result in a substitution of glycine with aspartate, valine, or arginine; resulting in a protein insensitive to GAPs and leading to persistent tumour promoting Ras kinase activity (Pylayeva-Gupta et al., 2011). Other commonly found genetic mutations in PDAC include inactivating mutations in tumour suppressor genes encoding p16, p53 and Smad4 (Perez-Mancera et al., 2012).

Recent advances in transgenic technology have enabled the development of clinically relevant mouse models to further understand the biology of PDAC. A major breakthrough emerged from the development of a conditional mutant *Kras*^{G12D} model (Hingorani et al., 2003; Jackson et al., 2001), where exon 1 of endogenous *Kras* was modified to contain G to A transition in codon 12. This mutation, frequently found in human pancreatic cancer, compromises its GTPase activity leading to constitutively active Kras protein and its downstream signalling. A stop cassette flanked by functional LoxP sites (LSL) was inserted upstream of the modified exon 1 (*LSL-Kras*^{G12D}), thus mutant protein is expressed only after Cre mediated excision of the Stop element (Fig. 4-1B). This model was further used in combination with different cooperating mutations to understand the biology of PDAC. Although a number of different mouse models have been developed so far, poor survival rate and intrinsically resistant pancreatic tumour demands development

of new mouse models for further understanding of the disease and identification of potential new drug targets.

A growing body of evidence supports a pivotal role for MYC in pancreatic cancer initiation and maintenance (Saborowski et al., 2014). Recently, a study using the *Kras*^{G12D} and mutant p53 (p53^{R172H}) driven mouse model for pancreatic cancer have shown that genetic deletion of just one allele of *Myc* significantly delayed pancreatic tumourigenesis (Walz et al., 2014). Genetic mutation of *MYC* in pancreatic cancer is infrequent however MYC lies downstream of multiple signalling pathways that are frequently deregulated in pancreatic cancer. For example, alterations of Hedgehog and Wnt/Notch signalling have been found in 100% of human PDAC tumours and MYC is a known target of both these pathways (Morris et al., 2010). Furthermore, the phosphatidylinositol 3-kinase (PI3K) pathway, which has been reported to be constitutively active in pancreatic cancer, leads to Nf-kB dependent MYC stabilization (Skoudy et al., 2011). Also, nuclear factor of activated T cells protein c1 (NFATc1), which was found to be significantly overexpressed in human pancreatic cancer, regulates MYC expression directly (Buchholz et al., 2006).

Given the role of MYC in pancreatic cancer, I wanted to characterize a new mouse model to determine whether MYC deregulation can act as a driver mutation for pancreatic tumourigenesis. Then, I aimed to determine whether there are synergistic interactions between MYC overexpression and *Kras*^{G12D} in pancreatic tumourigenesis. Importantly, establishing a MYC dependent pancreatic model will enable us to exploit MYC-induced vulnerabilities as a therapeutic strategy for pancreatic cancer.

4.1.1 Mouse models used to address these aims

To investigate the cooperation between oncogenic *Kras* and MYC in pancreatic tumourigenesis, I used the previously described conditional *Kras*^{G12D} mice, where exon 1 of endogenous *Kras* is modified to contain G to A transition in codon 12 (Jackson et al., 2001) (Fig. 4-1B). To overexpress MYC, human MYC cDNA is expressed under the control of the constitutive *Rosa26* locus, preceded by a LoxP-Stop-LoxP cassette (*R26*^{LSL-MYC}) (Fig. 4-1A). The transgenes are expressed only after Cre mediated excision of the Stop element.

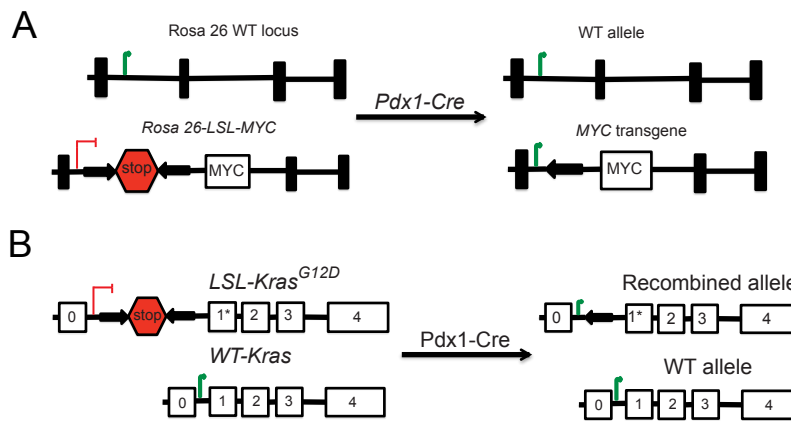


Figure 4-1- Schematic representation of Conditional *LSL-Kras*^{G12D/+} and *R26*^{LSL-MYC/+} mouse model

(A) Simplified schematic representation of transgene *MYC* under *Rosa26* locus, block arrows represent LoxP sites flanking a stop cassette, Cre mediated excision of the stop cassette results in the expression of *MYC* transgene. (B) Simplified schematic representation of conditional *Kras*^{G12D} allele (* represents modified exon) knocked into the endogenous locus. Block arrows represent LoxP sites flanking a stop cassette, Cre mediated excision of the stop cassette results in the expression of mutant *Kras*.

4.2 Results

4.2.1 Pancreas specific expression of mutant *Kras* and *MYC*

Pancreas specific expression of *Kras*^{G12D} and *MYC* was achieved by interbreeding above mentioned conditional mice with animals that express Cre recombinase from the pancreatic tissue specific promoter *Pdx1*. *Pdx1* is a transcription factor that is expressed as early as E8.5 in pancreatic progenitor cells (Burlison et al., 2008). Thus, tissues that do not express Cre recombinase are functionally heterozygous for the endogenous loci. To ascertain the presence or successful recombination of the targeted alleles, genomic DNA was extracted from the end stage pancreatic tumours of respective genotypes (Fig. 4-2) and PCR for recombined and/or targeted allele was carried out as described in section 2.4. The presence of a band corresponding to the modified *Rosa26* locus (320bp), confirmed the presence of transgene *MYC* in the pancreas (Fig. 4-2A). The presence of a band corresponding to the recombined *Kras*^{G12D} allele (620bp), confirmed that the gene is successfully recombined and retained (Fig. 4-2B). The presence of a band corresponding to the wild type *Rosa26* locus (605bp) or wild type *Kras* (600bp) confirmed that the respective allele was present in heterozygous condition (Fig. 4-2A, B). A pancreas tissue from a wild type (for the transgene) mouse was used as a negative control (Lane 2 of Fig. 4-2A, B).

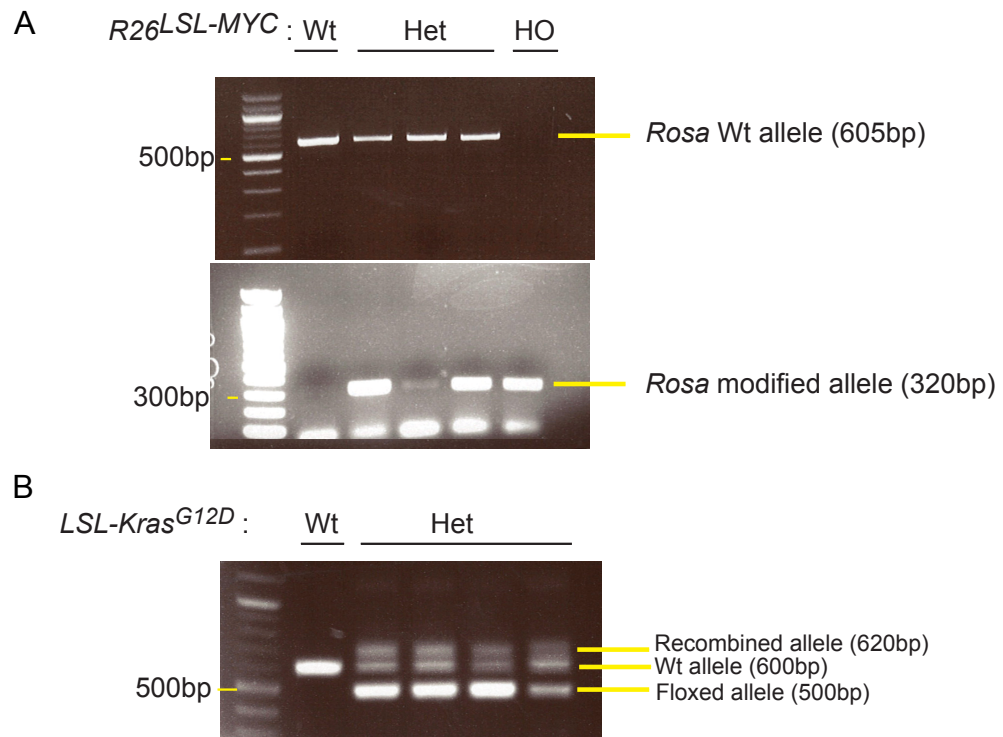


Figure 4-2- Pancreas specific expression of MYC and mutant *Kras*

(A) A PCR from the pancreas of wild type (wt) or end stage pancreatic tumour of heterozygous and homozygous $R26^{LSL-MYC}$ mice. 605 bp band represents wild type $Rosa26$ locus and 320 bp band represents $Rosa26$ locus with transgene MYC. (B) Recombined PCR from wild type or $Kras^{G12D}$ only mice (2nd and 3rd lane) or from pancreatic tumour of KMC ($Pdx1-Cre;R26^{LSL-MYC/+};LSL-Kras^{G12D/+}$) mice, recombined (620bp) and targeted (500bp) alleles were present in the pancreas of transgenic mice but not in the pancreas of wild type mice.

4.2.2 MYC accelerates $Kras^{G12D}$ induced pancreatic tumourigenesis

To determine whether there is synergistic interactions between MYC overexpression and $Kras^{G12D}$ to promote pancreatic tumourigenesis, cohorts of $Pdx1-Cre;R26^{LSL-MYC/+};LSL-Kras^{G12D/+}$ (KMC) and $Pdx1-Cre;R26^{LSL-MYC/+}$ (MC) mice were generated. It has been previously reported that pancreas specific expression of $Kras^{G12D}$ (KC) induces precursor lesions (PanINs) that rarely progress to adenocarcinoma (Hingorani et al., 2003). However, overexpression of MYC together with $Kras^{G12D}$ accelerated pancreatic tumourigenesis and dramatically reduced the lifespan of the compound mice (Fig. 4-3A). The median survival of KMC mice is 50 days (n=24) compared to 355 days of MC mice (n=12). 100% of the mice (24/24) with the pancreatic activation of MYC and $Kras^{G12D/+}$ succumbed to aggressive pancreatic tumours (Fig. 4-3B). As MC mice lived longer, a cohort of $Pdx1-Cre;R26^{LSL-MYC/+}$ (MC, n=3) was euthanized at 60 days of age and the pancreas was harvested. Similarly, a cohort of $Pdx1-Cre;LSL-Kras^{G12D}$ (KC, n=3) was euthanized at 60

days of age and the pancreas was harvested. They serve as age-matched controls to compare the histological features of pancreas from KC, MC and KMC mice. At this age (60 days), MC mice display histologically normal pancreas with abundant acinar tissue, scattered islets of Langerhans and normal looking ducts (Fig. 4-3B). KC mice on the other hand display PanIN lesions (Fig. 4-3B)

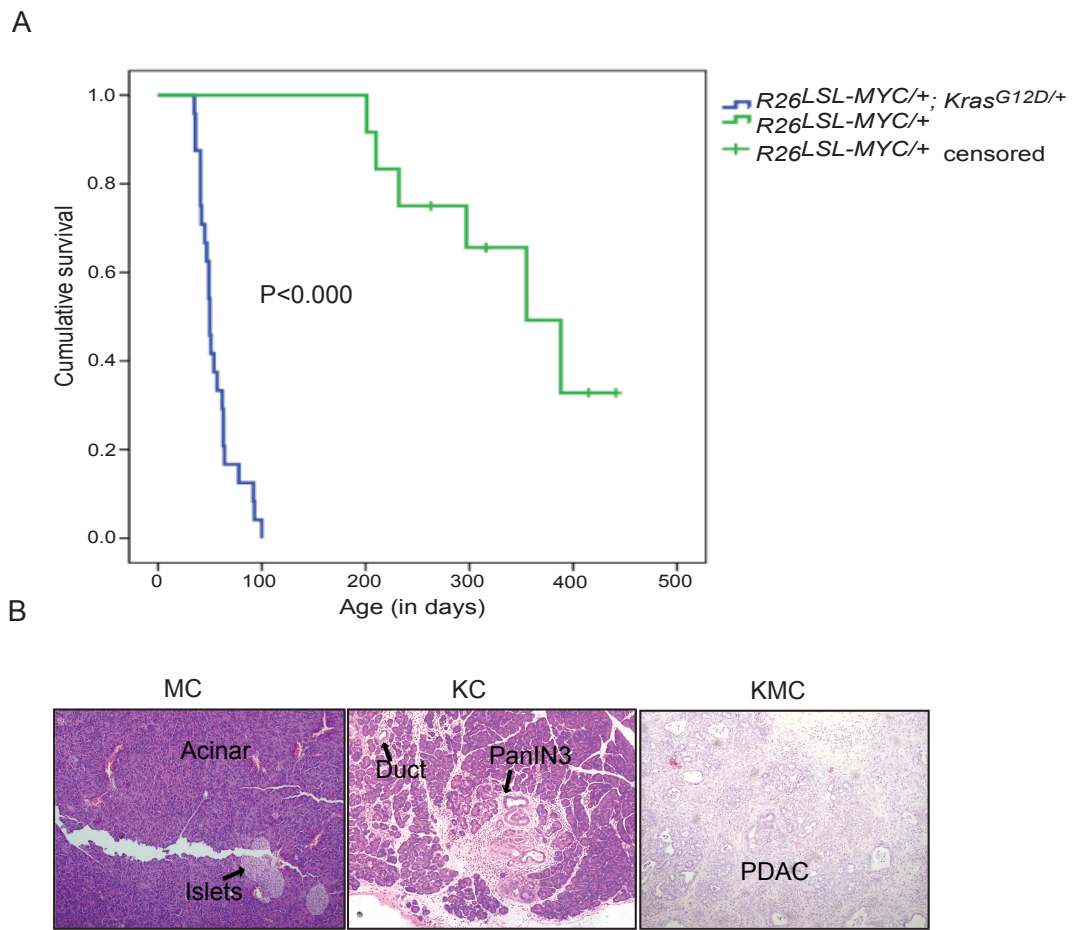


Figure 4-3- MYC cooperates with mutant Kras in driving pancreatic ductal adenocarcinoma

(A) Kaplan-Meier survival curve of *Pdx1-Cre;R26^{LSL-MYC/+};LSL-Kras^{G12D}* (KMC, n=24) and *Pdx1-Cre;R26^{LSL-MYC/+}* (MC, n=12) cohorts, P value is calculated using log-rank tests (SPSS) (B) Representative example of H&E staining of age matched *Pdx1-Cre;R26^{LSL-MYC/+}* (MC, n=3), *Pdx1-Cre; LSL-Kras^{G12D}* (KC, n=3) displaying PanIN3, and end stage PDAC from KMC cohorts. Scale bar represents 100 μ m.

The majority of KMC tumours were well-differentiated PDAC. 46% of mice exhibited exclusively tumours with ductal morphology with characteristic expression of epithelial marker pan-cytokeratin (Table 4-1 and Fig.4-4 left panel). 50% of mice displayed tumours with mixed pathology, ductal and neuro-endocrine tumours. Neuro-endocrine tumours display strong expression of neuro-endocrine marker synaptophysin, and a weak or patchy

cytokeratin staining (Fig. 4-4 right panel). One out of 24 (4%) mice exhibited exclusively tumours resembling neuro-endocrine or islet cell tumours. To examine the proliferation status of KMC tumours, IHC for proliferation marker Ki67 was performed. As shown in Fig. 4-5, both the tumour types (Neuro-endocrine and PDAC) were positive for Ki67, suggesting that they are actively proliferating.

On the other hand, only 50% (6/12) of *Pdx1-Cre;R26^{LSL-MYC/+}* (MC) mice developed pancreatic tumours (Table 4-1). These were primarily poorly differentiated tumours, which displayed different grades of synaptophysin staining and differential cytokeratin staining (Table 4-1 and Fig. 4-10 left panel).

Table 4-1 Table summarising the histological features of pancreatic tumours in KMC and MC mice

Genotype	PDAC	Neuro-Endocrine tumours	Mixed tumours	Others
KMC <i>Pdx1- Cre ;</i> <i>R26^{LSL-MYC/+}.</i> <i>LSL-Kras^{G12D/+}</i>	11/24	1/24	12/24	0/24
MC <i>Pdx1- Cre ;</i> <i>R26^{LSL-MYC/+}</i>	0/12	1/12	0/12	5/12

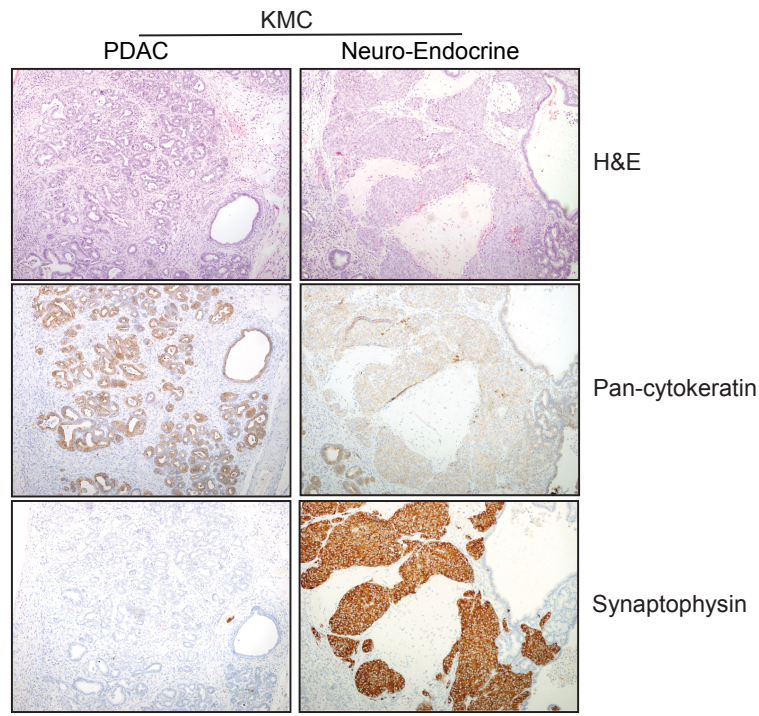


Figure 4-4- KMC mice exhibit tumours with mixed pathology

A representative example of KMC tumours showing histological features of PDAC (left panel) and neuro-endocrine tumours (right panel). Pan-cytokeratin and synaptophysin were used as a marker for epithelial and neuro-endocrine cells respectively. Scale bar represents 100µm and the original magnification is 10X.

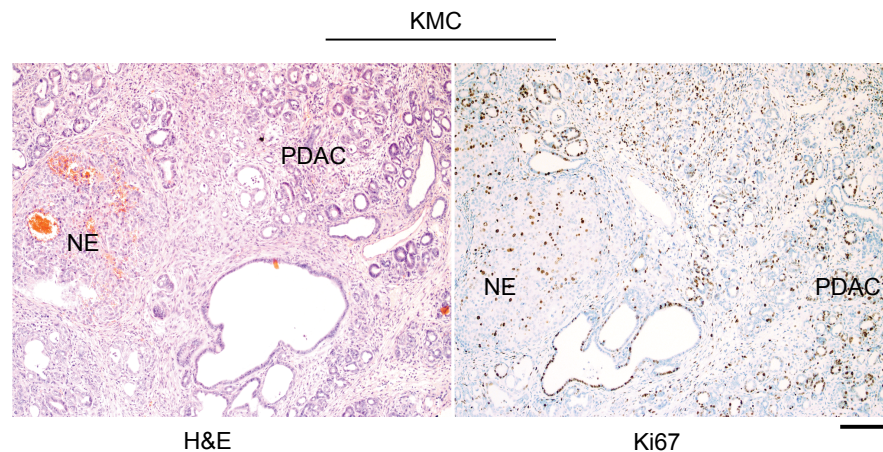


Figure 4-5- IHC for Ki67 revealed that KMC tumours are actively proliferating

H&E staining and adjacent section stained for Ki67 shows that both Neuro-endocrine (NE) tumours and PDAC are proliferating. Scale bar represents 100µm and the original magnification is 10X.

4.2.3 mTOR and Raf/MEK/Erk pathways are active in MYC and $Kras^{G12D}$ induced tumours

mTOR and MAPK pathway activation status in the KMC tumours were determined by IHC. PDAC is known to be very heterogeneous disease with different pathways activated

in different set of patients. A recent report, reported activation of the mTOR signalling cascade in a subset of human PDACs (Utomo et al., 2014). To evaluate the activity of the mTOR pathway, an IHC for phospho-S6 ribosomal protein (Ser240/244) (pS6), downstream target of mTOR was carried out. IHC for pS6 indicated that there was increase in staining intensity in KMC tumours compared to age matched *Kras^{G12D}* and *R26^{LSL-MYC/+}* tissue, suggesting that mTOR pathway is active in KMC tumours (Fig. 4-6). As shown in Fig.4-6, *Kras^{G12D}* (KC) induced PanIN displayed no staining, whereas small portion of acinar region of *R26^{LSL-MYC/+}* (MC) mice displayed weak staining to pS6. As there is no clear staining of pS6 in *R26^{LSL-MYC/+}* expressing pancreas or *Kras^{G12D}* induced PanINs, one can postulate that a spontaneous somatic mutation deregulating mTOR pathway must have occurred during progression of the tumour.

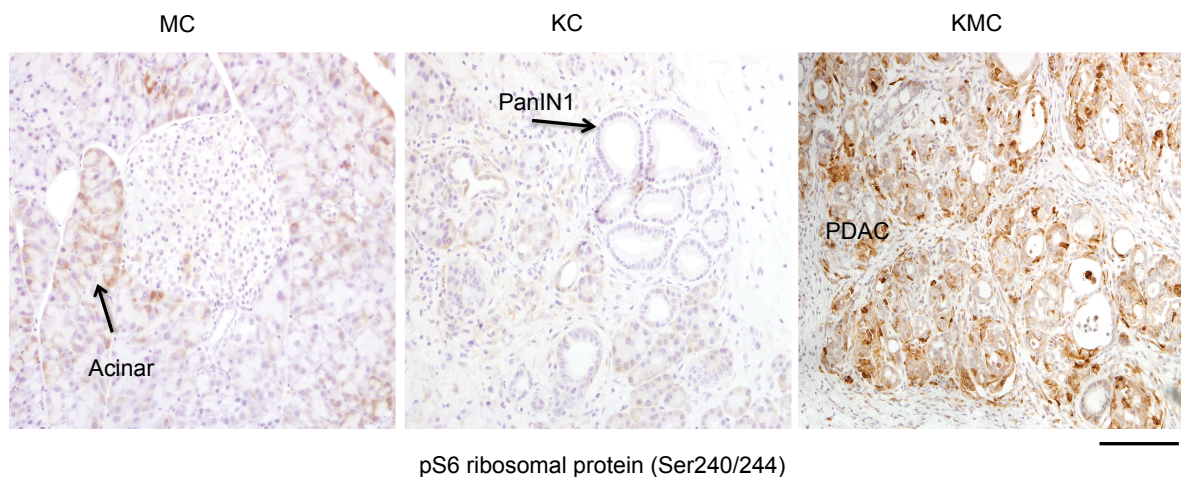


Figure 4-6- IHC for pS6 (ser240/244) confirmed activation of mTOR pathway in *R26^{LSL-MYC/+};LSL-Kras^{G12D}* driven pancreatic tumours

IHC against pS6 (Ser240/244) in the pancreas of 60 days old *Pdx1-Cre;R26^{LSL-MYC/+}* (MC, n=3); *Pdx1-Cre;LSL-Kras^{G12D}* (KC, n=3) mice and in end stage pancreatic tumours of *Pdx1-Cre;R26^{LSL-MYC/+};LSL-Kras^{G12D}* (KMC, n=5) mice. Scale bar represents 100µm.

Raf/MEK/Erk is one of the Ras effector pathways that has been linked to PDAC. For example, IHC analyses of human resected pancreatic carcinomas revealed that high p-ERK expression correlated with poor patient survival (Chadha et al., 2006). To evaluate the activity of Raf/MEK/Erk in KMC tumours, an IHC for phospho-P44/42 MAPK (Thr202/Tyr204) (p-ERK) was carried out. As shown in Fig. 4-7, pERK expression was evident in KMC tumours and *Kras^{G12D}* induced PanINs, but not in *R26^{LSL-MYC/+}* expressing age (60 days) matched controls.

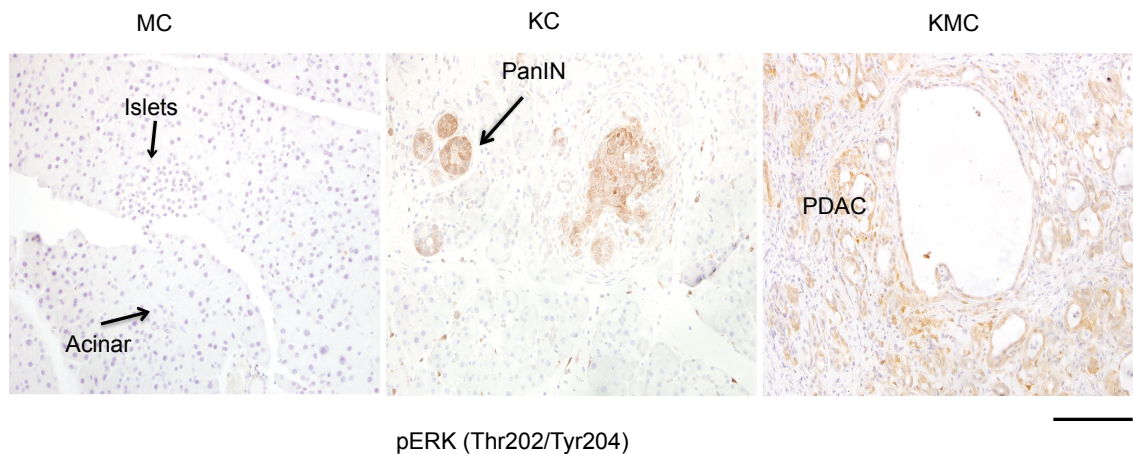


Figure 4-7- IHC for p-ERK revealed active Raf/MEK/Erk pathway in PanINs and PDAC

IHC against p-ERK (Thr202/Tyr204) in the pancreas of 60days old *Pdx1-Cre;R26^{LSL-MYC/+}* (MC, n=3); *Pdx1-Cre;LSL-Kras^{G12D}* (KC, n=3) mice and in end stage pancreatic tumours of *Pdx1-Cre;R26^{LSL-MYC/+};LSL-Kras^{G12D}* (KMC, n=5) mice. Scale bar represents 100 μ m.

4.2.4 KMC tumours resemble human pancreatic cancer in terms of mucin expression and collagen deposition

Overexpression of mucins is a characteristic feature of human PDAC. Mucins are high molecular weight glycoproteins, which show differential patterns of expression during different stages of pancreatic tumour progression (Jonckheere et al., 2010). Overexpression of mucins has been correlated with poor patient survival and poor response of pancreatic cancer cells to the cytotoxic drug 5-fluorouracil ((Kalra and Campbell, 2007). KMC tumours show high mucin expression (Fig. 4-8 top panel), as revealed by Alcian blue/PAS staining that stains mucins in blue/magenta/purple depending on their charge. In line with previous reports (Hingorani et al., 2003), *Kras^{G12D}* induced PanINs also show abundant mucin content (Fig. 4-8 top panel). Another striking feature of human pancreatic cancer is the abundant extracellular matrix components (ECM), commonly referred as desmoplasia. ECM components include collagen, fibronectin, proteoglycans and some active enzymes. Again, increased desmoplasia has been correlated with poor drug response in GEMMs (Feig et al., 2012; Olive et al., 2009). Intense picro sirus staining, an indicator of collagen fibres, confirms the high stromal content of KMC tumours compared to MC or KC mice (Fig. 4-8 lower panel).

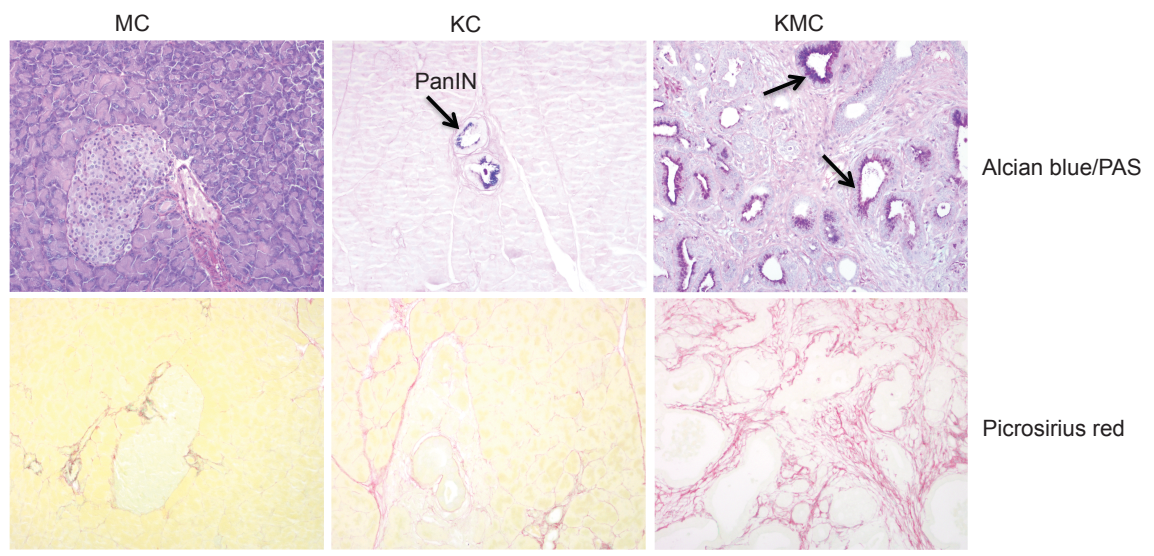


Figure 4-8- KMC tumours display high mucin expression and collagen deposition

Top Panel : Alcian blue/PAS staining of MC, KC pancreas (taken at 60days of age) and end stage tumour of KMC cohort. Original magnification of image is 10X. Lower panel: Representative images of Picro-sirius red staining of MC, KC pancreas (taken at 60days of age) and end stage tumour of KMC cohort. Original magnification of image is 10X. Scale bar represents 100µm.

4.2.5 Dose dependent effect of MYC on pancreatic tumourigenesis

To evaluate the effect of increased MYC expression on pancreatic tumourigenesis, cohorts of *Pdx1-Cre;R26^{LSL-MYC/+}* and *Pdx1-Cre;R26^{LSL-MYC/LSL-MYC}* mice were generated. Mice, which are homozygous for *Rosa-26* driven *MYC* had significantly reduced lifespan compared to their heterozygous counterparts (Fig. 4-9). 91% of *R26^{LSL-MYC/LSL-MYC}* mice (10/11) developed pancreatic tumours with the median survival of 185 days compared to median survival of 355 days for *Pdx1-Cre; R26^{LSL-MYC/+}* cohort. As described in table 4-2, heterozygous expression of *Rosa-26* driven *MYC* resulted in mostly poorly differentiated and some neuro-endocrinal tumours, whereas homozygous expression resulted in neuro-endocrine tumours in all the cases (Fig. 4-10). IHC for Ki67 staining revealed that both *R26^{LSL-MYC/+}*; *R26^{LSL-MYC/LSL-MYC}* tumours display high proliferative capacity (Fig. 4-11). This is in agreement with the previously published work, where ectopic MYC expression in the acinar compartment of the pancreas (using the acinar specific elastase promoter) in *Ink4a/Arf* null mice resulted in a subtype of neuro-endocrine tumour, insulinomas (Lewis et al., 2003).

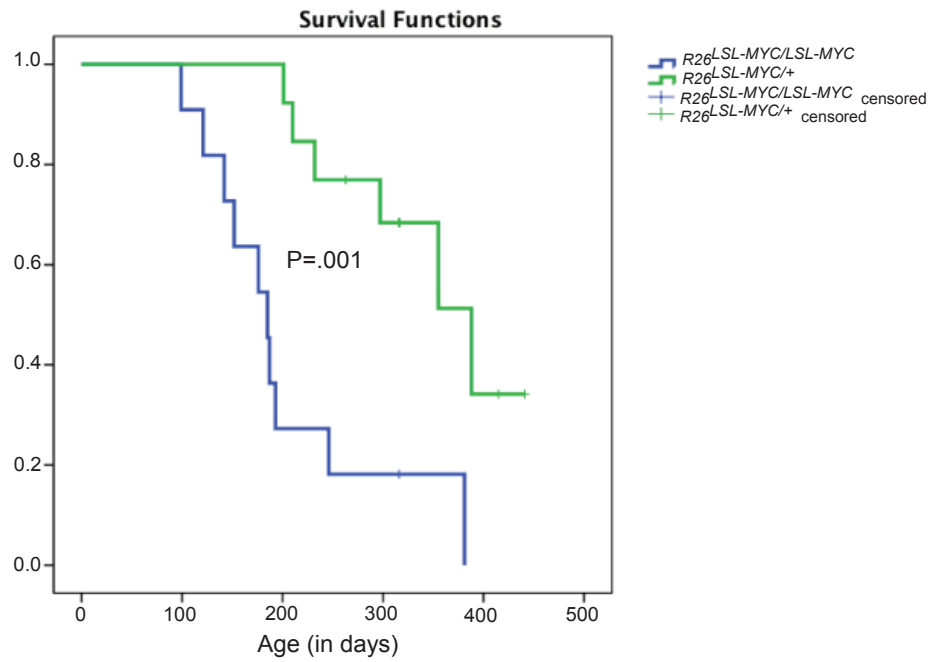


Figure 4-9- Dose dependent effect of MYC on pancreatic tumourigenesis

(A) Kaplan-Meier survival curve of $Pdx1-Cre;R26^{LSL-MYC/+}$ (n=12) represented in green and $Pdx1-Cre;R26^{LSL-MYC/LSL-MYC}$ (n=11) represented in blue, P value is calculated using log-rank tests (SPSS)

Table 4-2- Table summarising the histological features of tumours from $R26^{LSL-MYC}$ homozygous and heterozygous cohorts

Genotype	PDAC	Neuro Endocrine tumours	Mixed tumours	Others
$Pdx1-Cre ; R26^{LSL-MYC/LSL-MYC}$	0/11	10/11	0/11	0/11
$Pdx1-Cre ; R26^{LSL-MYC/+}$	0/12	1/12	0/12	5/12

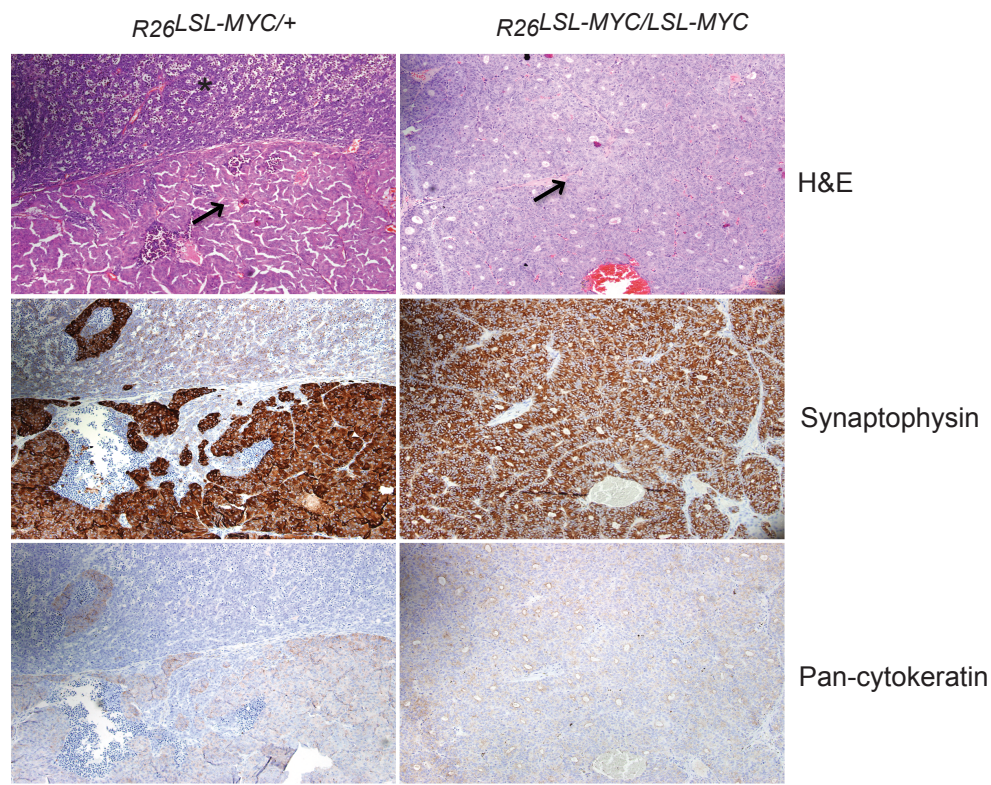


Figure 4-10- MYC induced tumours are primarily neuro-endocrine tumours

A representative example of H&E, synaptophysin and Pan-cytokeratin stainings of end stage $R26^{LSL-MYC/+}$ tumours (Left panel) and $R26^{LSL-MYC/LSL-MYC}$ tumours (Right Panel). Star represents poorly differentiated tumour and an arrow represents neuro-endocrine tumour. Scale bar indicates $100\mu\text{m}$ and the original magnification of the image is 10X.

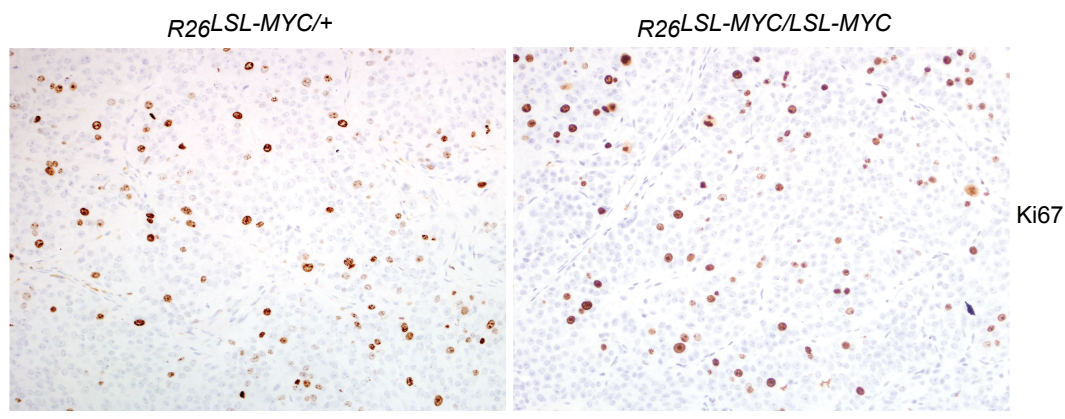


Figure 4-11- IHC for Ki67 on MYC only pancreatic tumours

IHC for Ki67 performed on pancreatic tumours of mice that are heterozygous for Rosa26 driven MYC (left) or Homozygous for Rosa26 driven MYC (Right). Scale bar indicates $100\mu\text{m}$ and the original magnification of the image is 20X.

4.2.6 mTOR but not Raf/MEK/Erk pathway is active in $R26^{LSL-MYC}$ tumours

To evaluate the activity of mTOR and Raf/MEK/Erk pathway in MYC-induced tumours, IHC for pS6 and p-ERK was carried out in end stage pancreatic tumour tissues of *Pdx1-Cre;R26^{LSL-MYC}* heterozygous and homozygous mice. The tumours showed differential staining for pS6 (Ser240/244), suggesting that mTOR is active in MYC only tumours. On the other hand, these tumours were stained negative for pERK (Thr202/Tyr204), suggesting that MYC only tumours unlike MYC and Kras^{G12D} induced PDAC, do not have active Raf/MEK/ERK pathway.

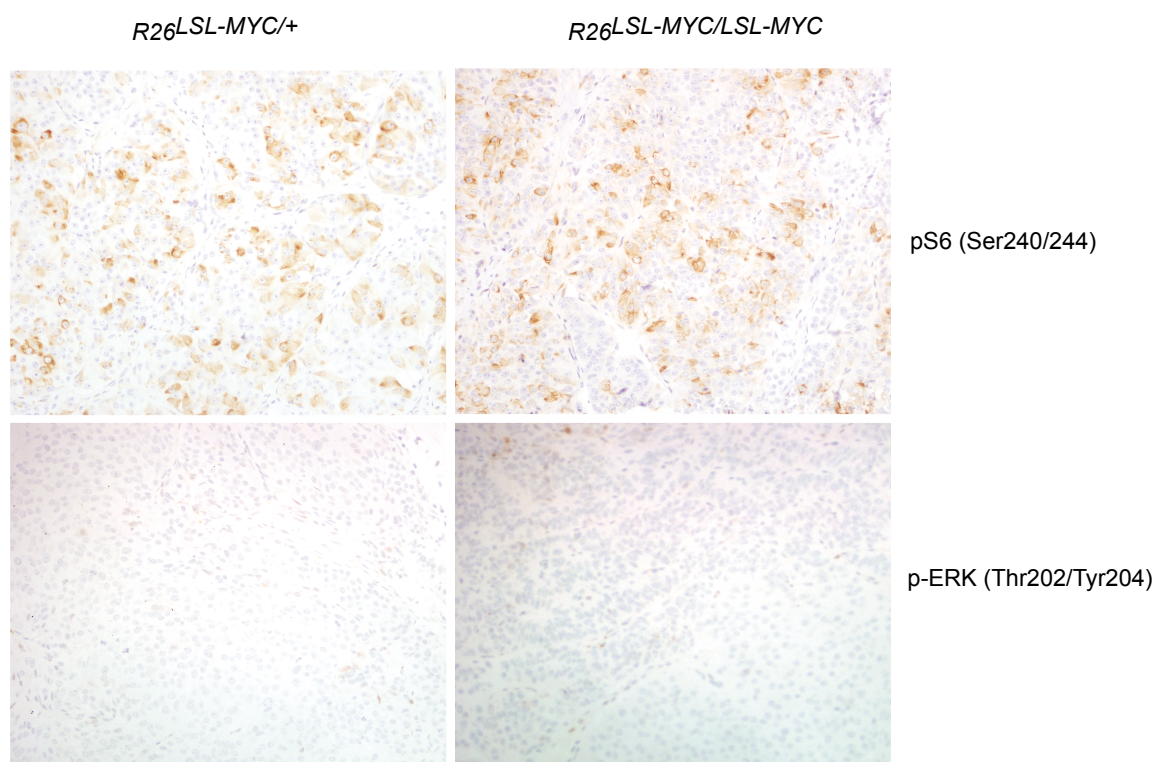


Figure 4-12- MYC only tumours have active mTOR pathway but not Raf/MEK/ERk pathway

IHC against pS6 (Ser240/244) and p-ERK (Thr202/Tyr204) in end stage tumours of *Pdx1-Cre;R26^{LSL-MYC/+}* and *Pdx1-Cre;R26^{LSL-MYC/LSL-MYC}* mice. Scale bar represents 100 μ m.

4.2.7 Primary pancreatic tumour cells are sensitive to BH3-mimetic, ABT-737

Pancreatic cancers are intrinsically resistant and respond poorly to chemotherapeutic agents. We and others have shown that overexpression of MYC can induce apoptosis and is also capable of sensitizing the cells to other apoptotic stimuli (Evan et al., 1992; Murphy et al., 2008; Muthalagu et al., 2014). ABT-737, a BH3 mimetic, induces apoptosis by

selectively targeting pro-survival Bcl2 proteins (e.g. Bcl2, Bcl-x_L, Bcl-w). It has been shown to be effective against MYC-driven lymphomas and other lymphoid tumours, however it is not very effective against solid tumours as a single agent with the exception of small cell lung cancer (Kelly et al., 2013; Mason et al., 2008; Oltersdorf et al., 2005).

To evaluate the sensitivity of MYC-induced pancreatic cancer to ABT-737, I have generated pancreatic tumour cell lines from the end stage KMC tumours as described in section 2.5.2. Sytox green, a fluorescent, cell impermeant nuclear dye was used as a marker for cell death and the IncuCyte imaging system was used to detect the fluorescence from dying cells. Two different tumour lines (KMC1 and 2) were used and both were found to be sensitive to the treatment of ABT-737. ABT-737 (10 μ M) treatment resulted in a progressive accumulation of dead cells (Sytox green positive) over time (Fig. 4-13). As shown in Fig. 4-13A&B, the kinetics of death in response to ABT-737 is different between two tumour lines, KMC 2 line appear to be an early responder to ABT-737 compared to KMC1 tumour line.

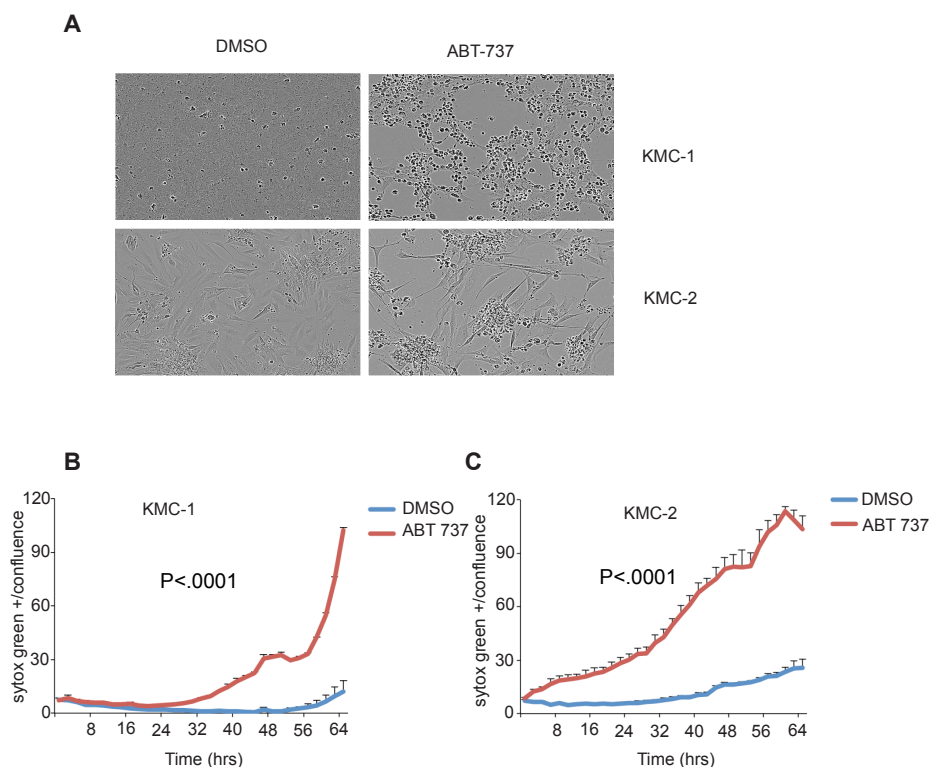


Figure 4-13- Primary pancreatic tumour cells derived from KMC tumours are sensitive to BH3-mimetic, ABT-737

(A) Light microscope images showing death after 60hrs of ABT-737 (10 μ M) treatment in two different pancreatic tumour lines KMC-1 and KMC-2. (B) & (C) Graphs showing increase in Sytox green positive cells over time in ABT-737 (10 μ M) treated cells (red) compared to vehicle (DMSO) treated cells (blue). Incucyte was used to calculate number of sytox green positive cells and confluence (Indirect measure of cell density) for each condition.

4.3 Discussion

MYC is an important contributor to the genesis of many human cancers. Here, I show that overexpression of MYC is alone sufficient to drive pancreatic tumourigenesis. In line with a previous report, MYC overexpression resulted in neuro-endocrine tumours (Lewis et al., 2003). This is not surprising given the prominent role of MYC in pancreatic endocrine cell biology. For example, MYC overexpression stimulated proliferation and ablated differentiation of human foetal islet cells (Demeterco et al., 2002). Similarly, overexpression of MYC in mouse pancreatic β cells (using a β cell specific Insulin promoter) resulted in an initial phase of proliferation followed by rapid cell death however, when apoptosis is blocked, MYC facilitated the formation of insulinomas (Pelengaris et al., 2002). It is to be noted that the Insulin promoter drives strong expression of 4-OHT dependent MycER in pancreatic β cells and a direct comparison between pIns-MycER^{TAM} and *Rosa26*^{MER/MER} model revealed that MYC is expressed ~ 15 fold higher in pIns-MycER^{TAM} model compared to the other (Murphy et al., 2008). Moreover, it is proved that thresholds of MYC for proliferation and apoptosis are set at different levels, low level for the former and high level for the latter (Murphy et al., 2008). The level of MYC deregulation in the pancreas of *R26*^{LSL-MYC/+} mice is below the apoptotic threshold, thereby avoiding the negative selection arising from the high level of MYC expression.

I also provide evidence for dose dependent effect of MYC in pancreatic tumourigenesis. Homozygous *Rosa26* MYC mice developed pancreatic tumours with short latency compared to their heterozygous counterparts. This suggests a potential therapeutic opportunity to explore, which is to destabilize MYC protein level in human cancers. Indeed, several groups are investigating the opportunity to inhibit proteins that are required for MYC protein stability (e.g. USP28). Interestingly, overexpression of MYC from the same promoter (*Rosa26*) in an adult mouse is not sufficient to drive lung tumourigenesis on its own, highlighting the tissue specific role of oncogenic MYC (Neidler and Murphy, unpublished).

Using conditional mouse models it has been shown that pancreatic expression of oncogenic *Kras* leads to precursor lesions of pancreatic cancer (PanINs). Also, mono or biallelic loss of different tumour suppressors such as p16Arf, and p53, cooperates with *Kras*^{G12D} to accelerate formation of pancreatic ductal adenocarcinoma (Aguirre et al., 2003; Bardeesy et al., 2006a; Hingorani et al., 2005; Morton et al., 2010). Here, I show

that the heterozygous expression of *Rosa26*-driven *MYC* cooperates with mutant *Kras* to produce aggressive pancreatic ductal adenocarcinoma, with significantly reduced median survival (50 days). The mouse model used in this study allows the concomitant expression of both mutant *Kras* and *MYC in utero* (E 8.5). In contrast, human pancreatic cancer is not a paediatric disease. Instead, neoplastic lesions arise in adulthood and acquire mutations sequentially only in a small subset of cells as the disease progresses. Hence, it is conceivable that the highly accelerated disease observed is due to the expression of oncogenes in all pancreatic precursor cells during embryogenesis. This issue can be largely addressed by using an inducible Cre system (e.g. *Pdx-CreER*), which allows for the activation of alleles in a fully developed adult/adolescent mouse pancreas.

Interestingly, *MYC* expression alone or concomitant expression of *MYC* and *Kras*^{G12D} drove development of pancreatic tumours with very different histological features. MC mice presented with poorly differentiated or neuro-endocrine tumours, whereas KMC mice displayed predominantly PDAC. This raises an important question about the cell of origin of tumours from KMC and MC mice. However, determining cell of origin for the pancreatic tumours is complicated due to developmental plasticity of the pancreas, which enable the trans-differentiation between cell lineages (Puri et al., 2015). Also, experimental studies have shown that different cell lineages (e.g. acinar cells, islet cells) can give rise to pancreatic tumours with ductal features in a context-dependent manner (Gidekel Friedlander et al., 2009). It also remains possible that specific initiating genetic lesions dictate the phenotypic endpoint of the tumour irrespective of cell of origin.

Importantly, establishing a *MYC* driven pancreatic model served as a tool to test for *MYC*-induced vulnerabilities. In chapter 3, I have shown that *MYC*, when expressed at sub-apoptotic level can sensitize the cells to different pro-apoptotic stimuli. In line with this, *MYC* driven pancreatic cancer cells are highly sensitive to BH3-mimetic ABT-737, whereas pancreatic cells derived from KPC tumours (*Pdx1-Cre;LSL-Kras*^{G12D};*LSL-Trp53*^{R172H}) are not equally sensitive (data not shown). This may provide a new therapeutic strategy to test ABT-737 against *MYC* driven tumours or tumour types where *MYC* is overexpressed. This model will be used to test the *MYC*-induced dependence of Nuak1 in pancreatic cancer (see chapter 5).

In conclusion, I have shown that *MYC* cooperates with mutant *Kras* to form aggressive PDAC, which resemble human pancreatic cancer. Also, *MYC* overexpression on its own leads to neuroendocrine/islet cell tumours, a cancer type that is rare in humans, in a dose

dependent manner. I have also provided evidence for exploiting the intrinsic tumour suppressive function of MYC by using the BH3-mimetic ABT-737 in murine pancreatic cancer cells.

4.4 Future work

The data presented in this chapter represent early findings into the investigation of MYC and Kras^{G12D} in pancreatic tumourigenesis, further work is needed to understand the mechanism of cooperation. To do this, Pdx1-CreER system should be used, which allows the temporal activation of both the alleles in an adult mouse pancreas by administration of tamoxifen. Short-term activation of both alleles (e.g. 3 days, 7 days, 14 days) will provide an opportunity to understand the course of tumour evolution.

IHC analyses of MYC/Kras tumours revealed that mTOR and Raf/MEK/Erk pathways were active. Further analysis to determine the status of other commonly deregulated pathways in human PDAC such as Wnt/ β -catenin and the TGF- β -pathway should be evaluated. Furthermore, primary pancreatic tumour lines derived from KMC tumour should be used as a tool to screen for efficacy of specific pathway inhibitors, selected based on IHC analyses. In longer term, specific inhibitors or combination of inhibitors that were shown to be effective *in vitro* should be tested *in vivo* (*Pdx1-creER*; *R26^{LSL-MYC}*; *LSL-Kras^{G12D}*).

5 Evaluating the role of Nuak1 in MYC driven pancreatic tumourigenesis

5.1 Introduction

Pancreatic ductal adenocarcinoma (PDAC) is a leading cause of cancer mortality and morbidity. PDAC is associated with accumulating somatic mutations in a subset of genes including the small GTPase protein KRAS. Embryonic pathways such as, Hedgehog, Wnt- β -catenin, Notch, and transforming growth factor- β have been implicated in PDAC development (Morris et al., 2010; Perez-Mancera et al., 2012). Gemcitabine, a nucleoside analogue has been used as the standard of care treatment for patients with advanced pancreatic cancer for many years, where median survival is extended from 4.4 to 5.6 months (Burris et al., 1997). Based on recent research into understanding of the molecular basis of the disease, a number of new-targeted therapies such as, small molecule inhibitors targeting RAS, the Hedgehog pathway, and EGFR have been investigated but with little success (Hidalgo, 2010; Perez-Mancera et al., 2012). For example, Phase III trial of NCI, Canada, revealed that a combination of Erlotinib, an EGFR inhibitor, with Gemcitabine in patients with locally advanced or metastatic PDAC, only increased median survival from 5.91 months to 6.24 months (Moore et al., 2007). Hence, identifying new potential therapeutic targets for pancreatic cancer are major goals in this field.

On average, 50% of all human cancers have high MYC expression (Vita and Henriksson, 2006). Several lines of evidence suggest an important role for MYC in pancreatic cancer initiation and maintenance (Saborowski et al., 2014; Walz et al., 2014). In chapter 4, I have shown that Rosa26 driven MYC cooperates with oncogenic Kras to accelerate PDAC. One of the strategies to target MYC is to exploit oncogene-induced addiction. Cell cycle kinases CDK1, Aurora kinases, Chk1 (an essential kinase involved in DNA damage) and SUMO-activating enzyme 1/2 (SAE1/2) have been reported to be critical for the survival for MYC overexpressing cells (Horiuchi et al., 2014). In addition, we have previously described a selective dependence upon an AMPK-related kinase Ark5 (NUAK1) in cells overexpressing MYC (Liu et al., 2012b). NUAK1 depletion in the context of MYC overexpression resulted in plethora of effects including, loss of ATP, unrestrained mTOR pathway activity, reactive oxygen species (ROS) production and cell death. As shown in Fig. 5-1, activation of MycER in NUAK1 depleted (using shRNA) osteosarcoma cell line U2OS resulted in cell death, whereas depletion of NUAK1 or MycER activation independently was not detrimental.

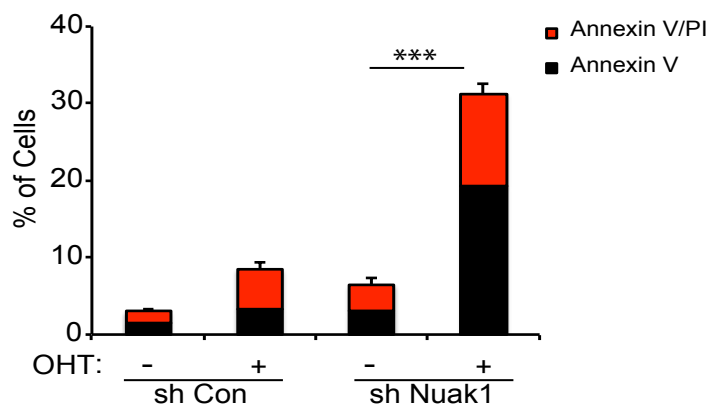


Figure 5-1- NUAK1 depletion kills MYC overexpressing cells

The graph shows the death (AnnexinV/PI positive) of MYC overexpressing (+OHT), NUAK1 depleted (shRNA against NUAK1) U2OS cells compared to NUAK1 depleted (-OHT) or MYC overexpressing sh Control cells. This data is reproduced based on the results from Liu et al., 2012b.

Nuak1 belongs to the AMPK related kinase family and was found to be involved in various biological processes such as, cell proliferation, adhesion and cellular ploidy (Banerjee et al., 2014; Humbert et al., 2010; Zagorska et al., 2010). Furthermore, NUAK1 has been closely associated with human cancers as it was found to be overexpressed in different cancer types including pancreatic cancer (Kusakai et al., 2004; Liu et al., 2012b) and there is evidence to suggest that NUAK1 can drive tumour invasion and metastasis (Kusakai et al., 2004; Lu et al., 2013). Given the role of MYC in pancreatic cancer, I hypothesized that Nuak1 may be required for pancreatic tumour initiation and/or maintenance. As the kinase activity of NUAK1 can be suppressed with small molecule inhibitors (Banerjee et al., 2014), a requirement for NUAK1 in pancreatic cancer could open an exciting new therapeutic avenue. Therefore, the aim of this chapter is to evaluate the requirement of Nuak1 for MYC and Kras^{G12D} driven pancreatic tumourigenesis.

5.2 Mouse models used to address the aim

The *Pdx1-Cre;R26^{LSL-MYC/+};LSL-Kras^{G12D}* (KMC) model, which was described in chapter 4, together with a previously described conditional *Nuak1^{FL/FL}* mouse model (Inazuka et al., 2012) was used to investigate the role of Nuak1 in pancreatic tumourigenesis. In *Nuak1^{FL/FL}* mouse model, exon 3 of endogenous *Nuak1* is flanked by functional LoxP sites and Cre mediated excision of LoxP sites results in *Nuak1* Knockout (Fig. 5-2).

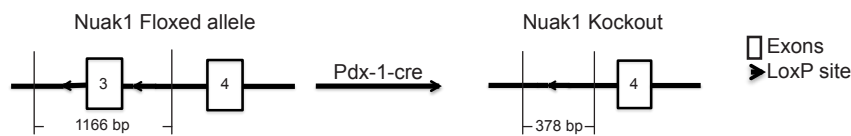


Figure 5-2- Schematic representation of *Nuak1* floxed allele

Simplified schematic representation of *Nuak1* floxed allele, block arrows represents LoxP sites flanking exon 3 of the endogenous *Nuak1*. Cre recombinase expression specifically in the pancreas (using *Pdx1* promoter) leads to excision of the intervening sequence between LoxP sites resulting in a *Nuak1* knockout.

5.3 Results

5.3.1 Pancreas specific Knockout of Ark5/*Nuak 1*

Pancreas specific knockout of *Nuak1* was achieved by interbreeding *Nuak1^{FL/FL}* conditional mice with animals that expresses Cre recombinase from the pancreatic specific promoter *Pdx1*. Thus, tissues that do not express Cre recombinase retain functional *Nuak1* alleles. To ascertain successful knockout of the targeted allele, genomic DNA was extracted from the pancreas of *Pdx1-Cre; Nuak1^{FL/FL}* mice of differing age (indicated in Fig. 5-3) and PCR for recombined and targeted alleles was carried out. The presence of a band corresponding to the recombined allele (378bp), confirmed the successful and complete deletion of the gene in the pancreas (Fig. 5-3).

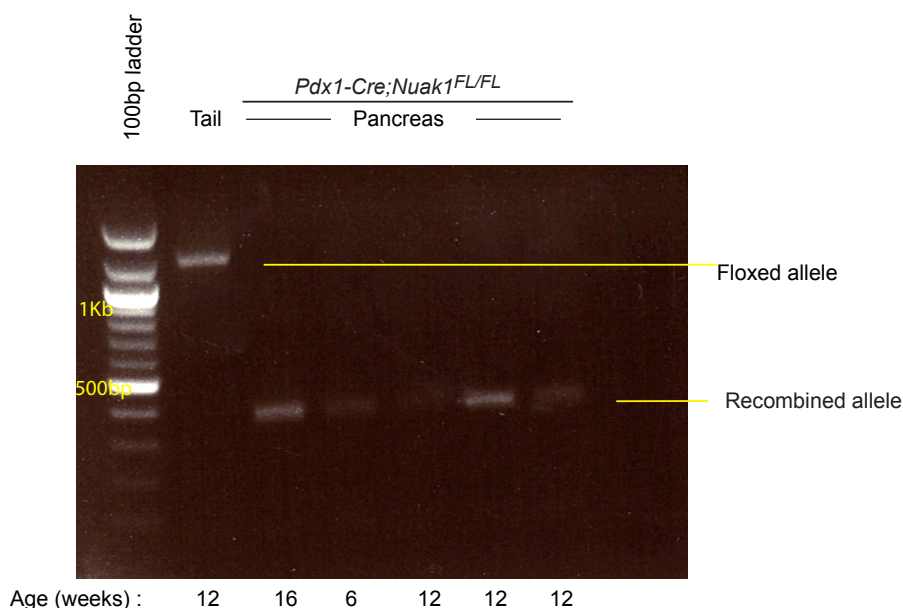


Figure 5-3- Pancreas specific deletion of *Nuak1*

PCR products visualised on an agarose gel showing complete recombination of *Nuak1* floxed allele from the pancreas of *Pdx-1cre;Nuak1^{FL/FL}* mice, but not from the tail sample of the same genotype. 378bp band represents recombined (Knockout) allele and 1166bp band represents unrecombined or floxed allele.

To investigate the effects of *Nuak1* deletion on pancreas development, histological features of *Nuak1* deleted pancreas were assessed. As shown in Fig. 5-4, *Nuak1* deleted mice displayed histologically normal pancreas with abundant acinar tissue, scattered islets of Langerhans and normal looking ducts similar to the wild type control (Fig. 5-4 top panel). Synaptophysin and Pan-cytokeratin were used as a marker to identify intact islets of Langerhans and pancreatic ducts respectively (Fig. 5-4). This data suggest that *Nuak1* deletion does not affect pancreatic development and pancreas-specific *Nuak1* deletion was tolerated.

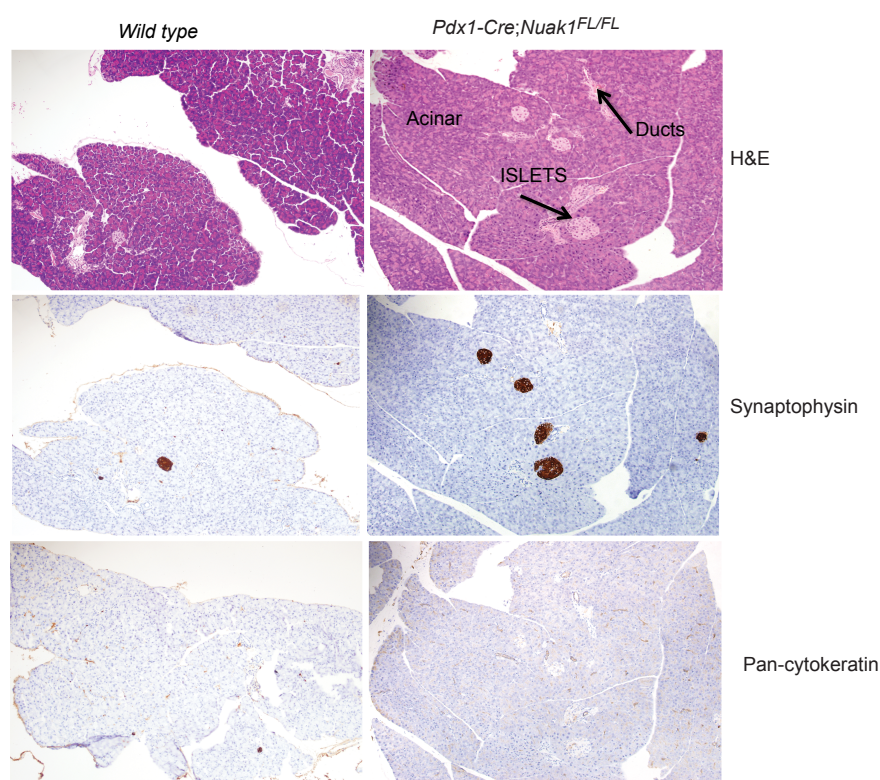


Figure 5-4- *Nuak1* deleted mice display pancreas with normal histological feature

Representative images of H&E stained pancreas showing normal ducts, islets and acinar compartments in wild type and *Nuak1^{FL/FL}* mice. Synaptophysin and Pan-cytokeartin staining from the pancreas of wild type and *Pdx1-Cre;Nuak1^{FL/FL}* mice. Original magnification of the image is 10X. Scale bar represents 100 μ m

5.3.2 MYC and mutant *Kras* impose selective pressure to retain *Nuak1*

To investigate the requirement of *Nuak1* for MYC driven pancreatic tumourigenesis, cohorts of *Pdx1-Cre;R26^{LSL-Myc+/-};LSL-Kras^{G12D/+};Nuak1^{FL/FL}* mice (KMC;*Nuak1^{FL/FL}*) were generated. Mice were monitored for pancreatic tumour development and sacrificed when symptomatic of the disease (see section 2.1.3.2). A cohort of KMC mice (described in chapter 4) was used as a control. As shown in Fig 5-5A, depletion of *Nuak1* did not

significantly increase the survival of KMC mice as *Nuak1* wild type and floxed KMC mice have similar median survival, 54 and 57 days respectively (Fig. 5-5A). Hematoxylin and Eosin (H&E) staining revealed that *Nuak1* floxed KMC tumours display histological features of PDAC similar to control counterparts (Fig. 5-5B)

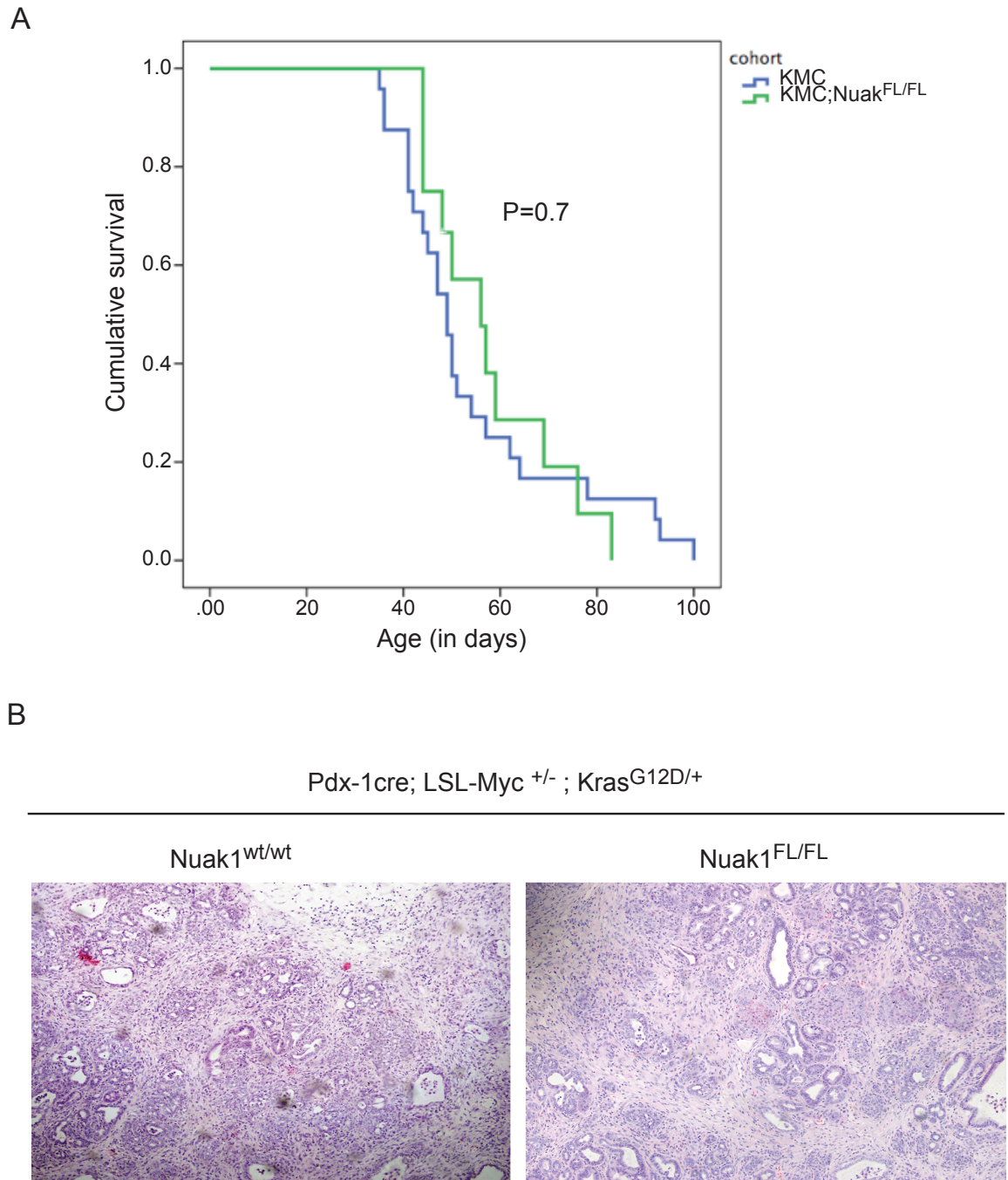


Figure 5-5- *Nuak1* deletion had no significant effect on survival of the KMC mice

(A) Kaplan-Meier survival curve of *Pdx1-Cre; R26^{LSL-MYC/+}; LSL- Kras^{G12D/+}* (KMC n=24) and *Pdx1-Cre; R26^{LSL-MYC/+}; LSL- Kras^{G12D/+}; Nuak1^{FL/FL}* (KMC;*Nuak1^{FL/FL}* n=12) cohorts, P value is calculated using log-rank test (B) Representative example of H&E staining of end stage tumours of KMC and KMC;*Nuak1^{FL/FL}* cohorts.

Although Fig. 5-3 demonstrates complete deletion of *Nuak1* allele in normal pancreas, it is important to determine the degree of *Nuak1* deletion in tumour bearing mice. To ascertain the successful knockout of the targeted allele, 7/12 KMC;*Nuak1*^{FL/FL} tumours were analysed. The genomic DNA was extracted from end stage tumours of KMC;*Nuak1*^{FL/FL} cohort and PCR for recombined and targeted allele was carried out. Surprisingly, 6/7 tumours show partial deletion of the allele, suggesting that tumours are comprised of two different populations of cells, one that deleted *Nuak1* allele and another that retain *Nuak1* expression (Fig. 5-6). This data suggests that pancreatic tumours arise by failing to knockout *Nuak1* completely.

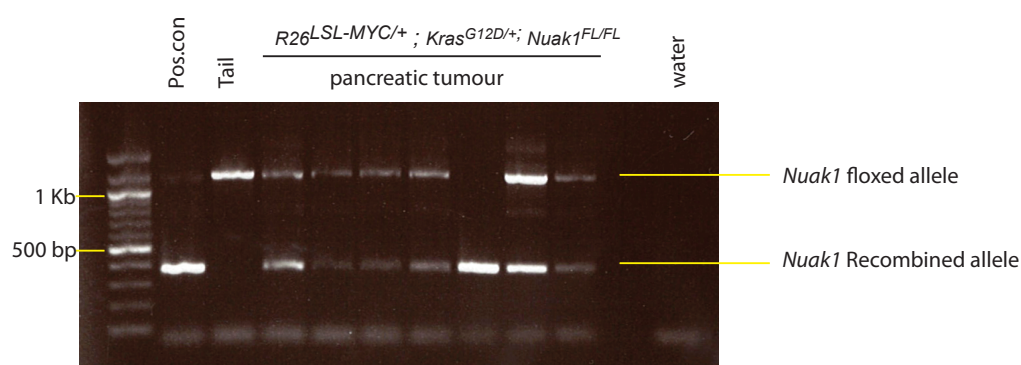


Figure 5-6- KMC *Nuak1*^{FL/FL} tumours show partial deletion of the allele

A PCR products visualised on an agarose gel showing partial recombination of end stage pancreatic tumour of KMC;*Nuak1*^{FL/FL} mice; a band corresponding to 1166bp represents floxed allele and a band corresponding to 378bp represents recombined (knockout) allele. A tail sample from the KMC;*Nuak1*^{FL/FL} mouse was used as a control for unrecombined *Nuak1* floxed allele.

5.3.3 Primary pancreatic tumour cells are sensitive to *Nuak1* inhibitor

Having shown that KMC tumours have selective pressure to retain *Nuak1* expression, I then tested the sensitivity of pancreatic tumour cells to *Nuak1* inhibitor *in vitro*. Recently identified *Nuak1* specific inhibitor HTH-01-015 serves as a valuable tool for probing the function of *Nuak1* *in vitro* (Banerjee et al., 2014). To evaluate the sensitivity of MYC induced pancreatic tumours to the *Nuak1* inhibitor HTH-01-015, primary murine pancreatic tumour cell lines generated from the end stage KMC tumours were used. Sytox green, a fluorescent, cell impermeant nuclear dye was used as a marker for cell death and the IncuCyte imaging system was used to detect the fluorescence. Two different tumour lines (KMC1 and 2) were used and both were found to be sensitive to the treatment of HTH-01-015 compared to vehicle (DMSO) treated controls. HTH-01-015 (10µM) treatment resulted in a progressive accumulation of dead cells over time in both tumour lines with different kinetics (Fig. 5.7). To determine if the *Nuak1* inhibitor is toxic to non-

transformed cells, mouse embryonic fibroblasts were treated with HTH-01-015 (10 μ M) for 72hrs. As shown in Fig. 5-8, crystal violet staining revealed that the same concentration of HTH-01-015 is not detrimental to the non-transformed primary mouse embryonic fibroblasts (MEFs)

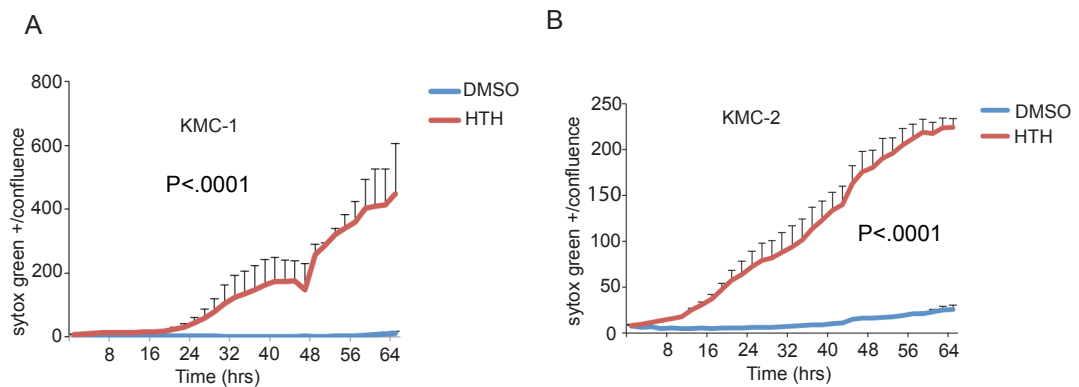


Figure 5-7- Primary murine pancreatic tumour cells are sensitive to Nuak1 inhibitor HTH-01-015

(A and B) Graphs showing increase in Sytox green positive cells over time in HTH-01-015 (10 μ M) treated cells (red) compared to vehicle (DMSO) treated (blue) pancreatic tumour lines KMC-1 and KMC-2, respectively. Incucyte was used to calculate the number of sytox green positive cells and confluence (Indirect measure of cell density) for each condition. P value is calculated using unpaired student t test (Graph pad prism)

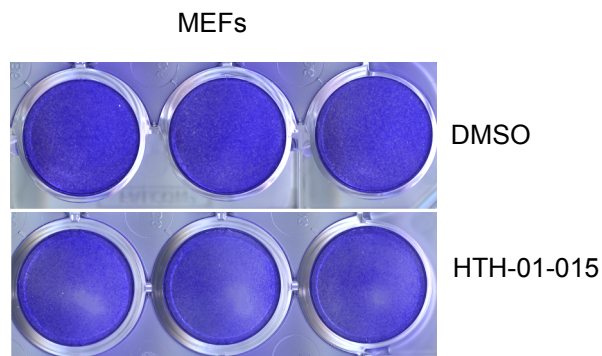


Figure 5-8- Nuak1 inhibition is not toxic to primary mouse embryonic fibroblasts

Crystal violet staining of MEFs treated with DMSO or HTH-01-015 (10 μ M) for 72hrs.

5.3.4 Discussion

MYC is deregulated in a variety of human cancers however, the fact that it encodes a critical transcription factor, which is important for coordinated expression of several genes, makes it a challenging therapeutic target. For the same reason, several efforts have been made to target MYC indirectly. A synthetic lethality i.e. exploiting oncogene-induced dependencies is one of the strategies to target MYC driven tumours. In an attempt to identify kinases that are required for the survival of MYC overexpressing cells, we have identified AMPK related kinase Ark5/Nuak1 as a potential target. We have previously shown that Ark5 depletion is lethal to MYC overexpressing osteosarcoma cells *in vitro* and

increased survival of mice with orthotopic liver tumours (Liu et al., 2012b). In a similar context, the data presented in this chapter aimed to evaluate the requirement of Nuak1 for MYC driven pancreatic cancer. The data suggests that deletion of Nuak1 did not increase the survival of KMC mice. However, it is to be noted that end stage tumours retained the Nuak1 allele, possibly indicating that tumour cells have strong selective pressure to retain Nuak1 expression. It has been shown that Nuak1 is required for cell proliferation as inhibition or depletion of NUA1 impaired the proliferation of U2OS cells (Banerjee et al., 2014; Liu et al., 2012b). Hence, I propose that NUA1 depletion in cells with MYC overexpression (and/or oncogenic Kras mutation) might have imposed selective growth disadvantage, causing the cells that retain Nuak1 allele to outgrow. In other words, MYC overexpressing pancreatic cells require Nuak1 expression for its survival. This hypothesis is consistent with our previous study, where we have shown that MYC overexpressing cells are sensitive to NUA1 depletion (Liu et al., 2012b). One other aspect to consider is the ability of the Cre recombinase, expressed from Pdx1 promoter, to recombine the *Nuak1* floxed allele efficiently and with high frequency. It has been reported that efficiency of Cre recombinase to recombine different alleles varies depending on specific factors such as, the distance between LoxP sites, the expression level of the target genes or the chromatin structure of the target genes (Vooijs et al., 2001). However, complete knockout of *Nuak1* was observed in the normal pancreas, suggesting that Cre recombinase can recombine the floxed *Nuak1* allele with high efficiency. It also suggests that the cells that do not have oncogenic mutations (MYC and KRAS in this case) can tolerate loss of Nuak1. It is true that PCR results should be interpreted with caution, because pancreatic tumours in our model are very heterogeneous with increased desmoplasia and the genotyping result depends on the region of pancreatic tumour taken for the analysis, further analyses is therefore required to ascertain the Nuak1 status in KMC;*Nuak1*^{FL/FL} tumours (see section 5.4)

In conclusion, although *Nuak1* deletion had no significant effect on the survival of KMC mice, a selective pressure to retain *Nuak1* allele was shown by the KMC tumours suggesting that a different strategy is required to evaluate Nuak1 as a potential therapeutic target. But the fact that tumours retained Nuak1 allele is by itself an interesting avenue to explore.

5.4 Future work

To strengthen the argument on selective pressure imposed by MYC overexpression, it would be useful to isolate DNA specifically from tumour regions using the Laser capture microdissection technique to determine the degree of *Nuak1* deletion. This can eliminate cross contaminations from stromal regions. Alternatively, RNA in situ hybridization assay, which will allow the detection of single RNA molecules per cell could be used to determine the expression of Nuak1 in *Nuak1* wild type and floxed tumours.

The data presented in this chapter is a preliminary work, further work is required to evaluate the effect of Nuak1 depletion in MYC driven pancreatic tumours. It would be useful to ascertain if pathways such as mTOR and Raf/MEK/Erk, which were active in KMC tumours was modulated in KMC;*Nuak1*^{FL/FL} tumours. Furthermore, Pdx1-CreER system could be used to evaluate the status of Nuak1 deleted cells after short term induction of MYC and Kras^{G12D}.

The mouse model used in this study allowed the deletion of *Nuak1* in embryonic stage (Day 8.5), before the tumour is initiated. Hence, it is suitable to study the role of Nuak1 in tumour initiation but not an ideal model to test the therapeutic efficacy of Nuak1 depletion. To specifically answer this question, Nuak1 could be inhibited or deleted in established tumours. Two different approaches could be used; in the first approach tumour-bearing mice can be treated with small molecule inhibitor targeting Nuak1. Alternatively, an inducible shRNA system could be used to deplete *Nuak1* in the established tumour.

6 Conclusion, discussion and future directions

6.1 Tumours are addicted to MYC

Myc family oncogenes are deregulated in a wide variety of human cancers and importantly many human cancer cell lines are addicted to MYC; they require MYC expression for their growth and proliferation. For example, depletion of MYC by short hairpin RNA (shRNA) resulted in proliferation arrest of 22 different human tumour cell lines tested (Wang et al., 2008). In line with this, experimental evidence from GEMMs also suggests that sustained expression of Myc is critical for tumour maintenance. In one study, conditional inactivation of transgenic Myc (tet-off system) led to regression of haematopoietic tumours and osteosarcomas (Felsher and Bishop, 1999). The expression of dominant interfering Myc bHLH-LZ dimerization domain mutant (Omomyc), which inhibits endogenous Myc functions, inhibited lung tumour initiation and maintenance in a LSL-*Kras*^{G12D} model (Soucek et al., 2008). Similarly, shRNA mediated depletion of Myc (Saborowski et al., 2014) or deletion of endogenous *Myc* (*Myc*^{FL/+}) allele (Walz et al., 2014) significantly delayed *Kras*^{G12D} and p53^{R172H} mediated pancreatic tumourigenesis. All of these observations indicate that targeting MYC could be a promising therapeutic strategy.

6.2 Targeting MYC

Expression of MYC is universal to all proliferating cells (Harris et al., 1992) and one argument is that targeting MYC could be detrimental to normal cells, leading to unwanted toxicities. However, most adult cells are quiescent and express little, if any, MYC (Murphy et al., 2008) and this could mean that the toxicities are largely restricted to haematopoietic and gastrointestinal systems, as is the case with many other standard treatments. MYC does not have any enzymatic activity and therefore developing a MYC specific inhibitor is a challenge. To overcome this, an alternative approach to target protein-protein interaction has been extensively studied. Inhibitors disrupting interaction of MYC with its partner protein Max, have been shown to be effective against different cancer cells *in vitro* (Clausen et al., 2010; Huang et al., 2006; Kiessling et al., 2006). There are also efforts being made to target transcription of MYC itself (Delmore et al., 2011), depleting MYC using siRNA (encapsulated in a nanoparticle) (Yang et al., 2012) or to target protein stability. In addition, MYC can also be targeted selectively by exploiting MYC-induced vulnerabilities (Fig. 6-1).

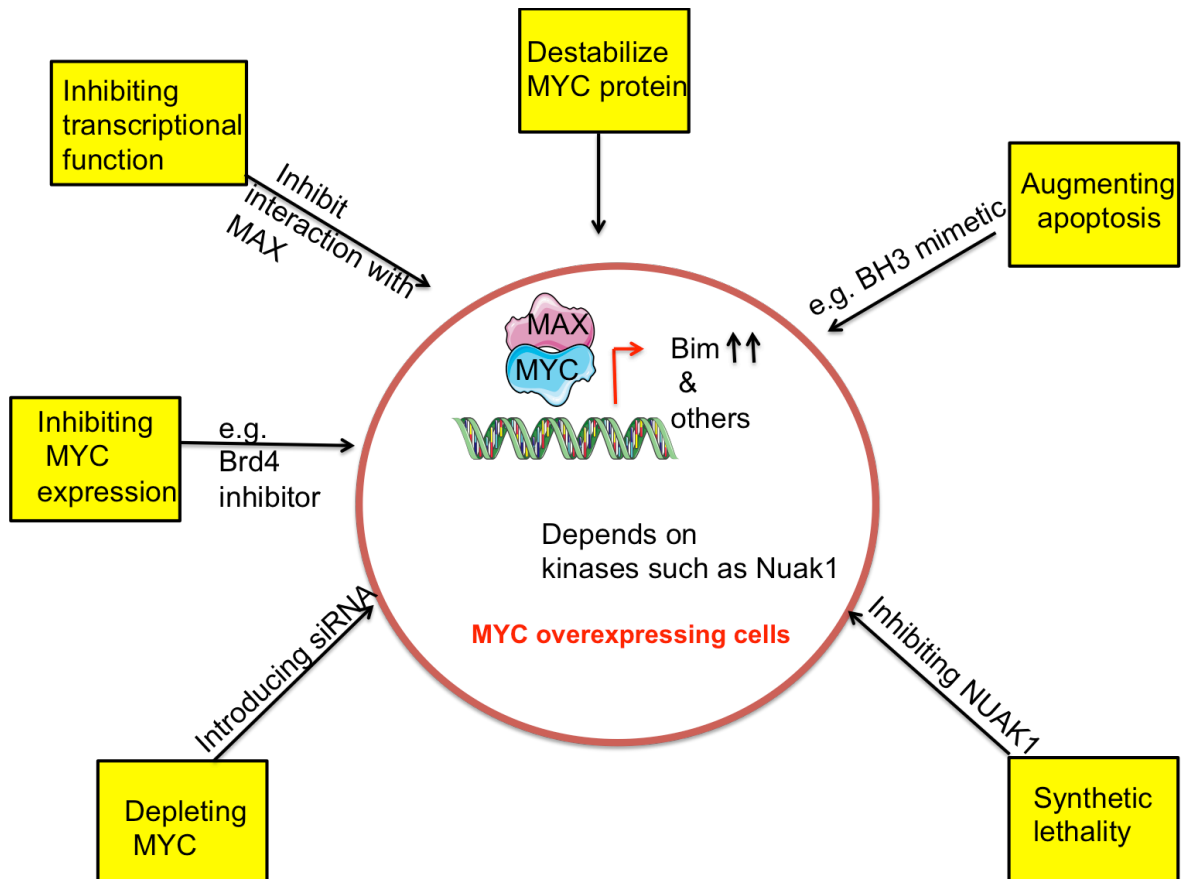


Figure 6-1- Schematic representation of ways of targeting MYC

Few of the several ways to target MYC is represented in this figure

MYC promotes cell growth, cell proliferation, reprogrammes metabolic pathways and also promotes metastasis and vasculogenesis in favour of cancer cells (Dang, 2013). However, MYC expression intrinsically leaves the cells in a vulnerable state by at least two different mechanisms. First, MYC can alone drive apoptosis, however a threshold level of MYC overexpression is required to induce apoptosis (Murphy et al., 2008). In a tumour setting it is possible that the level of MYC expressed in tumour cells is below the apoptotic threshold or unable to drive apoptosis because of the profound parallel survival signalling, but such cells would nevertheless be “primed” to die in the presence of other pro-apoptotic stimuli. For example, BH-3 mimetic ABT-737, which works primarily by engaging the mitochondrial pathway of apoptosis, has been shown to be effective against Eμ-Myc lymphoma model that expresses high levels of MYC (Kelly et al., 2013). MYC has been reported to be in synthetic lethal interaction with different kinases. MYC overexpressing cells have been shown to be dependent on the expression of kinases including, CDK1, Aurora-B, AMPK, and the AMPK related kinase Ark5 for their survival and targeting such kinases was shown to selectively kill MYC overexpressing cells and not normal cells (Kang et al., 2014; Liu et al., 2012b; Yang et al., 2010).

6.2.1 MYC-induced apoptosis

One aspect of the work detailed in this thesis was to better understand the mechanism of MYC-induced apoptosis. The p19Arf-Mdm2-p53 pathway has been implicated in MYC-induced apoptosis. Cells that lack either p19Arf or p53 were reported to be refractory to Myc-induced apoptosis (Zindy et al., 1998) and loss of either of these proteins was found to cooperate with Myc and accelerate lymphomagenesis in E μ -Myc mice (Bertwistle and Sherr, 2007; Schmitt et al., 1999). The majority of such lymphomas have either deletion of the *Cdkn2a* locus (coding p16& p19Arf), Mdm2 overexpression, or p53 mutations (Eischen et al., 1999). Given the link between p53 and apoptosis, it was concluded that mutations in the p19Arf-Mdm2-p53 pathway are necessary for tumours to evade Myc-induced apoptosis and maintain tumorigenicity. On the other hand, several other research groups have reported Myc-induced apoptosis independent of p53 suggesting the existence of an alternative pathway (Blyth et al., 2000; Eischen et al., 2001).

Several lines of evidence suggest a prominent role for mitochondrial Bcl2 family proteins in mediating MYC-induced apoptosis. Anti-apoptotic Bcl2 proteins buffer against pro-apoptotic members in order to maintain the mitochondrial outer membrane integrity and hence the survival. A fine balance of pro-and anti-apoptotic proteins is important and Myc has been reported to alter the balance of Bcl2 family proteins. For example, anti-apoptotic proteins Bcl2 and Bcl-x_L have been reported to be suppressed by Myc, although the precise mechanism of this suppression is as yet unresolved (Eischen et al., 2001; Maclean et al., 2003). Mutational analysis of MYC indicates that the regulation of transcription is key to MYC-induced apoptosis (Amati et al., 1993), thus the recent identification of *BIM* as a transcriptional target of MYC suggests that this BH-3 only protein may play an important role in mediating MYC-induced apoptosis (Campone et al., 2011).

Similar to the intrinsic mitochondrial pathway, the extrinsic death receptor pathway has also been linked to MYC-induced apoptosis. For instance, blocking death receptor CD95 (also termed as Fas or APO-1) using a monoclonal antibody reduced and delayed MYC-induced apoptosis in fibroblasts. However, it was found that CD95 expression was not increased upon MYC activation, suggesting that CD95 might not be a direct MYC target (Hueber et al., 1997). In line with this, CHIP-SEQ analysis in murine pancreatic tumour cells derived from KPC tumours (Pdx1-*Cre*;LSL-*Kras*^{G12D};LSL-*Trp53*^{R172H}) revealed no Myc binding on CD95 locus [GEO-entity :GSE44672, (Muthalagu et al., 2014)].

All these observations prompted us to re-evaluate the relative contribution of p19Arf and Bim in mediating MYC-induced apoptosis. To study MYC-induced apoptosis *in vivo*, I used the previously described Rosa26-MycER^{T2} model (R26^{MER/MER}), where MYC is expressed as a fusion protein with modified oestrogen receptor (ER^{T2}) under the control of the constitutive and ubiquitously active *Rosa26* locus. MYC activation can be achieved by administration of Tamoxifen, a synthetic ligand of oestrogen receptor (Murphy et al., 2008). In this model, MycER^{T2} drives apoptosis in the small intestine and colon, and sensitizes the tissues such as liver and islets of Langerhans to the pro-apoptotic stimuli Doxorubicin. On the other hand, tissues including kidney and exocrine pancreas are resistant to both MYC-induced apoptosis and MYC-induced sensitization to Doxorubicin. However, they are permissive to MYC-induced proliferation (Murphy et al., 2008). This difference in sensitivity could be partly explained by the level of MycER^{T2} expressed in different tissues, for example, MycER^{T2} expression is higher in the intestinal compartment compared to other tissues. Nevertheless, it might also reflect the differences in expression pattern of Bcl2 family proteins that is intrinsic to respective tissues.

To investigate the role of p19Arf and Bim, I interbred R26^{MER/MER} mice with *p19Arf* null (*Cdkn2a*^{tm1(GFP)Cjs}) and with *Bim* null (*Bcl2l1*^{tm1.1Ast}) mice to generate R26^{MER/MER}; *p19Arf* null and R26^{MER/MER}; *Bim* null cohorts respectively.

6.2.1.1 Role of Bim in MYC-induced apoptosis

Continuous activation of MycER^{T2} (for 3 days) in R26^{MER/MER} mice resulted in significant levels of apoptosis in the small intestine and colon compared to wild type controls (R26^{WT/WT}). To evaluate the role of Bim in MYC-induced apoptosis, MycER^{T2} was activated for 3 days in R26^{MER/MER} and R26^{MER/MER}; *Bim* null cohorts. As shown in Fig. 3-2, deletion of *Bim* suppressed MycER^{T2}-induced apoptosis in both small intestine and colon tissues. As described in the study performed by Murphy et al., 2008, the level of MycER^{T2} expressed in other tissues of R26^{MER/MER} mice is alone insufficient to breach the apoptotic threshold. However, combining MycER^{T2} activation with a dose of Doxorubicin that alone fails to drive apoptosis in most tissues, drove a significant amount of apoptosis in the liver and pancreatic islets of Langerhans, and enhanced MYC-induced killing in colon. To determine if sub-threshold apoptotic signalling by MYC is mediated by Bim, MycER^{T2} was activated for 3 days in R26^{MER/MER} and R26^{MER/MER}; *Bim* null mice, then a sub-apoptotic dose of Doxorubicin was administered. Again, deletion of *Bim* abrogated the apoptotic

response in all three tissues (Fig. 3-5 A and B), suggesting that Bim is required for MYC-induced sensitization to Doxorubicin.

It has been previously reported that MYC drives apoptosis only when the cells are deprived of serum and it is proposed that growth factors present in the serum might inhibit MYC-induced apoptosis (Evan et al., 1992). To determine the requirement of Bim for MYC-induced apoptosis *in vitro*, primary mouse embryonic fibroblasts (MEFs) generated from R26^{MER/WT} mice, wild type or nullizygous for *Bim*, were cultured in low serum conditions (0.2%) and treated with 4-OHT to activate MycER^{T2}. Apoptosis analysis by Annexin V/PI staining 30hrs after MycER^{T2} activation revealed that deletion of *Bim* attenuates MYC-induced apoptosis in the MEFs *in vitro* (Fig. 3-3A). Importantly, *Bim* null cells failed to undergo MYC-induced apoptosis even after 72hrs of MycER^{T2} activation, suggesting that Bim is required for both acute and chronic MYC signalling in MEFs (Fig. 3-4A). All these data suggest that Bim is required for both MYC-induced apoptosis and MYC-induced sensitization.

To determine whether Bim is a specific BH3-only protein required for MYC-induced apoptosis, the role of Puma, another closely related BH3-only protein, in MYC-induced apoptosis in the intestine was investigated. MycER^{T2} was activated for 3days in R26^{MER/MER} and R26^{MER/MER}; *Puma* null cohorts and as shown in Fig. 3-8, deletion of *Puma* had no effect on MYC-induced apoptosis in the intestine. However, in tissues where apoptosis is driven by the combination of MycER^{T2} activation and Doxorubicin treatment, both Bim and Puma are required (Fig. 3-9). I have shown that Bim lies downstream of MYC and I have also shown that Puma is required for Doxorubicin mediated apoptosis in the intestine, therefore it is hypothesized that combination of MycER^{T2} activation and Doxorubicin treatment require both Bim and Puma. The data presented in this thesis suggests that Puma failed to phenocopy Bim in MYC-induced apoptosis in the intestine, whereas Bim failed to phenocopy Puma in Doxorubicin mediated apoptosis in the small intestine (Fig. 3-10, 3-12). These data argue that there is a specific requirement of BH-3 only proteins to transduce specific pro-apoptotic signals and the parallel signals that engage multiple BH3-only proteins can cooperate in mediating apoptosis.

I next investigated if MYC regulates Bim directly. In line with previous reports (Campone et al., 2011), I have shown that MYC activates Bim expression both at the RNA and protein level (Fig. 3-15), and gene specific chromatin immunoprecipitation (CHIP) analysis in R26^{MER/WT} MEFs revealed increased occupancy of the *Bim* promoter region by

MYC in response to 4-OHT (Fig. 3-16A). This finding is not a species-specific or system-specific effect as I have shown binding of endogenous MYC to the *BIM* promoter region in a human cervical cancer cell line HeLa (Fig. 3-16B). Whole genome-CHIP coupled deep sequencing (CHIP-Seq) analysis using human breast cancer MCF-10A cells revealed an 4-OHT induced binding of MYC-ER exclusively to the *BIM* promoter region and not at the promoter region of genes encoding other Bcl2 family proteins, including *BCL2*, *BCLX*, *BBC3* (encoding *Puma*), *NOXA*, *BID*, *BAD*, *BAX* or *BAK*. However, similar analysis of promoter occupancy by Myc in primary murine pancreatic tumour cells derived from KPC tumours displayed promoter occupancy on all of the above mentioned genes except for *Noxa* and *Bak* (Muthalagu et al., 2014). This difference in promoter occupancy could be due to a variety of reasons, but a recent report suggests that target genes can be classified based on the presence of low-affinity or high-affinity MYC binding sites and different levels of MYC regulates distinct set of target genes (Walz et al., 2014). Hence, it can be hypothesized that the *BCL2L11* locus (encoding *Bim*) contains high-affinity binding sites and therefore even low-level of MYC can regulate its expression. On the other hand, promoters of other Bcl2 proteins encoding genes may contain low-affinity binding sites and thus require a high (tumourigenic) level of MYC for binding (Fig. 6-2).

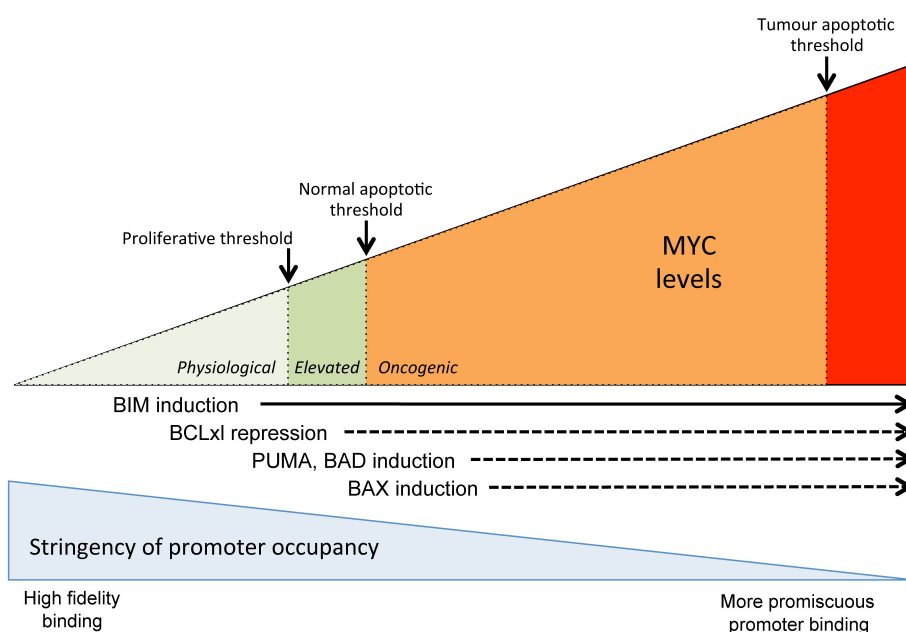


Figure 6-2- Model for the regulation of Bcl2 proteins by MYC

Proposed model showing regulation of Bcl2 proteins by different level of MYC. The data discussed in this thesis indicates that BIM promoter is bound by physiological level of MYC, whereas other Bcl2 proteins such as Puma require oncogenic level of MYC. Taken from (Murphy and Muthalagu, 2015)

6.2.1.2 Role of p19Arf in MYC-induced apoptosis

To evaluate the role of p19Arf in MYC-induced apoptosis in the intestine, MycER^{T2} was activated for 3 days in *R26^{MER/MER}*: p19Arf wild type and p19Arf null cohorts. As shown in Fig. 3-2, deletion of *p19Arf* did not affect the MYC-induced apoptosis in both small intestine and colon tissues. Similarly, apoptosis induced by the combination of MYC activation and Doxorubicin treatment (3dayTam+Dox) in the liver, pancreatic islets of Langerhans and colon was not affected by loss of *p19Arf* (Fig. 3-5). Consistent with the *in vivo* results, p19Arf is not required for MYC mediated apoptosis in MEFs cultured in low serum *in vitro* (Fig. 3-3, 3-4). All of these results suggest that p19Arf is dispensable for MYC-induced apoptosis *in vitro* and *in vivo*.

The results presented in this thesis are not consistent with previous data linking p19Arf to MYC-induced apoptosis. The first study showing the requirement of p19Arf for MYC-induced apoptosis in MEFs used retroviral based vector to overexpress MYC (pSR) (Zindy et al., 1998). It has been previously reported that the viral LTR are serum sensitive (Dutta et al., 1990). As pointed out earlier, MYC drives apoptosis only when the cells are deprived of serum. Accordingly, in their experiments, when the cells are deprived of serum to study MYC-induced apoptosis, they reported a decline in the level of MYC expressed over the course of the experiment, thus it is possible that the level of MYC that no longer breached the apoptotic threshold was inadvertently selected for. On the other hand, in the system used in this study, MycER^{T2} is expressed under the control of Rosa26 locus, which is not affected by serum conditions, thus a consistent level of MYC is maintained throughout the experimental conditions (Murphy et al., 2008).

Loss of *Ink4a/Arf* locus or deletion of *Trp53* have been shown to accelerate lymphomagenesis in the Eμ-Myc lymphoma model, which expresses Myc under the control of the immunoglobulin μ enhancer (Bertwistle and Sherr, 2007; Schmitt et al., 1999). This acceleration in lymphoma tumourigenesis was attributed to the suppression of MYC-induced apoptosis due to the loss of p19Arf and p53. However, because the level of MYC expressed from Rosa26 locus is not sufficient to drive apoptosis in B cells, one cannot exclude the possibility of tissue specific requirement of p19Arf for MYC-induced apoptosis.

Both p19Arf and p53 are bonafide tumour suppressors and the tumour suppressive role of Arf-p53 pathway during MYC-induced tumourigenesis is well documented. However, the

apoptosis function of Arf-p53 is not solely responsible for this tumour suppressive function. The Arf-p53 pathway acts as guardians of cells by mediating different tumour suppressive process such as apoptosis, cell cycle arrest and senescence. An elegant study using acetylation mutant of p53 (p53K117R), which abolishes apoptotic function of p53, demonstrated that apoptosis is dispensable for p53 mediated tumour suppression at least in the context of spontaneous tumourigenesis (Li et al., 2012). Different research groups have consistently showed increase in p19Arf expression upon MYC activation (Bertwistle and Sherr, 2007; Jacobs et al., 1999). In the R26^{MER/MER} system used in this study, the level of MycER^{T2} expressed was able to engage p19Arf pathway, by increasing its expression in the colonic epithelium (Murphy et al., 2008) but paradoxically it is not required for MYC-induced apoptosis in the same tissue, suggesting a possible requirement of p19Arf for a different biological output. Interestingly, p19Arf has been reported to complex with Myc/Max and inhibit the transactivation function of Myc. In this study, it has been shown that p19Arf specifically inhibits Myc-induced hyper proliferation but not apoptosis, suggesting that Myc-induced expression of p19Arf is a feedback mechanism to control the proliferation (Qi et al., 2004). Also, a study performed in pIns-MycER^{TAM} β cell model, which expresses ≈ 15 fold high MycER in the pancreatic islets compared to R26^{MER/MER} model, showed that Bcl-x_L gain of function and p19Arf loss of function cooperate with MYC in oncogenesis via distinct mechanisms. Bcl-x_L overexpression cooperates with MYC by specifically blocking MYC-induced apoptosis, whereas loss of p19Arf cooperates by facilitating MYC-induced proliferation (Finch et al., 2006). Therefore, I hypothesize that loss of *p19Arf* cooperates with Myc to accelerate tumourigenesis, possibly by accelerating MYC- induced proliferation.

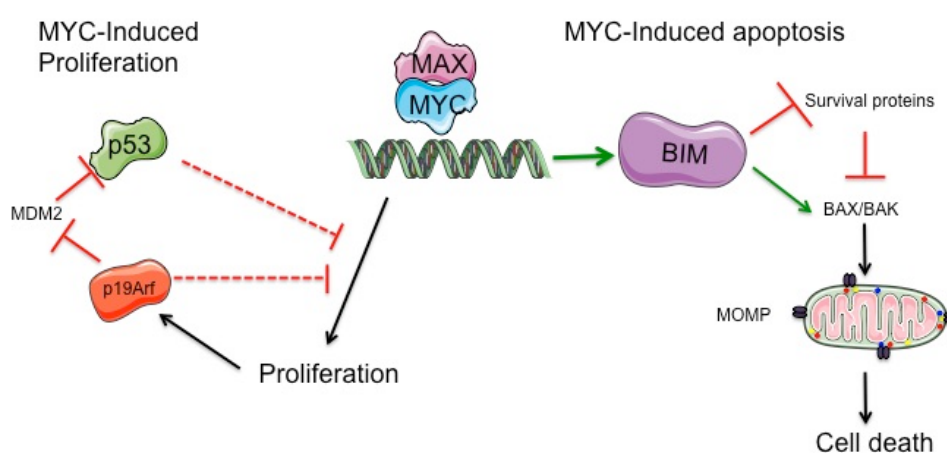


Figure 6-3- Proposed model for role of p19Arf and Bim in MYC-driven processes

MYC activates Bim transcriptionally, which in turn executes apoptosis through intrinsic mitochondrial pathway of apoptosis. p19Arf is induced upon MYC activation directly or indirectly, which in turn inhibits MYC-induced proliferation independently or by stabilizing p53. MOMP represents mitochondrial outer membrane permeabilization.

6.2.1.3 Exploiting MYC-induced apoptosis as a therapeutic strategy

In this study, I have shown that Bim is required and p19Arf is dispensable for MYC-induced apoptosis in various settings. It is clear from my data that a threshold level of Bim is required to overcome anti-apoptotic buffering and to drive MYC-induced apoptosis (Fig. 3-16). In such instances, I propose that augmenting MYC driven intrinsic pro-death signals by using BH3 mimetics (e.g. ABT-737, ABT-263) will hold great promise to target MYC overexpressing tumours. ABT-737 is a small molecule inhibitor that binds to the hydrophobic BH-3 binding groove of Bcl-x_L, Bcl2 and Bcl-w but not to Mcl1 or A1 (Oltersdorf et al., 2005). As a proof of principle, I have shown that the primary murine pancreatic cancer cells derived from KMC (*Pdx1-Cre;R26^{LSL-MYC/+};LSL-Kras^{G12D}*) tumours are sensitive to ABT-737 (Fig. 4-13). Strikingly, preliminary data suggests that primary murine pancreatic cancer cells derived from KPC (*Pdx1-Cre;LSL-Trp53^{R172H/+}; LSL-Kras^{G12D/+}*) tumours are not equally sensitive to the same dose of ABT-737 (data not shown). Although KPC cells express a high level of endogenous Myc, expression analysis of pro-and anti-apoptotic proteins needs to be performed in order to explain this result. For example, cells expressing high level of Mcl1 are generally resistant to ABT-737, as ABT-737 cannot inhibit Mcl1 (Hauck et al., 2009).

6.3 MYC in pancreatic tumourigenesis

The second aim of this thesis was to establish a MYC dependent pancreatic cancer mouse model. I used the *R26^{LSL-MYC}* model, where human MYC cDNA is expressed under the control of the constitutive Rosa26 locus, preceded by LoxP-Stop-LoxP cassette. Overexpression of MYC can be achieved by Cre recombinase mediated excision of Stop cassette (Neidler and Murphy, unpublished). In this study, pancreas specific expression of Rosa driven MYC was achieved by breeding *R26^{LSL-MYC/+}* mice with *Pdx1-Cre* mice, where Cre recombinase is expressed under the control of pancreas specific Pdx1 promoter. 50% of the mice that were heterozygous for Rosa26 driven MYC (*Pdx1-Cre;R26^{LSL-MYC/+}*) succumbed to pancreatic cancer with a median survival of 355days (Fig. 4-9). On the other hand, 91% of mice that were homozygous for Rosa26 driven MYC (*Pdx1-Cre;R26^{LSL-MYC/LSL-MYC}*) succumbed to pancreatic cancer with a median survival of 185days (Fig. 4-9). This data suggests that MYC can driver pancreatic tumourigenesis and that there is a dose dependent effect of MYC in pancreatic tumourigenesis. Interestingly, MYC driven by the same Rosa 26 locus when activated in the adult lung by administration of adenovirus expressing Cre recombinase, failed to initiate lung tumours on its own (Neidler and

Murphy, unpublished). This highlights the difference in response to the same oncogene by two different tissue types. However, it may also reflect a difference in response due to time of activation, MYC was activated *in utero* in the pancreatic cancer model and in the adult tissue in the lung tumour model. To answer this, MYC can be activated in the adult pancreas using Pdx1-CreER system, where Cre recombinase is activated by administration of tamoxifen.

A number of studies performed in GEMMs have demonstrated that *Kras* acts as a driver mutation and cooperates with a number of different oncogenes and tumour suppressors in accelerating pancreatic ductal adenocarcinoma (PDAC) (Perez-Mancera et al., 2012). Here, I have shown that MYC also cooperates with mutant *Kras* to accelerate pancreatic tumorigenesis (Fig. 4-3). MYC expression alone or concomitant expression of MYC and *Kras*^{G12D} drove the development of pancreatic tumours with distinct histological features. Overexpression of MYC resulted in poorly differentiated tumours that do not resemble PDAC. MYC in combination with *Kras*^{G12D} led to tumours with mixed pathology, but predominantly tumours that resemble PDAC histologically. Although the reason behind this is unclear, it is to be noted that MYC together with mutant p53 (p53^{R172H}) gave rise to poorly differentiated pancreatic tumours similar to MYC only tumours (Port and Murphy, unpublished). One possible explanation could be that in the absence of initiating *Kras*^{G12D} mutation, MYC overexpressing cells give rise to poorly differentiated tumours or it could be more complicated due to the developmental plasticity pertinent to the pancreas (Puri et al., 2015). However, *Myc* has also been reported to block differentiation and promote proliferation, in particular overexpression of MYC in pancreatic islet cells ablated the hormone producing ability of these cells and induces proliferation (Demeterco et al., 2002). Therefore, it is possible that MYC overexpression in the pancreatic precursor cells leads to poorly differentiated tumour. It will be insightful to evaluate the nature of pancreatic tumour, which arise when MYC is activated in a well differentiated, adolescent pancreas.

6.4 ‘Synthetic lethality’- an approach to target MYC selectively

The final aim of the thesis was to exploit MYC-induced dependence of Nuak1 (otherwise called Ark5) as a potential therapeutic strategy. NUA1 is an AMPK related kinase, which has been shown to be required for the survival of MYC overexpressing cells (Liu et al., 2012b). Having established the MYC dependent pancreatic cancer mouse model, I then

analysed the potential role for Nuak1 in MYC and Kras^{G12D} driven pancreatic tumorigenesis. Although, deletion of *Nuak1* did not provide any survival benefit to KMC mice, it is to be noted that tumours failed to knockout *Nuak1* allele completely (Fig. 5-6). This suggests that MYC (and/or KRAS) expressing cells might possibly have a selective pressure to retain Nuak1 expression for their survival. The primary murine pancreatic cancer cells derived from KMC tumours were sensitive to a small molecule inhibitor of Nuak1 (Fig. 5-7). This suggests that MYC overexpressing murine pancreatic cancer cells require Nuak1 function for their survival, and a different strategy is required to evaluate Nuak1 as a potential therapeutic target in MYC dependent pancreatic cancer (see below).

6.5 Future directions

6.5.1 Establishing tamoxifen inducible MYC/Kras^{G12D} pancreatic model

The pancreatic tumour model used in this study utilizes the Cre recombinase expression under the control of Pdx1 promoter. Pdx1 is expressed as early as E8.5, allowing the activation of alleles (MYC/Kras) in the embryonic stage. Constitutive expression of MYC and Kras^{G12D} is not ideal to understand the mechanism of cooperation in accelerating tumorigenesis. To mechanistically interrogate the course of tumour evolution, it would be useful to use the Pdx1-CreER system, where alleles (*R26^{LSL-MYC}* and *Kras^{G12D}*) can be activated by administration of tamoxifen (KMCⁱ model). This gives both spatial and temporal control over oncogene activation. Thus, by sacrificing mice at specific time points after allele activations, samples representing the entire course of PDAC development (from PanINs to PDAC) can be generated. RNA analysis comparing discrete stages of tumours could be used to link the phenotypic changes with underlying gene expression changes.

6.5.2 Exploiting MYC-induced vulnerabilities

Once established, this model (*Pdx1-CreER; R26^{LSL-MYC/+}; LSL-Kras^{G12D}* [KMCⁱ]) could be used to test if the intrinsic apoptosis signal and selective dependence to Nuak1 imposed by MYC can be used as a therapeutic strategy for pancreatic cancer. ABT-263, an orally available BH3-mimetic can be used to augment the MYC driven pro-apoptotic signalling and the effect on MYC driven PDAC should be evaluated.

To investigate the role of Nuak1 for the maintenance of MYC dependent pancreatic cancer, an intervention study should be carried out. The KMCⁱ model can be bred with mice carrying doxycycline dependent shRNA against Nuak1. Mice should be allowed to develop palpable pancreatic tumour and shNuak1 can be activated by the administration of doxycycline in the established tumours to evaluate effect of Nuak1 depletion in tumour growth and maintenance.

6.5.3 Characterizing the functions of Nuak1 in vitro

We have shown that Nuak1 inhibition resulted in suppression of electron transport chain components (ETC). ETC is one of the important sources of reactive oxygen species (ROS) production. In line with this, the preliminary data from my work suggests that NUA1 inhibition leads to mitochondrial ROS production and also modulation in Nrf2 anti-oxidant response. Cells have different anti-oxidant mechanisms to detoxify ROS and one of the important defence mechanisms is Nrf2 pathway. A study from Tuveson's laboratory has demonstrated that some oncogenes (e.g. *Kras* and *MYC*) elevate the basal Nrf2 anti-oxidant program, thereby conferring a more reduced intracellular environment. Moreover, Nrf2 ablation has been shown to impair *Kras*^{G12D} induced pancreatic tumourigenesis (DeNicola et al., 2011). Hence, it is hypothesized that Nuak1 mediated detoxification of ROS by activating Nrf2 pathway might represent a unique tumour promoting function of Nuak1, which will be investigated further.

6.6 Therapeutic implications

BIM mutations are rare in human cancer, however deletion polymorphism of *BIM* has been reported in East Asian communities. This deletion resulted in a splice variant of *BIM* that does not encode the BH3-domain, thereby compromising the apoptotic function of BIM. Furthermore, this polymorphism was sufficient to confer intrinsic resistance to tyrosine kinase inhibitor (TKI) in chronic myeloid leukaemia and non-small cell lung carcinoma, and the sensitivity to TKI was restored by using BH3-mimetic drugs (Ng et al., 2012). BH3-mimetic ABT-199 (GDC-0199), a selective Bcl2 inhibitor is in clinical trials for chronic lymphocytic leukaemia (CLL) and a variety of subtypes of non-Hodgkin lymphoma. The data presented in this thesis, linking BH3-only protein Bim and MYC-induced apoptosis; argue that this compound could be beneficial to patients with deregulated MYC expression.

Similar to MYC, NUA1 deregulation has been reported in a variety of human cancers including colorectal cancer, hepatocellular carcinoma, pancreatic cancer, and glioma. Preliminary data presented in this thesis and the data generated in our lab using GEMM for colorectal cancer (Raja et al., unpublished) suggest that targeting Nuak1 could be detrimental to MYC overexpressing cancer. Development and characterization of Nuak1 specific inhibitor in the available and established MYC dependent tumour models (Pancreas, lung and Colon) in the lab, will provide further insight.

References

- Adams, J. M., Harris, A. W., Pinkert, C. A., Corcoran, L. M., Alexander, W. S., Cory, S., Palmiter, R. D., and Brinster, R. L. (1985). The c-myc oncogene driven by immunoglobulin enhancers induces lymphoid malignancy in transgenic mice. *Nature* *318*, 533-538.
- Aguirre, A. J., Bardeesy, N., Sinha, M., Lopez, L., Tuveson, D. A., Horner, J., Redston, M. S., and DePinho, R. A. (2003). Activated Kras and Ink4a/Arf deficiency cooperate to produce metastatic pancreatic ductal adenocarcinoma. *Genes & development* *17*, 3112-3126.
- Akhoondi, S., Sun, D., von der Lehr, N., Apostolidou, S., Klotz, K., Maljukova, A., Cepeda, D., Fiegl, H., Dafou, D., Marth, C., *et al.* (2007). FBXW7/hCDC4 is a general tumor suppressor in human cancer. *Cancer research* *67*, 9006-9012.
- Akiyama, T., Dass, C. R., and Choong, P. F. (2009). Bim-targeted cancer therapy: a link between drug action and underlying molecular changes. *Molecular cancer therapeutics* *8*, 3173-3180.
- Alessi, D. R., Sakamoto, K., and Bayascas, J. R. (2006). LKB1-dependent signaling pathways. *Annual review of biochemistry* *75*, 137-163.
- Amati, B., Littlewood, T. D., Evan, G. I., and Land, H. (1993). The c-Myc protein induces cell cycle progression and apoptosis through dimerization with Max. *The EMBO journal* *12*, 5083-5087.
- Annibaldi, D., Whitfield, J. R., Favuzzi, E., Jauset, T., Serrano, E., Cuartas, I., Redondo-Campos, S., Folch, G., Gonzalez-Junca, A., Sodir, N. M., *et al.* (2014). Myc inhibition is effective against glioma and reveals a role for Myc in proficient mitosis. *Nature communications* *5*, 4632.
- Arabi, A., Wu, S., Ridderstrale, K., Bierhoff, H., Shiue, C., Fatyol, K., Fahlen, S., Hydbring, P., Soderberg, O., Grummt, I., *et al.* (2005). c-Myc associates with ribosomal DNA and activates RNA polymerase I transcription. *Nature cell biology* *7*, 303-310.
- Askew, D. S., Ashmun, R. A., Simmons, B. C., and Cleveland, J. L. (1991). Constitutive c-myc expression in an IL-3-dependent myeloid cell line suppresses cell cycle arrest and accelerates apoptosis. *Oncogene* *6*, 1915-1922.
- Ayer, D. E., Kretzner, L., and Eisenman, R. N. (1993). Mad: a heterodimeric partner for Max that antagonizes Myc transcriptional activity. *Cell* *72*, 211-222.
- Banerjee, S., Buhrlage, S. J., Huang, H. T., Deng, X., Zhou, W., Wang, J., Traynor, R., Prescott, A. R., Alessi, D. R., and Gray, N. S. (2014). Characterization of WZ4003 and HTH-01-015 as selective inhibitors of the LKB1-tumour-suppressor-activated NIAK kinases. *The Biochemical journal* *457*, 215-225.

- Bardeesy, N., Aguirre, A. J., Chu, G. C., Cheng, K. H., Lopez, L. V., Hezel, A. F., Feng, B., Brennan, C., Weissleder, R., Mahmood, U., *et al.* (2006a). Both p16(Ink4a) and the p19(Arf)-p53 pathway constrain progression of pancreatic adenocarcinoma in the mouse. *Proceedings of the National Academy of Sciences of the United States of America* *103*, 5947-5952.
- Bardeesy, N., Cheng, K. H., Berger, J. H., Chu, G. C., Pahler, J., Olson, P., Hezel, A. F., Horner, J., Lauwers, G. Y., Hanahan, D., and DePinho, R. A. (2006b). Smad4 is dispensable for normal pancreas development yet critical in progression and tumor biology of pancreas cancer. *Genes & development* *20*, 3130-3146.
- Barr, L. F., Campbell, S. E., Bochner, B. S., and Dang, C. V. (1998). Association of the decreased expression of alpha3beta1 integrin with the altered cell: environmental interactions and enhanced soft agar cloning ability of c-myc-overexpressing small cell lung cancer cells. *Cancer research* *58*, 5537-5545.
- Baudino, T. A., McKay, C., Pendeville-Samain, H., Nilsson, J. A., Maclean, K. H., White, E. L., Davis, A. C., Ihle, J. N., and Cleveland, J. L. (2002). c-Myc is essential for vasculogenesis and angiogenesis during development and tumor progression. *Genes & development* *16*, 2530-2543.
- Baykara, O., Bakir, B., Buyru, N., Kaynak, K., and Dalay, N. (2015). Amplification of chromosome 8 genes in lung cancer. *Journal of Cancer* *6*, 270-275.
- Bell, R. E., Khaled, M., Netanel, D., Schubert, S., Golan, T., Buxbaum, A., Janas, M. M., Postolsky, B., Goldberg, M. S., Shamir, R., and Levy, C. (2014). Transcription factor/microRNA axis blocks melanoma invasion program by miR-211 targeting NUA1. *The Journal of investigative dermatology* *134*, 441-451.
- Bertwistle, D., and Sherr, C. J. (2007). Regulation of the Arf tumor suppressor in Emicro-Myc transgenic mice: longitudinal study of Myc-induced lymphomagenesis. *Blood* *109*, 792-794.
- Bhatia, K., Huppi, K., Spangler, G., Siwarski, D., Iyer, R., and Magrath, I. (1993). Point mutations in the c-Myc transactivation domain are common in Burkitt's lymphoma and mouse plasmacytomas. *Nature genetics* *5*, 56-61.
- Bissonnette, R. P., Echeverri, F., Mahboubi, A., and Green, D. R. (1992). Apoptotic cell death induced by c-myc is inhibited by bcl-2. *Nature* *359*, 552-554.
- Blackwell, T. K., Kretzner, L., Blackwood, E. M., Eisenman, R. N., and Weintraub, H. (1990). Sequence-specific DNA binding by the c-Myc protein. *Science* *250*, 1149-1151.
- Blackwood, E. M., and Eisenman, R. N. (1991). Max: a helix-loop-helix zipper protein that forms a sequence-specific DNA-binding complex with Myc. *Science* *251*, 1211-1217.
- Blyth, K., Stewart, M., Bell, M., James, C., Evan, G., Neil, J. C., and Cameron, E. R. (2000). Sensitivity to myc-induced apoptosis is retained in spontaneous and transplanted lymphomas of CD2-mycER mice. *Oncogene* *19*, 773-782.

- Bouchard, C., Dittrich, O., Kiermaier, A., Dohmann, K., Menkel, A., Eilers, M., and Luscher, B. (2001). Regulation of cyclin D2 gene expression by the Myc/Max/Mad network: Myc-dependent TRRAP recruitment and histone acetylation at the cyclin D2 promoter. *Genes & development* *15*, 2042-2047.
- Bouchard, C., Lee, S., Paulus-Hock, V., Loddenkemper, C., Eilers, M., and Schmitt, C. A. (2007). FoxO transcription factors suppress Myc-driven lymphomagenesis via direct activation of Arf. *Genes & development* *21*, 2775-2787.
- Bouillet, P., Metcalf, D., Huang, D. C., Tarlinton, D. M., Kay, T. W., Kontgen, F., Adams, J. M., and Strasser, A. (1999). Proapoptotic Bcl-2 relative Bim required for certain apoptotic responses, leukocyte homeostasis, and to preclude autoimmunity. *Science* *286*, 1735-1738.
- Boxer, L. M., and Dang, C. V. (2001). Translocations involving c-myc and c-myc function. *Oncogene* *20*, 5595-5610.
- Bright, N. J., Thornton, C., and Carling, D. (2009). The regulation and function of mammalian AMPK-related kinases. *Acta physiologica* *196*, 15-26.
- Brodeur, G. M., Seeger, R. C., Schwab, M., Varmus, H. E., and Bishop, J. M. (1984). Amplification of N-myc in untreated human neuroblastomas correlates with advanced disease stage. *Science* *224*, 1121-1124.
- Buchholz, M., Schatz, A., Wagner, M., Michl, P., Linhart, T., Adler, G., Gress, T. M., and Ellenrieder, V. (2006). Overexpression of c-myc in pancreatic cancer caused by ectopic activation of NFATc1 and the Ca²⁺/calcineurin signaling pathway. *The EMBO journal* *25*, 3714-3724.
- Burlison, J. S., Long, Q., Fujitani, Y., Wright, C. V., and Magnuson, M. A. (2008). Pdx-1 and Ptf1a concurrently determine fate specification of pancreatic multipotent progenitor cells. *Developmental biology* *316*, 74-86.
- Burris, H. A., 3rd, Moore, M. J., Andersen, J., Green, M. R., Rothenberg, M. L., Modiano, M. R., Cripps, M. C., Portenoy, R. K., Storniolo, A. M., Tarassoff, P., *et al.* (1997). Improvements in survival and clinical benefit with gemcitabine as first-line therapy for patients with advanced pancreas cancer: a randomized trial. *Journal of clinical oncology : official journal of the American Society of Clinical Oncology* *15*, 2403-2413.
- Campone, M., Noel, B., Couriaud, C., Grau, M., Guillemin, Y., Gautier, F., Gouraud, W., Charbonnel, C., Campion, L., Jezequel, P., *et al.* (2011). c-Myc dependent expression of pro-apoptotic Bim renders HER2-overexpressing breast cancer cells dependent on anti-apoptotic Mcl-1. *Molecular cancer* *10*, 110.
- Chadha, K. S., Khoury, T., Yu, J., Black, J. D., Gibbs, J. F., Kuvshinoff, B. W., Tan, D., Brattain, M. G., and Javle, M. M. (2006). Activated Akt and Erk expression and survival after surgery in pancreatic carcinoma. *Annals of surgical oncology* *13*, 933-939.

Chang, X. Z., Yu, J., Liu, H. Y., Dong, R. H., and Cao, X. C. (2012). ARK5 is associated with the invasive and metastatic potential of human breast cancer cells. *Journal of cancer research and clinical oncology* 138, 247-254.

Chen, L., Willis, S. N., Wei, A., Smith, B. J., Fletcher, J. I., Hinds, M. G., Colman, P. M., Day, C. L., Adams, J. M., and Huang, D. C. (2005). Differential targeting of prosurvival Bcl-2 proteins by their BH3-only ligands allows complementary apoptotic function. *Molecular cell* 17, 393-403.

Cho, K. B., Cho, M. K., Lee, W. Y., and Kang, K. W. (2010). Overexpression of c-myc induces epithelial mesenchymal transition in mammary epithelial cells. *Cancer letters* 293, 230-239.

Clausen, D. M., Guo, J., Parise, R. A., Beumer, J. H., Egorin, M. J., Lazo, J. S., Prochownik, E. V., and Eiseman, J. L. (2010). In vitro cytotoxicity and in vivo efficacy, pharmacokinetics, and metabolism of 10074-G5, a novel small-molecule inhibitor of c-Myc/Max dimerization. *The Journal of pharmacology and experimental therapeutics* 335, 715-727.

Conacci-Sorrell, M., McFerrin, L., and Eisenman, R. N. (2014). An overview of MYC and its interactome. *Cold Spring Harbor perspectives in medicine* 4, a014357.

Cory, S., and Adams, J. M. (2002). The Bcl2 family: regulators of the cellular life-or-death switch. *Nature reviews Cancer* 2, 647-656.

Croce, C. M. (2008). Oncogenes and cancer. *The New England journal of medicine* 358, 502-511.

Cui, J., Yu, Y., Lu, G. F., Liu, C., Liu, X., Xu, Y. X., and Zheng, P. Y. (2013). Overexpression of ARK5 is associated with poor prognosis in hepatocellular carcinoma. *Tumour biology : the journal of the International Society for Oncodevelopmental Biology and Medicine* 34, 1913-1918.

Czabotar, P. E., Lessene, G., Strasser, A., and Adams, J. M. (2014). Control of apoptosis by the BCL-2 protein family: implications for physiology and therapy. *Nature reviews Molecular cell biology* 15, 49-63.

Dang, C. V. (2013). MYC, metabolism, cell growth, and tumorigenesis. *Cold Spring Harbor perspectives in medicine* 3.

Dansen, T. B., Whitfield, J., Rostker, F., Brown-Swigart, L., and Evan, G. I. (2006). Specific requirement for Bax, not Bak, in Myc-induced apoptosis and tumor suppression in vivo. *The Journal of biological chemistry* 281, 10890-10895.

Datta, S. R., Dudek, H., Tao, X., Masters, S., Fu, H., Gotoh, Y., and Greenberg, M. E. (1997). Akt phosphorylation of BAD couples survival signals to the cell-intrinsic death machinery. *Cell* 91, 231-241.

- Delmore, J. E., Issa, G. C., Lemieux, M. E., Rahl, P. B., Shi, J., Jacobs, H. M., Kastritis, E., Gilpatrick, T., Paranal, R. M., Qi, J., *et al.* (2011). BET bromodomain inhibition as a therapeutic strategy to target c-Myc. *Cell* *146*, 904-917.
- Demeterco, C., Itkin-Ansari, P., Tyrberg, B., Ford, L. P., Jarvis, R. A., and Levine, F. (2002). c-Myc controls proliferation versus differentiation in human pancreatic endocrine cells. *The Journal of clinical endocrinology and metabolism* *87*, 3475-3485.
- DeNicola, G. M., Karreth, F. A., Humpton, T. J., Gopinathan, A., Wei, C., Frese, K., Mangal, D., Yu, K. H., Yeo, C. J., Calhoun, E. S., *et al.* (2011). Oncogene-induced Nrf2 transcription promotes ROS detoxification and tumorigenesis. *Nature* *475*, 106-109.
- Doerflinger, M., Glab, J. A., and Puthalakath, H. (2015). BH3-only proteins: a 20-year stock-take. *The FEBS journal*.
- Dutta, A., Hamaguchi, M., and Hanafusa, H. (1990). Serum independence of transcription from the promoter of an avian retrovirus in v-src-transformed cells is a primary, intracellular effect of increased tyrosine phosphorylation. *Proceedings of the National Academy of Sciences of the United States of America* *87*, 608-612.
- Eberhardy, S. R., and Farnham, P. J. (2001). c-Myc mediates activation of the cad promoter via a post-RNA polymerase II recruitment mechanism. *The Journal of biological chemistry* *276*, 48562-48571.
- Eberhardy, S. R., and Farnham, P. J. (2002). Myc recruits P-TEFb to mediate the final step in the transcriptional activation of the cad promoter. *The Journal of biological chemistry* *277*, 40156-40162.
- Egle, A., Harris, A. W., Bouillet, P., and Cory, S. (2004). Bim is a suppressor of Myc-induced mouse B cell leukemia. *Proceedings of the National Academy of Sciences of the United States of America* *101*, 6164-6169.
- Eilers, M., and Eisenman, R. N. (2008). Myc's broad reach. *Genes & development* *22*, 2755-2766.
- Eilers, M., Picard, D., Yamamoto, K. R., and Bishop, J. M. (1989). Chimaeras of myc oncoprotein and steroid receptors cause hormone-dependent transformation of cells. *Nature* *340*, 66-68.
- Eischen, C. M., Weber, J. D., Roussel, M. F., Sherr, C. J., and Cleveland, J. L. (1999). Disruption of the ARF-Mdm2-p53 tumor suppressor pathway in Myc-induced lymphomagenesis. *Genes & development* *13*, 2658-2669.
- Eischen, C. M., Woo, D., Roussel, M. F., and Cleveland, J. L. (2001). Apoptosis triggered by Myc-induced suppression of Bcl-X(L) or Bcl-2 is bypassed during lymphomagenesis. *Molecular and cellular biology* *21*, 5063-5070.
- Escot, C., Theillet, C., Lidereau, R., Spyrtos, F., Champeme, M. H., Gest, J., and Callahan, R. (1986). Genetic alteration of the c-myc protooncogene (MYC) in human

primary breast carcinomas. *Proceedings of the National Academy of Sciences of the United States of America* *83*, 4834-4838.

Evan, G. I., Wyllie, A. H., Gilbert, C. S., Littlewood, T. D., Land, H., Brooks, M., Waters, C. M., Penn, L. Z., and Hancock, D. C. (1992). Induction of apoptosis in fibroblasts by c-myc protein. *Cell* *69*, 119-128.

Fanidi, A., Harrington, E. A., and Evan, G. I. (1992). Cooperative interaction between c-myc and bcl-2 proto-oncogenes. *Nature* *359*, 554-556.

Feig, C., Gopinathan, A., Neesse, A., Chan, D. S., Cook, N., and Tuveson, D. A. (2012). The pancreas cancer microenvironment. *Clinical cancer research : an official journal of the American Association for Cancer Research* *18*, 4266-4276.

Feil, R., Brocard, J., Mascrez, B., LeMeur, M., Metzger, D., and Chambon, P. (1996). Ligand-activated site-specific recombination in mice. *Proceedings of the National Academy of Sciences of the United States of America* *93*, 10887-10890.

Felsher, D. W., and Bishop, J. M. (1999). Reversible tumorigenesis by MYC in hematopoietic lineages. *Molecular cell* *4*, 199-207.

Fernandez, P. C., Frank, S. R., Wang, L., Schroeder, M., Liu, S., Greene, J., Cocito, A., and Amati, B. (2003). Genomic targets of the human c-Myc protein. *Genes & development* *17*, 1115-1129.

Finch, A., Prescott, J., Shchors, K., Hunt, A., Soucek, L., Dansen, T. B., Swigart, L. B., and Evan, G. I. (2006). Bcl-xL gain of function and p19 ARF loss of function cooperate oncogenically with Myc in vivo by distinct mechanisms. *Cancer cell* *10*, 113-120.

Frank, S. R., Parisi, T., Taubert, S., Fernandez, P., Fuchs, M., Chan, H. M., Livingston, D. M., and Amati, B. (2003). MYC recruits the TIP60 histone acetyltransferase complex to chromatin. *EMBO reports* *4*, 575-580.

Fridovich, I. (1995). Superoxide radical and superoxide dismutases. *Annual review of biochemistry* *64*, 97-112.

Frye, M., Gardner, C., Li, E. R., Arnold, I., and Watt, F. M. (2003). Evidence that Myc activation depletes the epidermal stem cell compartment by modulating adhesive interactions with the local microenvironment. *Development* *130*, 2793-2808.

Gao, P., Tchernyshyov, I., Chang, T. C., Lee, Y. S., Kita, K., Ochi, T., Zeller, K. I., De Marzo, A. M., Van Eyk, J. E., Mendell, J. T., and Dang, C. V. (2009). c-Myc suppression of miR-23a/b enhances mitochondrial glutaminase expression and glutamine metabolism. *Nature* *458*, 762-765.

Gidekel Friedlander, S. Y., Chu, G. C., Snyder, E. L., Girnius, N., Dibelius, G., Crowley, D., Vasile, E., DePinho, R. A., and Jacks, T. (2009). Context-dependent transformation of adult pancreatic cells by oncogenic K-Ras. *Cancer cell* *16*, 379-389.

- Gomez-Roman, N., Grandori, C., Eisenman, R. N., and White, R. J. (2003). Direct activation of RNA polymerase III transcription by c-Myc. *Nature* *421*, 290-294.
- Grandori, C., Gomez-Roman, N., Felton-Edkins, Z. A., Ngouenet, C., Galloway, D. A., Eisenman, R. N., and White, R. J. (2005). c-Myc binds to human ribosomal DNA and stimulates transcription of rRNA genes by RNA polymerase I. *Nature cell biology* *7*, 311-318.
- Guerra, C., and Barbacid, M. (2013). Genetically engineered mouse models of pancreatic adenocarcinoma. *Molecular oncology* *7*, 232-247.
- Guicciardi, M. E., and Gores, G. J. (2009). The Death Receptor Pathway. *Essentials of Apoptosis, Second Edition*, 119-150.
- Guo, J., Parise, R. A., Joseph, E., Egorin, M. J., Lazo, J. S., Prochownik, E. V., and Eisenman, J. L. (2009). Efficacy, pharmacokinetics, tissue distribution, and metabolism of the Myc-Max disruptor, 10058-F4 [Z,E]-5-[4-ethylbenzylidene]-2-thioxothiazolidin-4-one, in mice. *Cancer chemotherapy and pharmacology* *63*, 615-625.
- Hanahan, D., and Weinberg, R. A. (2000). The hallmarks of cancer. *Cell* *100*, 57-70.
- Hanson, K. D., Shichiri, M., Follansbee, M. R., and Sedivy, J. M. (1994). Effects of c-myc expression on cell cycle progression. *Molecular and cellular biology* *14*, 5748-5755.
- Happo, L., Strasser, A., and Cory, S. (2012). BH3-only proteins in apoptosis at a glance. *Journal of cell science* *125*, 1081-1087.
- Harada, Y., Katagiri, T., Ito, I., Akiyama, F., Sakamoto, G., Kasumi, F., Nakamura, Y., and Emi, M. (1994). Genetic studies of 457 breast cancers. Clinicopathologic parameters compared with genetic alterations. *Cancer* *74*, 2281-2286.
- Hardie, D. G. (2014). AMPK: positive and negative regulation, and its role in whole-body energy homeostasis. *Current opinion in cell biology* *33C*, 1-7.
- Harrington, E. A., Bennett, M. R., Fanidi, A., and Evan, G. I. (1994a). c-Myc-induced apoptosis in fibroblasts is inhibited by specific cytokines. *The EMBO journal* *13*, 3286-3295.
- Harrington, E. A., Fanidi, A., and Evan, G. I. (1994b). Oncogenes and cell death. *Current opinion in genetics & development* *4*, 120-129.
- Harris, L. L., Talian, J. C., and Zelenka, P. S. (1992). Contrasting patterns of c-myc and N-myc expression in proliferating, quiescent, and differentiating cells of the embryonic chicken lens. *Development* *115*, 813-820.
- Hauck, P., Chao, B. H., Litz, J., and Krystal, G. W. (2009). Alterations in the Noxa/Mcl-1 axis determine sensitivity of small cell lung cancer to the BH3 mimetic ABT-737. *Molecular cancer therapeutics* *8*, 883-892.

He, T. C., Sparks, A. B., Rago, C., Hermeking, H., Zawel, L., da Costa, L. T., Morin, P. J., Vogelstein, B., and Kinzler, K. W. (1998). Identification of c-MYC as a target of the APC pathway. *Science* 281, 1509-1512.

Hemann, M. T., Bric, A., Teruya-Feldstein, J., Herbst, A., Nilsson, J. A., Cordon-Cardo, C., Cleveland, J. L., Tansey, W. P., and Lowe, S. W. (2005). Evasion of the p53 tumour surveillance network by tumour-derived MYC mutants. *Nature* 436, 807-811.

Hermeking, H., Rago, C., Schuhmacher, M., Li, Q., Barrett, J. F., Obaya, A. J., O'Connell, B. C., Mateyak, M. K., Tam, W., Kohlhuber, F., *et al.* (2000). Identification of CDK4 as a target of c-MYC. *Proceedings of the National Academy of Sciences of the United States of America* 97, 2229-2234.

Hezel, A. F., Kimmelman, A. C., Stanger, B. Z., Bardeesy, N., and Depinho, R. A. (2006). Genetics and biology of pancreatic ductal adenocarcinoma. *Genes & development* 20, 1218-1249.

Hidalgo, M. (2010). Pancreatic cancer. *The New England journal of medicine* 362, 1605-1617.

Hingorani, S. R., Petricoin, E. F., Maitra, A., Rajapakse, V., King, C., Jacobetz, M. A., Ross, S., Conrads, T. P., Veenstra, T. D., Hitt, B. A., *et al.* (2003). Preinvasive and invasive ductal pancreatic cancer and its early detection in the mouse. *Cancer cell* 4, 437-450.

Hingorani, S. R., Wang, L., Multani, A. S., Combs, C., Deramaudt, T. B., Hruban, R. H., Rustgi, A. K., Chang, S., and Tuveson, D. A. (2005). Trp53R172H and KrasG12D cooperate to promote chromosomal instability and widely metastatic pancreatic ductal adenocarcinoma in mice. *Cancer cell* 7, 469-483.

Hirano, M., Kiyonari, H., Inoue, A., Furushima, K., Murata, T., Suda, Y., and Aizawa, S. (2006). A new serine/threonine protein kinase, Omphk1, essential to ventral body wall formation. *Developmental dynamics : an official publication of the American Association of Anatomists* 235, 2229-2237.

Hoffman, B., and Liebermann, D. A. (2008). Apoptotic signaling by c-MYC. *Oncogene* 27, 6462-6472.

Horiuchi, D., Anderton, B., and Goga, A. (2014). Taking on challenging targets: making MYC druggable. *American Society of Clinical Oncology educational book / ASCO American Society of Clinical Oncology Meeting*, e497-502.

Hou, X., Liu, J. E., Liu, W., Liu, C. Y., Liu, Z. Y., and Sun, Z. Y. (2011). A new role of NUA1: directly phosphorylating p53 and regulating cell proliferation. *Oncogene* 30, 2933-2942.

Hruban, R. H., Takaori, K., Klimstra, D. S., Adsay, N. V., Albores-Saavedra, J., Biankin, A. V., Biankin, S. A., Compton, C., Fukushima, N., Furukawa, T., *et al.* (2004). An illustrated consensus on the classification of pancreatic intraepithelial neoplasia and

- intraductal papillary mucinous neoplasms. *The American journal of surgical pathology* *28*, 977-987.
- Huang, M. J., Cheng, Y. C., Liu, C. R., Lin, S., and Liu, H. E. (2006). A small-molecule c-Myc inhibitor, 10058-F4, induces cell-cycle arrest, apoptosis, and myeloid differentiation of human acute myeloid leukemia. *Experimental hematology* *34*, 1480-1489.
- Hueber, A. O., Zornig, M., Lyon, D., Suda, T., Nagata, S., and Evan, G. I. (1997). Requirement for the CD95 receptor-ligand pathway in c-Myc-induced apoptosis. *Science* *278*, 1305-1309.
- Humbert, N., Navaratnam, N., Augert, A., Da Costa, M., Martien, S., Wang, J., Martinez, D., Abbadie, C., Carling, D., de Launoit, Y., *et al.* (2010). Regulation of ploidy and senescence by the AMPK-related kinase NUA1. *The EMBO journal* *29*, 376-386.
- Ijichi, H., Chytil, A., Gorska, A. E., Aakre, M. E., Fujitani, Y., Fujitani, S., Wright, C. V., and Moses, H. L. (2006). Aggressive pancreatic ductal adenocarcinoma in mice caused by pancreas-specific blockade of transforming growth factor-beta signaling in cooperation with active Kras expression. *Genes & development* *20*, 3147-3160.
- Inazuka, F., Sugiyama, N., Tomita, M., Abe, T., Shioi, G., and Esumi, H. (2012). Muscle-specific knock-out of NUA1 family SNF1-like kinase 1 (NUAK1) prevents high fat diet-induced glucose intolerance. *The Journal of biological chemistry* *287*, 16379-16389.
- Izeradjene, K., Combs, C., Best, M., Gopinathan, A., Wagner, A., Grady, W. M., Deng, C. X., Hruban, R. H., Adsay, N. V., Tuveson, D. A., and Hingorani, S. R. (2007). Kras(G12D) and Smad4/Dpc4 haploinsufficiency cooperate to induce mucinous cystic neoplasms and invasive adenocarcinoma of the pancreas. *Cancer cell* *11*, 229-243.
- Jackson, E. L., Willis, N., Mercer, K., Bronson, R. T., Crowley, D., Montoya, R., Jacks, T., and Tuveson, D. A. (2001). Analysis of lung tumor initiation and progression using conditional expression of oncogenic K-ras. *Genes & development* *15*, 3243-3248.
- Jacobs, J. J., Scheijen, B., Voncken, J. W., Kieboom, K., Berns, A., and van Lohuizen, M. (1999). Bmi-1 collaborates with c-Myc in tumorigenesis by inhibiting c-Myc-induced apoptosis via INK4a/ARF. *Genes & development* *13*, 2678-2690.
- Janiak, F., Leber, B., and Andrews, D. W. (1994). Assembly of Bcl-2 into microsomal and outer mitochondrial membranes. *The Journal of biological chemistry* *269*, 9842-9849.
- Jenkins, R. B., Qian, J., Lieber, M. M., and Bostwick, D. G. (1997). Detection of c-myc oncogene amplification and chromosomal anomalies in metastatic prostatic carcinoma by fluorescence in situ hybridization. *Cancer research* *57*, 524-531.
- Johnston, L. A., Prober, D. A., Edgar, B. A., Eisenman, R. N., and Gallant, P. (1999). *Drosophila myc* regulates cellular growth during development. *Cell* *98*, 779-790.
- Jonckheere, N., Skrypek, N., and Van Seuning, I. (2010). Mucins and pancreatic cancer. *Cancers* *2*, 1794-1812.

Juin, P., Hueber, A. O., Littlewood, T., and Evan, G. (1999). c-Myc-induced sensitization to apoptosis is mediated through cytochrome c release. *Genes & development* *13*, 1367-1381.

Juin, P., Hunt, A., Littlewood, T., Griffiths, B., Swigart, L. B., Korsmeyer, S., and Evan, G. (2002). c-Myc functionally cooperates with Bax to induce apoptosis. *Molecular and cellular biology* *22*, 6158-6169.

Kaczmarek, L., Hyland, J. K., Watt, R., Rosenberg, M., and Baserga, R. (1985). Microinjected c-myc as a competence factor. *Science* *228*, 1313-1315.

Kaelin, W. G., Jr. (2005). The concept of synthetic lethality in the context of anticancer therapy. *Nature reviews Cancer* *5*, 689-698.

Kalra, A. V., and Campbell, R. B. (2007). Mucin impedes cytotoxic effect of 5-FU against growth of human pancreatic cancer cells: overcoming cellular barriers for therapeutic gain. *British journal of cancer* *97*, 910-918.

Kamijo, T., Weber, J. D., Zambetti, G., Zindy, F., Roussel, M. F., and Sherr, C. J. (1998). Functional and physical interactions of the ARF tumor suppressor with p53 and Mdm2. *Proceedings of the National Academy of Sciences of the United States of America* *95*, 8292-8297.

Kanazawa, S., Soucek, L., Evan, G., Okamoto, T., and Peterlin, B. M. (2003). c-Myc recruits P-TEFb for transcription, cellular proliferation and apoptosis. *Oncogene* *22*, 5707-5711.

Kang, J., Sergio, C. M., Sutherland, R. L., and Musgrove, E. A. (2014). Targeting cyclin-dependent kinase 1 (CDK1) but not CDK4/6 or CDK2 is selectively lethal to MYC-dependent human breast cancer cells. *BMC cancer* *14*, 32.

Kato, G. J., Barrett, J., Villa-Garcia, M., and Dang, C. V. (1990). An amino-terminal c-myc domain required for neoplastic transformation activates transcription. *Molecular and cellular biology* *10*, 5914-5920.

Kato, G. J., Lee, W. M., Chen, L. L., and Dang, C. V. (1992). Max: functional domains and interaction with c-Myc. *Genes & development* *6*, 81-92.

Kelly, P. N., Grabow, S., Delbridge, A. R., Adams, J. M., and Strasser, A. (2013). Prophylactic treatment with the BH3 mimetic ABT-737 impedes Myc-driven lymphomagenesis in mice. *Cell death and differentiation* *20*, 57-63.

Kern, S. E., Hruban, R. H., Hidalgo, M., and Yeo, C. J. (2002). An introduction to pancreatic adenocarcinoma genetics, pathology and therapy. *Cancer biology & therapy* *1*, 607-613.

Khanna, A., Bockelman, C., Hemmes, A., Junttila, M. R., Wiksten, J. P., Lundin, M., Junnila, S., Murphy, D. J., Evan, G. I., Haglund, C., *et al.* (2009). MYC-dependent

- regulation and prognostic role of CIP2A in gastric cancer. *Journal of the National Cancer Institute* *101*, 793-805.
- Kiessling, A., Sperl, B., Hollis, A., Eick, D., and Berg, T. (2006). Selective inhibition of c-Myc/Max dimerization and DNA binding by small molecules. *Chemistry & biology* *13*, 745-751.
- Kim, J., Woo, A. J., Chu, J., Snow, J. W., Fujiwara, Y., Kim, C. G., Cantor, A. B., and Orkin, S. H. (2010). A Myc network accounts for similarities between embryonic stem and cancer cell transcription programs. *Cell* *143*, 313-324.
- Knies-Bamforth, U. E., Fox, S. B., Poulsom, R., Evan, G. I., and Harris, A. L. (2004). c-Myc interacts with hypoxia to induce angiogenesis in vivo by a vascular endothelial growth factor-dependent mechanism. *Cancer research* *64*, 6563-6570.
- Kusakai, G., Suzuki, A., Ogura, T., Miyamoto, S., Ochiai, A., Kaminishi, M., and Esumi, H. (2004). ARK5 expression in colorectal cancer and its implications for tumor progression. *The American journal of pathology* *164*, 987-995.
- Kuwana, T., Bouchier-Hayes, L., Chipuk, J. E., Bonzon, C., Sullivan, B. A., Green, D. R., and Newmeyer, D. D. (2005). BH3 domains of BH3-only proteins differentially regulate Bax-mediated mitochondrial membrane permeabilization both directly and indirectly. *Molecular cell* *17*, 525-535.
- Laurenti, E., Varnum-Finney, B., Wilson, A., Ferrero, I., Blanco-Bose, W. E., Ehninger, A., Knoepfler, P. S., Cheng, P. F., MacDonald, H. R., Eisenman, R. N., *et al.* (2008). Hematopoietic stem cell function and survival depend on c-Myc and N-Myc activity. *Cell stem cell* *3*, 611-624.
- Le, Y., and Sauer, B. (2001). Conditional gene knockout using Cre recombinase. *Molecular biotechnology* *17*, 269-275.
- Lee, Y. Y., Moujalled, D., Doerflinger, M., Gangoda, L., Weston, R., Rahimi, A., de Alboran, I., Herold, M., Bouillet, P., Xu, Q., *et al.* (2013). CREB-binding protein (CBP) regulates beta-adrenoceptor (beta-AR)-mediated apoptosis. *Cell death and differentiation* *20*, 941-952.
- Letai, A., Bassik, M. C., Walensky, L. D., Sorcinelli, M. D., Weiler, S., and Korsmeyer, S. J. (2002). Distinct BH3 domains either sensitize or activate mitochondrial apoptosis, serving as prototype cancer therapeutics. *Cancer cell* *2*, 183-192.
- Lewis, B. C., Klimstra, D. S., and Varmus, H. E. (2003). The c-myc and PyMT oncogenes induce different tumor types in a somatic mouse model for pancreatic cancer. *Genes & development* *17*, 3127-3138.
- Lewis, B. C., Shim, H., Li, Q., Wu, C. S., Lee, L. A., Maity, A., and Dang, C. V. (1997). Identification of putative c-Myc-responsive genes: characterization of rcl, a novel growth-related gene. *Molecular and cellular biology* *17*, 4967-4978.

- Li, F., Wang, Y., Zeller, K. I., Potter, J. J., Wonsey, D. R., O'Donnell, K. A., Kim, J. W., Yustein, J. T., Lee, L. A., and Dang, C. V. (2005). Myc stimulates nuclearly encoded mitochondrial genes and mitochondrial biogenesis. *Molecular and cellular biology* 25, 6225-6234.
- Li, T., Kon, N., Jiang, L., Tan, M., Ludwig, T., Zhao, Y., Baer, R., and Gu, W. (2012). Tumor suppression in the absence of p53-mediated cell-cycle arrest, apoptosis, and senescence. *Cell* 149, 1269-1283.
- Lin, C. Y., Loven, J., Rahl, P. B., Paranal, R. M., Burge, C. B., Bradner, J. E., Lee, T. I., and Young, R. A. (2012). Transcriptional amplification in tumor cells with elevated c-Myc. *Cell* 151, 56-67.
- Liu, H., Radisky, D. C., Yang, D., Xu, R., Radisky, E. S., Bissell, M. J., and Bishop, J. M. (2012a). MYC suppresses cancer metastasis by direct transcriptional silencing of alpha v and beta3 integrin subunits. *Nature cell biology* 14, 567-574.
- Liu, L., Ulbrich, J., Muller, J., Wustefeld, T., Aeberhard, L., Kress, T. R., Muthalagu, N., Rycak, L., Rudalska, R., Moll, R., *et al.* (2012b). Deregulated MYC expression induces dependence upon AMPK-related kinase 5. *Nature* 483, 608-612.
- Lizcano, J. M., Goransson, O., Toth, R., Deak, M., Morrice, N. A., Boudeau, J., Hawley, S. A., Udd, L., Makela, T. P., Hardie, D. G., and Alessi, D. R. (2004). LKB1 is a master kinase that activates 13 kinases of the AMPK subfamily, including MARK/PAR-1. *The EMBO journal* 23, 833-843.
- Llambi, F., Moldoveanu, T., Tait, S. W., Bouchier-Hayes, L., Temirov, J., McCormick, L. L., Dillon, C. P., and Green, D. R. (2011). A unified model of mammalian BCL-2 protein family interactions at the mitochondria. *Molecular cell* 44, 517-531.
- Lu, S., Niu, N., Guo, H., Tang, J., Guo, W., Liu, Z., Shi, L., Sun, T., Zhou, F., Li, H., *et al.* (2013). ARK5 promotes glioma cell invasion, and its elevated expression is correlated with poor clinical outcome. *Eur J Cancer* 49, 752-763.
- Maclean, K. H., Keller, U. B., Rodriguez-Galindo, C., Nilsson, J. A., and Cleveland, J. L. (2003). c-Myc augments gamma irradiation-induced apoptosis by suppressing Bcl-XL. *Molecular and cellular biology* 23, 7256-7270.
- Marhin, W. W., Chen, S., Facchini, L. M., Fornace, A. J., Jr., and Penn, L. Z. (1997). Myc represses the growth arrest gene gadd45. *Oncogene* 14, 2825-2834.
- Mason, K. D., Vandenberg, C. J., Scott, C. L., Wei, A. H., Cory, S., Huang, D. C., and Roberts, A. W. (2008). In vivo efficacy of the Bcl-2 antagonist ABT-737 against aggressive Myc-driven lymphomas. *Proceedings of the National Academy of Sciences of the United States of America* 105, 17961-17966.
- Mateyak, M. K., Obaya, A. J., Adachi, S., and Sedivy, J. M. (1997). Phenotypes of c-Myc-deficient rat fibroblasts isolated by targeted homologous recombination. *Cell growth & differentiation : the molecular biology journal of the American Association for Cancer Research* 8, 1039-1048.

- McMahon, S. B., Van Buskirk, H. A., Dugan, K. A., Copeland, T. D., and Cole, M. D. (1998). The novel ATM-related protein TRRAP is an essential cofactor for the c-Myc and E2F oncoproteins. *Cell* *94*, 363-374.
- Menssen, A., and Hermeking, H. (2002). Characterization of the c-MYC-regulated transcriptome by SAGE: identification and analysis of c-MYC target genes. *Proceedings of the National Academy of Sciences of the United States of America* *99*, 6274-6279.
- Meyer, N., Kim, S. S., and Penn, L. Z. (2006). The Oscar-worthy role of Myc in apoptosis. *Seminars in cancer biology* *16*, 275-287.
- Michalak, E. M., Jansen, E. S., Hoppo, L., Cragg, M. S., Tai, L., Smyth, G. K., Strasser, A., Adams, J. M., and Scott, C. L. (2009). Puma and to a lesser extent Noxa are suppressors of Myc-induced lymphomagenesis. *Cell death and differentiation* *16*, 684-696.
- Miller, D. M., Thomas, S. D., Islam, A., Muench, D., and Sedoris, K. (2012). c-Myc and cancer metabolism. *Clinical cancer research : an official journal of the American Association for Cancer Research* *18*, 5546-5553.
- Minn, A. J., Rudin, C. M., Boise, L. H., and Thompson, C. B. (1995). Expression of bcl-xL can confer a multidrug resistance phenotype. *Blood* *86*, 1903-1910.
- Moore, M. J., Goldstein, D., Hamm, J., Figer, A., Hecht, J. R., Gallinger, S., Au, H. J., Murawa, P., Walde, D., Wolff, R. A., *et al.* (2007). Erlotinib plus gemcitabine compared with gemcitabine alone in patients with advanced pancreatic cancer: a phase III trial of the National Cancer Institute of Canada Clinical Trials Group. *Journal of clinical oncology : official journal of the American Society of Clinical Oncology* *25*, 1960-1966.
- Morris, J. P. t., Wang, S. C., and Hebrok, M. (2010). KRAS, Hedgehog, Wnt and the twisted developmental biology of pancreatic ductal adenocarcinoma. *Nature reviews Cancer* *10*, 683-695.
- Morton, J. P., Jamieson, N. B., Karim, S. A., Athineos, D., Ridgway, R. A., Nixon, C., McKay, C. J., Carter, R., Brunton, V. G., Frame, M. C., *et al.* (2010). LKB1 haploinsufficiency cooperates with Kras to promote pancreatic cancer through suppression of p21-dependent growth arrest. *Gastroenterology* *139*, 586-597, 597 e581-586.
- Murphy, D. J., Junttila, M. R., Pouyet, L., Karnezis, A., Shchors, K., Bui, D. A., Brown-Swigart, L., Johnson, L., and Evan, G. I. (2008). Distinct thresholds govern Myc's biological output in vivo. *Cancer cell* *14*, 447-457.
- Murphy, D. J., and Muthalagu, N. (2015). Bim's up first. *Molecular & cellular oncology* *2*.
- Murphy, M. J., Wilson, A., and Trumpp, A. (2005). More than just proliferation: Myc function in stem cells. *Trends in cell biology* *15*, 128-137.
- Muthalagu, N., Junttila, M. R., Wiese, K. E., Wolf, E., Morton, J., Bauer, B., Evan, G. I., Eilers, M., and Murphy, D. J. (2014). BIM is the primary mediator of MYC-induced apoptosis in multiple solid tissues. *Cell reports* *8*, 1347-1353.

- Nau, M. M., Brooks, B. J., Battey, J., Sausville, E., Gazdar, A. F., Kirsch, I. R., McBride, O. W., Bertness, V., Hollis, G. F., and Minna, J. D. (1985). L-myc, a new myc-related gene amplified and expressed in human small cell lung cancer. *Nature* *318*, 69-73.
- Nesbit, C. E., Tersak, J. M., and Prochownik, E. V. (1999). MYC oncogenes and human neoplastic disease. *Oncogene* *18*, 3004-3016.
- Ng, K. P., Hillmer, A. M., Chuah, C. T., Juan, W. C., Ko, T. K., Teo, A. S., Ariyaratne, P. N., Takahashi, N., Sawada, K., Fei, Y., *et al.* (2012). A common BIM deletion polymorphism mediates intrinsic resistance and inferior responses to tyrosine kinase inhibitors in cancer. *Nature medicine* *18*, 521-528.
- Nie, Z., Hu, G., Wei, G., Cui, K., Yamane, A., Resch, W., Wang, R., Green, D. R., Tessarollo, L., Casellas, R., *et al.* (2012). c-Myc is a universal amplifier of expressed genes in lymphocytes and embryonic stem cells. *Cell* *151*, 68-79.
- Offield, M. F., Jetton, T. L., Labosky, P. A., Ray, M., Stein, R. W., Magnuson, M. A., Hogan, B. L., and Wright, C. V. (1996). PDX-1 is required for pancreatic outgrowth and differentiation of the rostral duodenum. *Development* *122*, 983-995.
- Olive, K. P., Jacobetz, M. A., Davidson, C. J., Gopinathan, A., McIntyre, D., Honess, D., Madhu, B., Goldgraben, M. A., Caldwell, M. E., Allard, D., *et al.* (2009). Inhibition of Hedgehog signaling enhances delivery of chemotherapy in a mouse model of pancreatic cancer. *Science* *324*, 1457-1461.
- Oltersdorf, T., Elmore, S. W., Shoemaker, A. R., Armstrong, R. C., Augeri, D. J., Belli, B. A., Bruncko, M., Deckwerth, T. L., Dinges, J., Hajduk, P. J., *et al.* (2005). An inhibitor of Bcl-2 family proteins induces regression of solid tumours. *Nature* *435*, 677-681.
- Orian, A., van Steensel, B., Delrow, J., Bussemaker, H. J., Li, L., Sawado, T., Williams, E., Loo, L. W., Cowley, S. M., Yost, C., *et al.* (2003). Genomic binding by the Drosophila Myc, Max, Mad/Mnt transcription factor network. *Genes & development* *17*, 1101-1114.
- Pan, J., Deng, Q., Jiang, C., Wang, X., Niu, T., Li, H., Chen, T., Jin, J., Pan, W., Cai, X., *et al.* (2014). USP37 directly deubiquitinates and stabilizes c-Myc in lung cancer. *Oncogene*.
- Pelengaris, S., Khan, M., and Evan, G. I. (2002). Suppression of Myc-induced apoptosis in beta cells exposes multiple oncogenic properties of Myc and triggers carcinogenic progression. *Cell* *109*, 321-334.
- Perez-Mancera, P. A., Guerra, C., Barbacid, M., and Tuveson, D. A. (2012). What we have learned about pancreatic cancer from mouse models. *Gastroenterology* *142*, 1079-1092.
- Peukert, K., Staller, P., Schneider, A., Carmichael, G., Hanel, F., and Eilers, M. (1997). An alternative pathway for gene regulation by Myc. *The EMBO journal* *16*, 5672-5686.
- Popov, N., Wanzel, M., Madiredjo, M., Zhang, D., Beijersbergen, R., Bernards, R., Moll, R., Elledge, S. J., and Eilers, M. (2007). The ubiquitin-specific protease USP28 is required for MYC stability. *Nature cell biology* *9*, 765-774.

- Pourdehnad, M., Truitt, M. L., Siddiqi, I. N., Ducker, G. S., Shokat, K. M., and Ruggero, D. (2013). Myc and mTOR converge on a common node in protein synthesis control that confers synthetic lethality in Myc-driven cancers. *Proceedings of the National Academy of Sciences of the United States of America* *110*, 11988-11993.
- Puri, S., Folias, A. E., and Hebrok, M. (2015). Plasticity and dedifferentiation within the pancreas: development, homeostasis, and disease. *Cell stem cell* *16*, 18-31.
- Pylayeva-Gupta, Y., Grabocka, E., and Bar-Sagi, D. (2011). RAS oncogenes: weaving a tumorigenic web. *Nature reviews Cancer* *11*, 761-774.
- Qi, Y., Gregory, M. A., Li, Z., Brousal, J. P., West, K., and Hann, S. R. (2004). p19ARF directly and differentially controls the functions of c-Myc independently of p53. *Nature* *431*, 712-717.
- Rahl, P. B., Lin, C. Y., Seila, A. C., Flynn, R. A., McCuine, S., Burge, C. B., Sharp, P. A., and Young, R. A. (2010). c-Myc regulates transcriptional pause release. *Cell* *141*, 432-445.
- Rapp, U. R., Korn, C., Ceteci, F., Karreman, C., Luetkenhaus, K., Serafin, V., Zanucco, E., Castro, I., and Potapenko, T. (2009). MYC is a metastasis gene for non-small-cell lung cancer. *PloS one* *4*, e6029.
- Rodriguez-Pinilla, S. M., Jones, R. L., Lambros, M. B., Arriola, E., Savage, K., James, M., Pinder, S. E., and Reis-Filho, J. S. (2007). MYC amplification in breast cancer: a chromogenic in situ hybridisation study. *Journal of clinical pathology* *60*, 1017-1023.
- Ryan, D. P., Hong, T. S., and Bardeesy, N. (2014). Pancreatic adenocarcinoma. *The New England journal of medicine* *371*, 2140-2141.
- Sabo, A., Kress, T. R., Pelizzola, M., de Pretis, S., Gorski, M. M., Tesi, A., Morelli, M. J., Bora, P., Doni, M., Verrecchia, A., *et al.* (2014). Selective transcriptional regulation by Myc in cellular growth control and lymphomagenesis. *Nature* *511*, 488-492.
- Saborowski, M., Saborowski, A., Morris, J. P. t., Bosbach, B., Dow, L. E., Pelletier, J., Klimstra, D. S., and Lowe, S. W. (2014). A modular and flexible ESC-based mouse model of pancreatic cancer. *Genes & development* *28*, 85-97.
- Sahai, V., Kumar, K., Knab, L. M., Chow, C. R., Raza, S. S., Bentrem, D. J., Ebine, K., and Munshi, H. G. (2014). BET bromodomain inhibitors block growth of pancreatic cancer cells in three-dimensional collagen. *Molecular cancer therapeutics* *13*, 1907-1917.
- Schleger, C., Arens, N., Zentgraf, H., Bleyl, U., and Verbeke, C. (2000). Identification of frequent chromosomal aberrations in ductal adenocarcinoma of the pancreas by comparative genomic hybridization (CGH). *The Journal of pathology* *191*, 27-32.
- Schmitt, C. A., McCurrach, M. E., de Stanchina, E., Wallace-Brodeur, R. R., and Lowe, S. W. (1999). INK4a/ARF mutations accelerate lymphomagenesis and promote chemoresistance by disabling p53. *Genes & development* *13*, 2670-2677.

- Schmitt, C. A., Rosenthal, C. T., and Lowe, S. W. (2000). Genetic analysis of chemoresistance in primary murine lymphomas. *Nature medicine* 6, 1029-1035.
- Schuhmacher, M., Kohlhuber, F., Holzel, M., Kaiser, C., Burtscher, H., Jarsch, M., Bornkamm, G. W., Laux, G., Polack, A., Weidle, U. H., and Eick, D. (2001). The transcriptional program of a human B cell line in response to Myc. *Nucleic acids research* 29, 397-406.
- Sears, R. C. (2004). The life cycle of C-myc: from synthesis to degradation. *Cell cycle* 3, 1133-1137.
- Shao, Q., Kannan, A., Lin, Z., Stack, B. C., Jr., Suen, J. Y., and Gao, L. (2014). BET Protein Inhibitor JQ1 Attenuates Myc-Amplified MCC Tumor Growth In Vivo. *Cancer research* 74, 7090-7102.
- Sheiness, D., and Bishop, J. M. (1979). DNA and RNA from uninfected vertebrate cells contain nucleotide sequences related to the putative transforming gene of avian myelocytomatosis virus. *Journal of virology* 31, 514-521.
- Sherr, C. J. (1998). Tumor surveillance via the ARF-p53 pathway. *Genes & development* 12, 2984-2991.
- Shi, C., Hong, S. M., Lim, P., Kamiyama, H., Khan, M., Anders, R. A., Goggins, M., Hruban, R. H., and Eshleman, J. R. (2009). KRAS2 mutations in human pancreatic acinar-ductal metaplastic lesions are limited to those with PanIN: implications for the human pancreatic cancer cell of origin. *Molecular cancer research : MCR* 7, 230-236.
- Shim, H., Dolde, C., Lewis, B. C., Wu, C. S., Dang, G., Jungmann, R. A., Dalla-Favera, R., and Dang, C. V. (1997). c-Myc transactivation of LDH-A: implications for tumor metabolism and growth. *Proceedings of the National Academy of Sciences of the United States of America* 94, 6658-6663.
- Siveke, J. T., Einwachter, H., Sipos, B., Lubeseder-Martellato, C., Kloppel, G., and Schmid, R. M. (2007). Concomitant pancreatic activation of Kras(G12D) and Tgfa results in cystic papillary neoplasms reminiscent of human IPMN. *Cancer cell* 12, 266-279.
- Skoudy, A., Hernandez-Munoz, I., and Navarro, P. (2011). Pancreatic ductal adenocarcinoma and transcription factors: role of c-Myc. *Journal of gastrointestinal cancer* 42, 76-84.
- Small, M. B., Hay, N., Schwab, M., and Bishop, J. M. (1987). Neoplastic transformation by the human gene N-myc. *Molecular and cellular biology* 7, 1638-1645.
- Smith, A. P., Verrecchia, A., Faga, G., Doni, M., Perna, D., Martinato, F., Guccione, E., and Amati, B. (2009). A positive role for Myc in TGFbeta-induced Snail transcription and epithelial-to-mesenchymal transition. *Oncogene* 28, 422-430.
- Soucek, L., Nasi, S., and Evan, G. I. (2004). Omomyc expression in skin prevents Myc-induced papillomatosis. *Cell death and differentiation* 11, 1038-1045.

- Soucek, L., Whitfield, J., Martins, C. P., Finch, A. J., Murphy, D. J., Sodikin, N. M., Karnezis, A. N., Swigart, L. B., Nasi, S., and Evan, G. I. (2008). Modelling Myc inhibition as a cancer therapy. *Nature* 455, 679-683.
- Staller, P., Peukert, K., Kiermaier, A., Seoane, J., Lukas, J., Karsunky, H., Moroy, T., Bartek, J., Massague, J., Hanel, F., and Eilers, M. (2001). Repression of p15INK4b expression by Myc through association with Miz-1. *Nature cell biology* 3, 392-399.
- Strasser, A., Harris, A. W., Bath, M. L., and Cory, S. (1990). Novel primitive lymphoid tumours induced in transgenic mice by cooperation between myc and bcl-2. *Nature* 348, 331-333.
- Strasser, A., Harris, A. W., and Cory, S. (1991). bcl-2 transgene inhibits T cell death and perturbs thymic self-censorship. *Cell* 67, 889-899.
- Sun, X., Gao, L., Chien, H. Y., Li, W. C., and Zhao, J. (2013). The regulation and function of the NUAK family. *Journal of molecular endocrinology* 51, R15-22.
- Suzuki, A., Iida, S., Kato-Uranishi, M., Tajima, E., Zhan, F., Hanamura, I., Huang, Y., Ogura, T., Takahashi, S., Ueda, R., *et al.* (2005). ARK5 is transcriptionally regulated by the Large-MAF family and mediates IGF-1-induced cell invasion in multiple myeloma: ARK5 as a new molecular determinant of malignant multiple myeloma. *Oncogene* 24, 6936-6944.
- Suzuki, A., Kusakai, G., Kishimoto, A., Lu, J., Ogura, T., and Esumi, H. (2003a). ARK5 suppresses the cell death induced by nutrient starvation and death receptors via inhibition of caspase 8 activation, but not by chemotherapeutic agents or UV irradiation. *Oncogene* 22, 6177-6182.
- Suzuki, A., Kusakai, G., Kishimoto, A., Lu, J., Ogura, T., Lavin, M. F., and Esumi, H. (2003b). Identification of a novel protein kinase mediating Akt survival signaling to the ATM protein. *The Journal of biological chemistry* 278, 48-53.
- Suzuki, A., Ogura, T., and Esumi, H. (2006). NDR2 acts as the upstream kinase of ARK5 during insulin-like growth factor-1 signaling. *The Journal of biological chemistry* 281, 13915-13921.
- Swanson, P. J., Kuslak, S. L., Fang, W., Tze, L., Gaffney, P., Selby, S., Hippen, K. L., Nunez, G., Sidman, C. L., and Behrens, T. W. (2004). Fatal acute lymphoblastic leukemia in mice transgenic for B cell-restricted bcl-xL and c-myc. *J Immunol* 172, 6684-6691.
- Tait, S. W., and Green, D. R. (2013). Mitochondrial regulation of cell death. *Cold Spring Harbor perspectives in biology* 5.
- Takahashi, K., and Yamanaka, S. (2006). Induction of pluripotent stem cells from mouse embryonic and adult fibroblast cultures by defined factors. *Cell* 126, 663-676.

Tikhonenko, A. T., Black, D. J., and Linial, M. L. (1996). Viral Myc oncoproteins in infected fibroblasts down-modulate thrombospondin-1, a possible tumor suppressor gene. *The Journal of biological chemistry* *271*, 30741-30747.

Turrens, J. F. (2003). Mitochondrial formation of reactive oxygen species. *The Journal of physiology* *552*, 335-344.

Utomo, W. K., Narayanan, V., Biermann, K., van Eijck, C. H., Bruno, M. J., Peppelenbosch, M. P., and Braat, H. (2014). mTOR is a promising therapeutical target in a subpopulation of pancreatic adenocarcinoma. *Cancer letters* *346*, 309-317.

van Riggelen, J., Yetil, A., and Felsher, D. W. (2010). MYC as a regulator of ribosome biogenesis and protein synthesis. *Nature Reviews Cancer* *10*, 301-309.

Vander Heiden, M. G., Cantley, L. C., and Thompson, C. B. (2009). Understanding the Warburg effect: the metabolic requirements of cell proliferation. *Science* *324*, 1029-1033.

Vaux, D. L., Cory, S., and Adams, J. M. (1988). Bcl-2 gene promotes haemopoietic cell survival and cooperates with c-myc to immortalize pre-B cells. *Nature* *335*, 440-442.

Villunger, A., Michalak, E. M., Coultas, L., Mullauer, F., Bock, G., Ausserlechner, M. J., Adams, J. M., and Strasser, A. (2003). p53- and drug-induced apoptotic responses mediated by BH3-only proteins puma and noxa. *Science* *302*, 1036-1038.

Vita, M., and Henriksson, M. (2006). The Myc oncoprotein as a therapeutic target for human cancer. *Seminars in cancer biology* *16*, 318-330.

Vooijs, M., Jonkers, J., and Berns, A. (2001). A highly efficient ligand-regulated Cre recombinase mouse line shows that LoxP recombination is position dependent. *EMBO reports* *2*, 292-297.

Wallace, D. C. (2012). Mitochondria and cancer. *Nature reviews Cancer* *12*, 685-698.

Walz, S., Lorenzin, F., Morton, J., Wiese, K. E., von Eyss, B., Herold, S., Rycak, L., Dumay-Odelot, H., Karim, S., Bartkuhn, M., *et al.* (2014). Activation and repression by oncogenic MYC shape tumour-specific gene expression profiles. *Nature* *511*, 483-487.

Wang, H., Mannava, S., Grachtchouk, V., Zhuang, D., Soengas, M. S., Gudkov, A. V., Prochownik, E. V., and Nikiforov, M. A. (2008). c-Myc depletion inhibits proliferation of human tumor cells at various stages of the cell cycle. *Oncogene* *27*, 1905-1915.

Weinberg, R. A. (1991). Tumor suppressor genes. *Science* *254*, 1138-1146.

Weng, A. P., Millholland, J. M., Yashiro-Ohtani, Y., Arcangeli, M. L., Lau, A., Wai, C., Del Bianco, C., Rodriguez, C. G., Sai, H., Tobias, J., *et al.* (2006). c-Myc is an important direct target of Notch1 in T-cell acute lymphoblastic leukemia/lymphoma. *Genes & development* *20*, 2096-2109.

Wilentz, R. E., Geradts, J., Maynard, R., Offerhaus, G. J., Kang, M., Goggins, M., Yeo, C. J., Kern, S. E., and Hruban, R. H. (1998). Inactivation of the p16 (INK4A) tumor-suppressor gene in pancreatic duct lesions: loss of intranuclear expression. *Cancer research* *58*, 4740-4744.

Wilson, A., Murphy, M. J., Oskarsson, T., Kaloulis, K., Bettess, M. D., Oser, G. M., Pasche, A. C., Knabenhans, C., Macdonald, H. R., and Trumpp, A. (2004). c-Myc controls the balance between hematopoietic stem cell self-renewal and differentiation. *Genes & development* *18*, 2747-2763.

Wise, D. R., DeBerardinis, R. J., Mancuso, A., Sayed, N., Zhang, X. Y., Pfeiffer, H. K., Nissim, I., Daikhin, E., Yudkoff, M., McMahon, S. B., and Thompson, C. B. (2008). Myc regulates a transcriptional program that stimulates mitochondrial glutaminolysis and leads to glutamine addiction. *Proceedings of the National Academy of Sciences of the United States of America* *105*, 18782-18787.

Wolfer, A., and Ramaswamy, S. (2011). MYC and metastasis. *Cancer research* *71*, 2034-2037.

Wolfer, A., Wittner, B. S., Irimia, D., Flavin, R. J., Lupien, M., Gunawardane, R. N., Meyer, C. A., Lightcap, E. S., Tamayo, P., Mesirov, J. P., *et al.* (2010). MYC regulation of a "poor-prognosis" metastatic cancer cell state. *Proceedings of the National Academy of Sciences of the United States of America* *107*, 3698-3703.

Wu, S., Cetinkaya, C., Munoz-Alonso, M. J., von der Lehr, N., Bahram, F., Beuger, V., Eilers, M., Leon, J., and Larsson, L. G. (2003). Myc represses differentiation-induced p21CIP1 expression via Miz-1-dependent interaction with the p21 core promoter. *Oncogene* *22*, 351-360.

Yada, M., Hatakeyama, S., Kamura, T., Nishiyama, M., Tsunematsu, R., Imaki, H., Ishida, N., Okumura, F., Nakayama, K., and Nakayama, K. I. (2004). Phosphorylation-dependent degradation of c-Myc is mediated by the F-box protein Fbw7. *The EMBO journal* *23*, 2116-2125.

Yang, D., Liu, H., Goga, A., Kim, S., Yuneva, M., and Bishop, J. M. (2010). Therapeutic potential of a synthetic lethal interaction between the MYC proto-oncogene and inhibition of aurora-B kinase. *Proceedings of the National Academy of Sciences of the United States of America* *107*, 13836-13841.

Yang, Y., Li, J., Liu, F., and Huang, L. (2012). Systemic delivery of siRNA via LCP nanoparticle efficiently inhibits lung metastasis. *Molecular therapy : the journal of the American Society of Gene Therapy* *20*, 609-615.

Ye, X. T., Guo, A. J., Yin, P. F., Cao, X. D., and Chang, J. C. (2014). Overexpression of NUA1 is associated with disease-free survival and overall survival in patients with gastric cancer. *Medical oncology* *31*, 61.

Yin, X., Giap, C., Lazo, J. S., and Prochownik, E. V. (2003). Low molecular weight inhibitors of Myc-Max interaction and function. *Oncogene* *22*, 6151-6159.

Zagorska, A., Deak, M., Campbell, D. G., Banerjee, S., Hirano, M., Aizawa, S., Prescott, A. R., and Alessi, D. R. (2010). New roles for the LKB1-NUAK pathway in controlling myosin phosphatase complexes and cell adhesion. *Science signaling* *3*, ra25.

Zhou, M., Wang, J., Ouyang, J., Xu, J. Y., Chen, B., Zhang, Q. G., Zhou, R. F., Yang, Y. G., Shao, X. Y., Xu, Y., *et al.* (2014). MYC protein expression is associated with poor prognosis in diffuse large B cell lymphoma patients treated with RCHOP chemotherapy. *Tumour biology : the journal of the International Society for Oncodevelopmental Biology and Medicine* *35*, 6757-6762.

Zimmerman, K. A., Yancopoulos, G. D., Collum, R. G., Smith, R. K., Kohl, N. E., Denis, K. A., Nau, M. M., Witte, O. N., Toran-Allerand, D., Gee, C. E., and *et al.* (1986). Differential expression of myc family genes during murine development. *Nature* *319*, 780-783.

Zindy, F., Eischen, C. M., Randle, D. H., Kamijo, T., Cleveland, J. L., Sherr, C. J., and Roussel, M. F. (1998). Myc signaling via the ARF tumor suppressor regulates p53-dependent apoptosis and immortalization. *Genes & development* *12*, 2424-2433.

Zindy, F., Williams, R. T., Baudino, T. A., Reh, J. E., Skapek, S. X., Cleveland, J. L., Roussel, M. F., and Sherr, C. J. (2003). Arf tumor suppressor promoter monitors latent oncogenic signals in vivo. *Proceedings of the National Academy of Sciences of the United States of America* *100*, 15930-15935.